



Published in final edited form as:

J Biomed Nanotechnol. 2015 November ; 11(11): 1859–1898.

Recent Developments in Active Tumor Targeted Multifunctional Nanoparticles for Combination Chemotherapy in Cancer Treatment and Imaging

Micah D. K. Glasgow¹ and Mahavir B. Chougule^{1,2,*}

¹Department of Pharmaceutical Sciences, Daniel K. Inouye College of Pharmacy, University of Hawai'i at Hilo, Hilo, Hawai'i 96720, China

²Natural Products and Experimental Therapeutics Program, University of Hawaii Cancer Center, Honolulu, Hawaii, USA

Abstract

Nanotechnology and combination therapy are two major fields that show great promise in the treatment of cancer. The delivery of drugs via nanoparticles helps to improve drug's therapeutic effectiveness while reducing adverse side effects associated with high dosage by improving their pharmacokinetics. Taking advantage of molecular markers over-expressing on tumor tissues compared to normal cells, an "active" molecular marker targeted approach would be beneficial for cancer therapy. These actively targeted nanoparticles would increase drug concentration at the tumor site, improving efficacy while further reducing chemo-resistance. The multidisciplinary approach may help to improve the overall efficacy in cancer therapy. This review article summarizes recent developments of targeted multifunctional nanoparticles in the delivery of various drugs for a combinational chemotherapy approach to cancer treatment and imaging.

Keywords

Cancer; Multi-Drug Resistance; Combination Chemotherapy; Nanoparticles; Drug Delivery; Targeted Nanoparticles; Multifunctional Nanoparticles

INTRODUCTION

Nanotechnologies were first described in the 1960s through liposomal carriers assisting in the delivery of proteins and drugs to various diseases.¹ Since then, the field has made a significant impact on the development of drug delivery systems and clinical therapeutics for cancer therapy.^{1–3} Currently, there are over two dozen nanotechnology-based therapeutic products approved by the Food and Drug Administration (FDA) for clinical use with more being evaluated under clinical trials.^{2–4} Some notable examples of chemotherapeutic nanoparticles on the market include doxorubicin (DOX) encapsulated liposomal nanocarriers Doxil⁵ and paclitaxel (PTX)-bound albumin nanocarriers Abraxane,⁶ both administered intravenously (i.v.) for the treatment of various cancers. Further advances in the

* Author to whom correspondence should be addressed. mahavir@hawaii.edu, mahavirchougule@gmail.com.

biocompatibility of these nanoscale drug carriers have allowed for safer, more efficient delivery of a variety of chemotherapeutic drugs. Advantages in nanoparticle assisted delivery of these drugs, particularly at the systemic level, include longer circulation half-lives, improved pharmacokinetics, and reduced adverse side effects.^{3,7,8} Nanoparticles may also take advantage of the enhanced permeability and retention (EPR) effect caused by “leaky” tumor vasculatures, increasing drug accumulation at the tumor site,⁹ thereby improving pharmacokinetics, and reducing dose and associated toxicities.

In recent years, researchers have been exploring different approaches to delivering multiple therapeutic agent loaded nanoparticles for cancer therapy.⁷ The use of multiple drugs may suppress the phenomenon known as cancer chemo-resistance that is accountable for the majority of failed cases for cancer therapy.⁷ Cancer cells have been observed to show a diminished response over a period of chemo-treatment as they acquire defense mechanisms by enhancing self-repair pathways, overexpressing drug efflux pumps, increasing drug metabolism or expressing altered drug targets.⁷ Combination chemotherapy has been adopted in clinics as a primary cancer treatment regimen to help overcome and reduce cancer drug resistance for an overall improved therapeutic effectiveness.⁸ If multiple drugs were applied with different molecular targets, then genetic barriers could be raised to overcome the cancer cell mutations, thereby delaying the cancer adaptation process. It has also been demonstrated that in the treatment with multiple drugs that target the same cellular pathways, the drugs do function synergistically, yielding an improved therapeutic efficacy and increased target selectivity.⁸ However, with all their benefits, current combination chemotherapies do have their shortcomings. Dosing and scheduling optimization may be extremely difficult due to the varying pharmacokinetics, bio-distributions, and membrane transport properties among various drug molecules.^{8,9} Furthermore, highly potent drug combinations are often associated with severe side effects. These challenges have driven researchers, engineers, and clinicians to investigate rationalized approaches to using the targeted nanotechnology with combination chemotherapy for a more precise and effective route of cancer treatment.

This article reviews the latest status of targeted nanoparticle-assisted co-delivery of multiple drugs in cancer therapy and imaging. The focus of this article is distinct from the broader generalization of targeted nanoparticle-based combination therapy, which touches on co-administration of multiple different single drug-containing vehicles, as recently discussed in a review by Greco et al.¹⁰ We emphasize a targeted approach to multidrug/siRNA-containing nanoparticles over delivery of single agent loaded nanoparticles due to the vehicle uniformity, ratio-metric drug loading and temporal drug release. All of these features carry significant therapeutic implications and will be discussed in detail.

CANCER THERAPY

Cancer is a major public health problem since it is the second leading cause of illness-related death, only exceeded by heart disease.¹¹ The pathogenesis of cancer involves the structural and quantitative alterations in cellular molecules that control different aspects of cell behavior.¹² Molecular changes that cause the development and progression of cancer have been commonly linked to genetic alterations.¹¹ Research efforts are on-going to identify

common genetic modifications and the underlying target genes involved in cancer pathways. Alterations in a person's genetic makeup may be inherited, as in hereditary cancers, or induced by endogenous and exogenous carcinogenic factors as in most sporadic cancers.¹¹ There are six essential changes in cell physiology suggested to collectively dictate malignant growth; self-sufficiency in growth signals, insensitivity to anti-growth signals, tissue invasion and metastasis, limitless replicative potential, sustained angiogenesis and evading apoptosis.¹²

Chemotherapeutic agents used in current clinical practice have played a significant role in reducing mortality/morbidity and in increasing patients' quality of life.¹³ Despite the recent advances in early diagnosis and in clinical protocols for cancer treatment, the development of anticancer agents that combine efficacy, safety and convenience for the patient remains a great challenge.¹⁴

Most anticancer drugs have narrow therapeutic index, develop multidrug resistance (MDR) and present non-specific bio-distribution upon i.v. administration leading to severe side effects to healthy tissues, mainly bone marrow and gastrointestinal tract.¹³ These limitations of conventional chemotherapeutic strategies frequently result in suboptimal dosing, treatment delay or discontinuance and reduced patient compliance to therapy.¹⁴

MECHANISMS OF DRUG RESISTANCE

Resistance can manifest as a result of decreased drug activity and can be primary (present prior to drug exposure, with the tumor insensitive to initial treatment) or acquired (tumor resistance developing during or after the course of treatment). This innate and/or adaptive resistance to chemotherapy critically limits treatment outcomes and remains a key challenge for clinicians.¹⁵ Because a particular mechanism can affect agents from completely unrelated classes of chemotherapy agents, subsequent treatment options may be compromised.¹⁵ This so-called MDR phenomenon constrains the efficacy of anthracyclines, taxanes, and several other cytotoxic and biologic agents.¹⁶ On a cellular level, there are multiple active mechanisms of resistance, which include increased activity of efflux pumps, such as adenosine-triphosphate (ATP) dependent transporters or reduced drug influx; activation of detoxifying proteins, such as cytochrome P450 mixed function oxidases; activation of mechanisms that repair drug induced DNA damage; and disruptions in apoptotic signaling pathways, which may decrease susceptibility to drug-induced cell death.¹⁵

Alterations in drug efflux mechanisms are a common cause of MDR.¹⁷ Overexpression of ATP-binding cassette (ABC) transporter proteins, such as P-glycoprotein (P-gp), and MDR-associated protein 1 (MRP1) may be involved.¹⁸ ABC transporters act by pumping anticancer agents out of the intracellular milieu into the extracellular matrix, thereby preventing the agents from reaching their minimally effective intracellular concentrations.¹⁷ Substrates for P-gp include anthracyclines, taxanes, antimetabolites, and vinca alkaloids.¹⁸ In a meta-analysis of 31 breast cancer clinical trials, overexpression of P-gp was associated with 3-fold increased risk of failure to respond to chemotherapy, and its expression was noted to increase after chemotherapy exposure.¹⁹ Although MRP1 expression is increased in

chemotherapy-naive tumors, its expression has shown to increase with exposure to cytotoxic agents.¹⁸ MRP1 has been shown to confer resistance to anthracyclines and vinca alkaloids, but not taxanes.¹⁸

The chemotherapy-resistant phenotype of cancer cells has been developed by multiple gene aberration.²⁰ Although multidrug and taxane resistance mechanisms are among the best characterized, agents targeted against MDR have yielded poor results.²¹ Since it is recognized that multiple genetic defects namely, DNA mutations, translocations, truncations, deletions, or duplications are present in cancer cells, the role of drug-induced epigenetic aberrations such as histone posttranslational modifications, DNA hypermethylation, and subsequent gene silencing is of increasing importance.^{22–24} Epigenetic changes can occur rapidly upon chemotherapy exposure.²⁴ This article is focused on nanoparticle based combination therapy for cancer. The mechanism of MDR is explained in detail in literature.

COMBINATION CHEMOTHERAPEUTICS

There are several potential advantages to combination chemotherapeutics, such as reversal of drug resistance, synergistically acting drugs, and improving efficacy as compared to single drug therapy.¹⁰ However, with each drug having its own distinct pharmacokinetic profile, the synergistic drug ratio optimized for *in vitro* analysis will undoubtedly change after the conventional administration of drug “cocktails,” which may lead to insufficient therapeutic results *in vivo*.¹⁰ Polymer and/or lipid-based nanoscale systems that have been previously developed for single drug therapy are now being utilized for co-delivery of more than one drug.²⁵ Mayer et al. have successfully tuned the relative dosage of various drugs in single particle levels, and simultaneously delivered them to target sites with a maintained drug ratio.²⁵ When it comes to other drug combinations, novel delivery vehicles must be developed having desired functionalities that allow for the co-encapsulation of both hydrophobic and hydrophilic drugs, active targeting, and/or controlled drug release.² These functionalities of the nanoparticle are essential for the co-delivery of nucleic acids and drugs, both of which require intracellular delivery to elicit their therapeutic effects.^{26,27} For example, when co-delivering chemotherapy and RNAi therapy for the treatment of multidrug resistant cancers, it is ideal that the nanoparticle first releases siRNA to reduce the expression of MDR transporters followed by the release of the anticancer drugs.²⁷

Co-delivery may also give the ability to combine both targeted imaging and therapeutic agents for the development of theranostics nanoparticles, allowing for the simultaneous visualization of sites targeted nanoparticles and delivery of therapeutic agents.²⁸ Theranostics technology is innovative in concept and holds significant promise for making large medical impacts within the next few decades. Theranostics may provide us with crucial information on intracellular targets, visualization that the therapeutic agents are efficiently reaching their target sites, and enabling effective early detection and treatment of various cancers and diseases.²⁸ Present day research is mainly focused on the design of such multifunctional nanosystems and proof-of-concept tests,^{29–32} however, more systematic *in vivo* studies are needed. Future research in the area of multifunctional nanoparticles will also help to trace the absorption, distribution, metabolism, and excretion of nanoparticles *in vivo*. Understanding the pharmacokinetics of the drug and its drug delivery system will help

improve-formulations, estimate clinical doses, and guarantee safety to patients.³³ Presently, radionuclide labeling is the only technique that can be used to provide *in situ* quantitative information-, but radio emitters may be too unstable to conjugate with nano-materials.³³ With the help of recently developed *in vivo* imaging probes like magnetic nanoparticles,^{34, 35} quantum dots,^{36, 37} gold nanoparticles,^{38, 39} and carbon nanotubes,^{40, 41} more imaging modalities may become available to track the distribution of nano-therapeutics in the body.

COMBINATION CHEMOTHERAPY NANOPARTICLES AGAINST MULTI-DRUG RESISTANT (MDR) CANCER

Multifunctional nanoparticles co-delivering combinations of chemotherapy agents and chemo-sensitizing agents have been shown to be successful in reversing MDR both *in vitro* and *in vivo*.^{42,43} The two underlying mechanisms through which cancer cells acquire MDR to multiple structurally and mechanistically different drugs, among the many cellular mutations that diminish the effectiveness of anticancer drugs, are by the over-expression of multidrug transporters and the altered apoptosis cycle.⁴⁴ MDR that are transporter-dependent have an up-regulated level of transmembrane drug efflux pumps, part of the ABC-superfamily that actively export drugs to reduce their effective intracellular concentration. Many anticancer drugs are affected by these transporters.⁴⁴ For example, the ATP-driven P-gp, is over-expressed in liver, pancreatic, ovarian and gastrointestinal cancers, and readily pumps out DOX, PTX, and Vinblastine.⁴⁴ Pro-survival mutations such as the deregulation of a human proto-oncogene located on chromosome 18, BCL2, and nuclear factor kappa B (NF- κ B), found in apoptotic pathway-dependent MDR, enable cancer cells to tolerate drug-inflicted injuries and significantly decrease their apoptotic response.⁴⁴⁻⁵⁰ A number of chemo-sensitizers have been developed to date which inhibit drug-efflux pumps and help to restore the proper apoptotic signaling within cancer cells. The emergence of siRNA as gene therapy has also made possible the silencing of MDR related genes.⁵⁰ Multifunctional nanoparticles that combine these MDR modulators and cytotoxic drugs have the ability to sensitize MDR cancer cells to the chemotherapeutic payloads.

NANOPARTICLES AS MULTIFUNCTIONAL DRUG DELIVERY SYSTEMS

Nanoparticulate systems such as liposomes, polymeric micelles, polymer-drug nano-conjugates, and dendrimers have led to about two dozen clinically approved therapeutic products.⁷ This review article will discuss nanoparticles that have been demonstrated to carry two or more types of therapeutic payloads for the treatment of various cancers. Controlled combinatorial drug delivery share the common aim in promoting synergism-; however, each drug platform has its unique strength and characteristics. The different particle structures, materials, and preparation processes are emphasized in this article to provide design considerations toward developing combinatorial nanoparticulate systems. The structure of most commonly used nanoparticle systems such as liposome, polymeric micelle, polymer-drug nano-conjugate, and dendrimers has been represented in Figure 1. A wide-range of nanoparticles have also been discussed in literature which utilize different physiochemical properties to chemotherapy⁵¹ but this review article will mainly focus on multifunctional nanoparticles described earlier.⁵²⁻⁵⁷

Liposomes

Liposomes are spherical vesicles consisting of amphiphilic phospholipid bilayers.⁵⁸ The most common building blocks for liposomal preparation are phosphatidylcholine and phosphatidylethanolamine with cholesterol being used as a frequent additive to modify the rigidity of the lipid membranes. Liposomal nanoparticle drug delivery systems have been used for the treatment of various diseases, including cancer. Liposomes may also be formed through the rehydration of lipid films to form multilamellar vesicles (MLV), which undergo further mechanical extrusions to form unilaminar vesicles.⁵⁸ The end structure of this procedure produces a lipid bilayer having an inner aqueous core, with the capability of carrying lipophilic and hydrophilic drugs, respectively. Liposomal drug loading can be accomplished either through active extrusion or through passive diffusion.⁵⁸ In the active extrusion approach, drugs are suspended along with the phospholipids in aqueous solution. The mixture of MLV and drugs is then extruded through membranes with a defined pore size to form drug-loaded liposomes.⁵⁸ Liposomes are first prepared and then mixed with solubilized drugs in the passive diffusion approach. The drug molecules then enter the liposome by diffusion through the lipid bilayers. Liposomes loaded with multiple chemotherapeutic agents can use either active or passive loading schemes for the formulation of combinatorial nanoparticles followed by the removal of the unloaded drug. For example, in the preparation of Cytarabine:Daunorubicin liposome injection (CPX-351), a combinatorial liposome for leukemia treatment, cytarabine is hydrated and extruded with the lipid components yielding cytarabine-loaded liposomes. These liposomes are then incubated with daunorubicin to achieve dual-drug encapsulation.⁵⁹ CPX-351 will be described in greater detail in the liposome section of this article. Currently liposomes are the only nanoparticle-based combinatorial drug delivery platform that has entered clinical trials.⁵⁹

The prevalence of MDR in cancer patients, both prior to treatment and de novo,^{60, 61} fueled the application of combinatorial chemotherapy to treat cancer as an alternative to increased doses of chemotherapeutics associated with life threatening side effects.⁶²⁻⁶⁴

Chen et al. studied the co-delivery of 3 different siRNA and one miRNA.⁶⁵ In their study, liposome-polycation-hyaluronic acid nanoparticles (LPH-NP) were developed and targeted by post insertion of DSPE-PEGGC4, the co-delivery of 3 different siRNA and one miRNA was achieved. LPH-NP showed a 80% reduction in tumor volume as compared to control. Their work allowed for the simultaneous study by targeting multiple pathways; proliferation pathways with Cellular-myc (C-myc) siRNA and miR34a miRNA,^{66,67} apoptosis with mouse double minute 2 homolog (MDM2) siRNA,⁶⁸ and angiogenesis using vascular endothelial growth factor (VEGF) siRNA.⁶⁹ Liposomal co-delivery of apoptosis resistance inhibitor PD0325901 with siRNA against the apoptosis regulator myeloid cell leukemia sequence 1 (Mcl-1) and the mitogen-activated extracellular kinase (MEK) resulted in significant enhanced tumor growth inhibition as compared to each treatment alone.⁷⁰ Chen et al. group also developed trilysinoyl oleyamide (trilysin peptide linked to oleyamine by a peptide bond) based PEGylated liposomes for co-delivery of Mcl-1 siRNA and the histone deacetylase inhibitor suberoylanilide hydroxamic acid (SAHA).⁷¹ The PEGylated liposomes were administered i.v. and showed a significant reduction in tumor growth as compared to

SAHA or scrambled siRNA loaded liposomes. Xiao and coworkers did a similar approach by using targeted liposomes to co-deliver DOX and DNA encoding a dominant mutant of survivin for the treatment of lung cancer.⁶⁶ The liposomal drug delivery system conjugated truncated basic fibroblast growth factor (tbFGF) peptides, that recognize the bFGF receptor over-expressed in lung cancers, for a targeted approach along with DOX and pDNA encoding for a dominant negative mutant of-survivin to counter survivin-mediated apoptosis resistance.⁷² Co-delivering both chemotherapeutic agents produced an increased therapeutic response against Lewis lung carcinoma tumors—over liposomes with either agent alone.

Saad et al. took a further step in the combination of an anticancer agent with the modulation of drug resistance by formulating peptide-targeted liposomes encapsulating DOX or cisplatin together with oligonucleotides against Bcl-2 and MDR1, two main drug resistance mechanisms of cancer cells.⁷³ The efficacy of combining a targeted chemotherapy with a gene therapy were evaluated using xenografts established from human ovarian malignant ascites.⁷³ Cisplatin or DOX-loaded targeted liposomes, with the inclusion of either Bcl-2 or MDR1 antisense oligonucleotides, decreased primary tumor volume and intraperitoneal metastases load. Tumor growth was further inhibited with targeted liposomes containing DOX or cisplatin, Bcl-2 and MDR1 antisense oligonucleotides together resulting in the complete prevention of the development of detectable intraperitoneal metastases or ascites.⁷³ Saad et al. first proposed this liposomal system as a platform for personalized cancer therapy. These liposomal formulations would contain antisense oligonucleotides targeting individually relevant resistance mechanisms.

Sawant et al. formulated PEGylated liposomes co-loaded with a palmitoyl-ascorbate conjugate and PTX.⁷⁴ The therapeutic efficacy of co-delivering both agents against 4T1 mammary carcinoma was evident at 10 mg/kg as compared to PTX or palmitoyl-ascorbate-loaded liposomes alone. The liposomal formulation, Atu027, was developed by Silence Therapeutics, London, UK and showed promising results in neuroendocrine and breast cancer patients during phase 1 clinical trials.⁷⁵ The liposomal formulation contains siRNA against protein kinase N3, a downstream effector of the mitogenic PI3K/PTEN pathway involved in prostate cancer metastasis.^{76,77} Atu027 was composed of 2-O-methyl-stabilized siRNA encapsulated in cationic liposomes (50 mol% cationic lipid-Larginyl-2,3-L-diaminopropionic acid-N-palmitoyl-N-oleylamidetrihydrochloride (AtuFECT01), 49 mol% co-lipid 1,2-diphytanoyl-sn-glycero-3-phosphoethanolamine (DPhyPE), and 1 mol% DSPE-PEG2000).⁷⁷ This formulation showed tumor regression during phase I clinical trials and—has entered phase II clinical trials with a focus on breast cancer patients.⁷⁸

Dai et al. co-delivered an antiangiogenic and anticancer agent using targeted PEGylated liposomes.⁷⁹ The combinatorial delivery of the antiangiogenic agent, combrestin A-4 in the lipid bilayer, and the anticancer drug, DOX in the aqueous core, resulted in increased therapeutic efficacy against breast cancer cells. Hu et al. also combined liposomal delivery of honokiol with irradiation for maximal therapeutic efficacy against lung cancer.⁸⁰ It was hypothesized that the co-delivery of this formulation would combine the destruction of tumor cells by irradiation followed by the inhibition of irradiation-induced neo-angiogenesis by honokiol.⁸¹ These PEGylated honokiol-loaded and radiotherapy showed an increase in survival of Lewis lung carcinoma-bearing mice as compared to honokiol or radiotherapy

liposomes alone. The formulation resulted in an overall decrease of angiogenesis *in vivo*.⁷⁹ Maitani et al. followed a similar approach and also combined an anti-cancer agent with an antiangiogenic agent. Maitani et al. co-loaded irinotecan, the anticancer agent, and sunitinib, antiangiogenic agent within liposomes for the treatment of pheochromocytoma neuroendocrine tumors *in vivo*.⁸² The co-delivery of both agents showed higher therapeutic effectiveness within tumors versus administration of sunitinib liposomes plus irinotecan liposomes alone. The co-delivery of both agents in a liposome also had higher drug accumulation at the site of action as compared to free drug. Similarly, folate-targeted DOX-loaded liposomes co-loaded with a bi-functional peptide capable of vascular disruption and antitumor activities were more effective against KB human nasopharyngeal carcinoma *in vivo* than untargeted co-loaded liposomes than either monotherapy.⁸³ RGD-targeted liposomes co-loaded with DOX and the vascular disrupting drug combrestatin A-4 increased tumor regression of B16F10 melanoma compared to untargeted co-loaded liposomes or targeted liposomes with either drug.⁸⁴

As mentioned earlier, CPX-351, a liposomal formulation developed by Celator Pharmaceuticals Inc. (Princeton, NJ) co-loaded with cytarabine and daunorubicin (5:1 molar ratio), was found to be effective in the treatment of acute myeloid leukemia (AML).^{85–88} The same company co-loaded the weakly acidic drug, 5-fluoroorotic acid and the amphiphatic drug, irinotecan (CPT-11) at a 5:1 ratio within PEGylated liposomes. These drugs showed synergism with increased therapeutic efficacy than free drug cocktails *in vivo*.^{88, 89} Liposomes were first prepared before active loading of CPT-11 by a pH gradient method, with protonated CPT-11 being retained in the liposomes after complex formation with 5-fluoroorotic acid. An increase in mice survival was observed when treated with co-loaded liposomes as compared to the combination with separate liposomes. However, the therapeutic efficacy was less than with liposomes loaded with 5-fluoroorotic acid only. It may be because the 5-fluoroorotic acid content had to be lowered for CPT-11 co-loading. This further demonstrates the difficulty of reproducing a synergy with liposomes relative to free drugs. CPX-351 has been tested in phase I trial with acute leukemia patients with the 5:1 ratio being maintained in plasma for 24 h. CPX-351 induced complete responses in 9 out of 43 patients during these trials.⁸⁹ Celator Pharmaceuticals also developed CPX-1, a liposomal formulation co-loaded with irinotecan and floxuridine agents (1:1 molar ratio). CPX-1 is currently in phase I clinical trials with the drug ratio of 1:1 being maintained in plasma for up to 12 h after infusion. Phase I trials showed a positive clinical response in patients with colorectal cancer when treated with CPX-1.⁹⁰ It should be noted that the high therapeutic efficacy of liposome encapsulating two anticancer drugs was always correlated with the maintenance of their synergistic molar ratio in plasma and therapeutic efficacy in preclinical and⁹⁰ as well as clinical studies^{87, 89, 90} which indicates that the optimization of drug loading and liposomal stability are essential for effective combination therapy. Falcao et al. co-delivered the Bcl-2 antisense oligodeoxynucleotide G3139 and the pro-apoptotic peptide D-(KLAKKLAK)-2.⁹¹ The research group used the electrostatic properties of the therapeutic molecules to their advantage. The authors formulated a negatively charged complex between G3139 and the peptide before mixing with the positively charged liposomes. Co-loaded liposomes were then injected intratumoral leading to enhanced tumor growth suppression as compared to liposomes containing a single agent and free drug.

Bajelan et al. co-encapsulated stealth nanoliposomes containing PSC 833 (Valspodar), an efficient MDR modulator, and DOX in order to increase the effectiveness and decrease adverse effects of the anticancer drug.⁹² Different methods for liposome preparation were tested in an attempt to increase the encapsulation efficiency of both therapeutic agents with different parameters such as drug to lipid molar ratio, cholesterol mole percent and lipid compositions, being investigated. The final formulation had a lipid composition of egg phosphatidylcholine (EPC):disteroylphosphoethamine (DSPE)-PEG2000:cholesterol (60:5:30 %mol) that was prepared by the thin layer film hydration method. Empty liposomes were first prepared with DOX and PSC 833 loaded after using ammonium sulfate gradient and remote film loading methods, respectively. An *in vitro* cytotoxicity study of various liposomal formulations as well as drugs, solutions against the resistant human breast cancer cell line, T47D/TAMR-6, were evaluated using MTT assay. The best formulation showed a narrow size distribution with average diameter of 91.3 ± 0.2 nm with zeta potential of -6 ± 1.2 , and with the encapsulation efficiency for DOX and PSC 833-more than 95% and 65.5%, respectively. In DOX-resistant T47D/TAMR-6 cells, dual-agent stealth liposomes showed significantly greater cytotoxicity ($P < 0.05$) than free DOX and liposomal DOX plus free PSC 833 treatments. Cell viability assays of dual-agent stealth liposomes showed an approximate 60% decrease as compared to the control with free DOX and PSC 833 solutions displaying a 40% decrease in cell viability. Co-encapsulation of DOX and PSC 833 presents a promising anticancer formulation, capable of effective reversal of drug resistance, and should be explored further in therapeutic studies with animal tumor xenograft models.

Finally, the co-delivery of magnetic fluid hyperthermia and photodynamic therapy liposomes⁹³ using magnetic fluid and zinc phthalocyanine as the photosensitizer demonstrated superior activity *in vitro* of combined light and magnetic stimuli over their separate applications.⁹⁴ This approach suggests a new treatment modality for enhanced tumor therapy.

Polymeric Micelles Nanoparticles

Micelles are colloidal particles with a size of about 5–150 nm that consist of self-assembled aggregates of amphiphilic molecules or surfactants.⁹⁵ At low concentrations these amphiphiles may exist as unimers in aqueous media.⁹⁵ -As the concentration increases, thermodynamic processes drive the formation of aggregates. These aggregates sequester hydrophobic regions into the core surrounded by a hydrophilic corona or shell. The critical micelle concentration (CMC) is the concentration at which aggregation occurs. Pharmaceutical formulations use low molecular weight surfactants (i.e., polysorbates, sodium dodecyl sulfate, etc.) with relatively high CMCs in the range of 10^{-3} to 10^{-4} M, primarily as excipients to increase the aqueous solubility of poorly water soluble drugs.⁹⁵ The core of these micelles encapsulate hydrophobic drugs which also-associate with the hydrophobic regions of the micelle. However, after administration, dilution of a given pharmaceutical formulation occurs rapidly, and as the micelle concentration drops below its CMC, its stability will be compromised.⁹⁵

Work by Kataoka,⁹⁶ Kabanov,⁹⁷ and authors demonstrated the potential use of amphiphilic polymers as drug carriers. As described earlier, the polymeric micelles are mostly composed

of block-copolymers with a hydrophobic and hydrophilic constituent that self-assemble into a hydrophobic core surrounded by the hydrophilic shell (Fig. 1).⁹⁸ Micellar unimer units can be assembled in a variety of ways, such as A–B diblock copolymers, A–B–A triblock copolymers, and grafted copolymers. One of the major advantages to using polymeric micelles, as compared to the traditional low molecular weight surfactant derived systems, is their increased stability. Polymeric micelles commonly exhibit CMCs in the 10^{-6} to 10^{-7} M range.⁹⁹ The ideal polymeric micelle should display the following: higher drug loading ability, controlled drug release, and suitable biological compatibility and stability. The characteristics and lengths of the hydrophilic and hydrophobic block polymers primarily determine the physiochemical properties of the polymeric micelles. The most commonly utilized hydrophilic polymer is Polyethylene glycol (PEG). Due to PEG's highly hydrated nature, it is able to resist uptake by the reticuloendothelial system (RES).⁹⁹ There are a number of other hydrophilic polymer chemistries currently being applied for this very reason: poly(N-vinyl-2-pyrrolidone) (PVP),¹⁰⁰ poly(vinyl alcohol) (PVA),¹⁰¹ and poly(ethyleneimine) (PEI).¹⁰² PEG remains the polymer of choice due to its widespread acceptance and availability. The hydrophobic core of the polymeric micelles uses a large variety of hydrophobic block polymers, which include propylene oxide, L-lysine, caprolactone, D, L-lactic acid, styrene, aspartic acid, β -benzoyl-L-aspartate, and spermine among others.¹⁰³ More hydrophobic unimers, such as styrene, tend to form micelle cores spontaneously, whereas less hydrophobic unimers (i.e., lysine) will first interact via electrostatic interactions with hydrophobic drug molecules, before formation of a micelle.¹⁰⁴ CMC tends to depend more on the type and length of the hydrophobic block, with lower CMCs associated with greater hydrophobicity and increased hydrophobic block length.^{105,106}

The majority of polymer micelles investigated form no covalent bond between the drug and the micellar carrier, as polymer drug conjugates do, and technically cannot be classified as conjugates. There are, however, a number of polymeric micelles where the therapeutic agent is covalently bound to the hydrophobic chains in the micelle core. For example, work by Mikhail et al. focused on poly-(ethylene glycol)-b-poly(ϵ -caprolactone) polymeric micelles containing chemically conjugated DTX.¹⁰⁷ Cationic ring-opening polymerization was implemented to first synthesize PEG-b-polycaprolactone (PCL). Once polymerization was complete, the terminal hydroxyl of PCL was reacted with succinic anhydride to form a terminal carboxylic acid. The terminal end was subsequently coupled to 2' hydroxyl of the therapeutic agent, DTX, a potent anti-mitotic chemotherapy agent. The conjugated DTX coupled to its hydrophobic block polymer resulted in higher drug loading as well as increased stability which was evident by a reduced release rate of DTX from the hydrophobic core.

Polymeric micelles are undergoing continued advances in the nanotechnology field. A trend has been shown towards the development of "smart" polymeric micelles, with their ability to recognize and target specific tissues and their response to various biological stimuli, characteristics which have been elaborated on in the section dealing with polymeric targeting. Another use of polymeric micelles involves the formation of poly-ion complex (PIC) micelles, wherein the micelle core is composed of a polycation block, for the delivery of negatively charged DNA or small interfering RNA (siRNA).^{108,109} Polymeric micelles

based on N-(2-Hydroxypropyl)methacrylamide (HPMA) copolymers have also been described. Poly HPMA can be generated either with the hydrophilic block comprising the shell^{110–113} or as the hydrophobic core after chemical modification.^{114,115} Poly HPMA micelles have shown to encapsulate a variety of hydrophobic drugs; however, the majority of the data on the activity of these systems to date have been obtained *in vitro*^{115–117} and more *in vivo* data is needed to ascertain their potential as carriers.

Lee et al. employed cationic micellar nanoparticles as carriers to co-deliver PTX and Herceptin for achieving targeted delivery of PTX to human epidermal growth factor receptor-2 (HER2/neu)-overexpressing human breast cancer cells, and enhanced cytotoxicity through synergistic activities.¹¹⁸ PTX-loaded nanoparticles had an average size less than 120 nm and a zeta potential of about 60 mV. Herceptin was complexed onto the surface of the nanoparticles. The drug-loaded nanoparticle/Herceptin complexes remained stable under physiologically-simulating conditions with sizes at around 200 nm. Their formulated nanoparticles delivered Herceptin much more efficiently than BioPorter, a commercially available lipid-based protein carrier, and displayed a much higher anti-cancer effectiveness. Lee et al. daily treatment, twice-repeated, with Herceptin showed significantly higher cytotoxicity especially in HER2-overexpressing breast cancer cells when compared to single treatment. Anticancer effects of this co-delivery system was investigated in human breast cancer cell lines with varying degrees of HER2 expression level, namely, MCF7, T47D and BT474.¹¹⁸ The co-delivery of Herceptin increased the cytotoxicity of PTX and this enhancement showed a dependency on their HER2 expression levels. Targeting ability of this co-delivery system was demonstrated through confocal images, which showed significantly higher cellular uptake in HER2-overexpressing BT474 cells as compared to HER2-negative HEK293 cells. This co-delivery system may have important clinical implications against HER2-overexpressing breast cancers.¹¹⁸

An advantage of polymeric micelles as compared to other polymeric drug carriers is their relative ease of fabrication, due to their inherent self-assembly properties. This has resulted in a number of polymeric micelles currently under clinical investigation.¹¹⁹ However, - further investigations are -warranted to explore the use of micellar systems to co-deliver the chemotherapeutic agents.

Poly(Lactic-Co-Glycolic Acid)-Based Nanoparticles

Poly(lactic-co-glycolic acid) (PLGA) is one of the most successfully developed biodegradable polymers.¹²⁰ Various polymers developed may be used to formulate polymeric nanoparticles-; however, PLGA has attracted considerable attention due to its properties:

- I.** biodegradability and biocompatibility,
- II.** FDA and European Medicine Agency approval in drug delivery systems for parenteral administration,
- III.** well described formulations and methods of production adapted to various types of drugs e.g., hydrophilic or hydrophobic small molecules or macromolecules,
- IV.** protection of drug from degradation,

- V. possibility of sustained release,
- VI. possibility to modify surface properties to provide –stealthiness and/or better interaction with biological materials and
- VII. possibility to target nanoparticles to specific organs or cells.¹²⁰

Schleich et al. developed dual PTX/superparamagnetic iron oxide (SPIO)-loaded PLGA-based nanoparticles for a theranostic purpose (Fig. 2). Their formulation produced nanoparticles with a spherical morphology and a size of 240 nm. The PTX and iron loading were 1.84 ± 0.4 and 10.4 ± 1.93 mg/100 mg, respectively.¹²¹ Relaxometry studies and phantom MRI demonstrated their efficacy as T2 contrast agent. Co-loaded PLGA-based nanoparticles showed significant cellular uptake by CT26 colon carcinoma cells executed by Prussian blue staining and fluorescent microscopy. While SPIO did not show any toxicity in CT26 cells, PTX-loaded nanoparticles displayed cytotoxic activity. PTX-loaded nanoparticles, at a concentration of 5 mg/kg, with or without co-encapsulated SPIO induced *in vivo* a regrowth delay of CT26 tumors (colon carcinoma).¹²¹ Together these multifunctional nanoparticles may be considered as future nano-medicine for simultaneous molecular imaging, drug delivery and real-time monitoring of therapeutic effectiveness within patients.

Zhu et al. report a strategy to make use of PLGA nanoparticles (PLGA NPs) for co-delivery of docetaxel (DTX) as a model anticancer drug together with d-alpha-tocopheryl-co-poly-(ethylene glycol) 1000 succinate (TPGS) (Fig. 3).¹²¹ Vitamin E TPGS plays a role as a pore-forming agent in the nanoparticles which may result in smaller particle size, faster drug release and a higher drug encapsulation efficiency. It also acts a bioactive agent that may inhibit P-gp to help overcome MDR of cancer cells. DTX-loaded PLGA NPs were prepared by the nano-precipitation method, encapsulating 0, 10, 20 and 40% TPGS and then characterized for size and size distribution, surface morphology, physical status and encapsulation efficiency of the therapeutic agent in the nanoparticles. It was found that all four formulations had a size ranging from 100–120 nm and entrapment efficiencies between 85–95% with a drug loading level around 10%. *In vitro* evaluation showed that the 48 h IC₅₀ values of free DTX and the DTX-loaded PLGA NPs of 0, 10, 20% TPGS were 2.619 and 0.474, 0.040, 0.009 $\mu\text{g}/\text{mL}$ respectively, which means that PLGA NPs formulations could be 5.57 fold more effective than free DTX. Also, DTX-loaded PLGA NPs of 10 or 20% TPGS were 11.85 and 52.7 fold more effective than DTX-loaded PLGA NPs containing no TPGS (therefore, 66.0 and 284 fold enhanced effectiveness than the free DTX alone). Nude mice with HeLa cell xenograft tumor model and immunohistological staining analysis further confirmed the advantages of the strategy of co-delivery of anticancer drugs with TPGS utilizing PLGA NPs.¹²²

Wang et al. reported core-shell nanoparticles that were doubly emulsified from an amphiphilic copolymer methoxy poly(ethylene glycol)-poly(lactide-co-glycolide) (mPEG-PLGA). These mPEG-PLGA nanoparticles offered advantages as described earlier; they were easy to fabricate by the improved double emulsion method, biocompatible, and showed high loading efficacy.¹²² The mPEG-PLGA nanoparticles were formulated to co-deliver hydrophilic DOX and hydrophobic PTX (Fig. 4). Co-loaded nanoparticles possessed a lower

polydispersity of 0.1, indicating the controlled size distribution of nanoparticles. Studies on drug release and cellular uptake of the co-loaded system demonstrated that both drugs were effectively internalized and released drugs simultaneously in the cells. Furthermore, the co-loaded nanoparticles suppressed tumor cell growth significantly, as compared to the delivery of either free DTX or PTX at the same concentrations, indicating a synergistic effect. Moreover, the nanoparticles loading drugs with a DTX/PTX concentration ratio of 2:1 showed the highest antitumor activity against three different types of tumor cells: A549 human lung cancer cells, B16 mouse melanoma cells and HepG2 human hepatocellular carcinoma cells. These mPEG-PLGA nanoparticles may have potential in clinical implications for co-delivery of multiple anti-tumor drugs with different properties.¹²³

Roy et al. reported better tumor regression and enhancement of antitumor immune response at the tumor microenvironment by co-delivering PTX and a toll-like receptor-4 (TLR4) agonist using a PLGA based nanoparticle preparation (TLNP).¹²⁴ TLR agonists have been shown to activate macrophages and dendritic cells to generate an antitumor immune response. TLR also plays a very crucial role in inducing both innate and adaptive immune response against cancer. The PLGA based nanoparticles entrapping both therapeutic agents had a mean diameter of 255 nm with a polydispersity index of less than 0.1. Particle characterization showed high encapsulation of PTX and TLR4, 87.43% and 62.14% respectively, with retention of their biological activities. *In vivo* tumor regression studies demonstrated the clear benefit of TLNP over free PTX and TLR4. B16-F10 melanoma cells were inoculated into the right flank of 6 to 8-week old C57BL/6 mice. The mean tumor weight of the TLNP treated animals was found to be 0.68 g, whereas that of PTX alone treated animals was 1.8 g. Survival of the TLNP-treated tumor-bearing mice was also found to be significantly higher than that of PTX treated animals. 70% of tumor-bearing mice treated with TLNP survived 30 days after treatment, whereas only 50% of PTX-treated and 30% of TLR4 agonist-treated mice survived 30 days post-treatment. These data suggest that combined chemo-immunotherapy with TLNP had better anticancer efficacy as compared to commercial PTX. *In vivo* results are promising and could pave the way for novel chemo-immunotherapeutic treatment-modalities.

Mesoporous Silica-Based Nanoparticles (MSNPs)

Kresge et al.¹²⁵ described the means of combining sol-gel chemistry with liquid-crystalline templating, creating a new class of ordered porous molecular sieves characterized by periodic arrangements of uniformly sized mesopores (defined by IUPAC as pores with diameters between 2 and 50 nm) incorporated within an amorphous silica matrix.¹²⁵ The controlled synthesis of spherical and other shaped mesoporous silica nanoparticles (MSNPs) has since been achieved using solution routes or an aerosol based evaporation-induced self-assembly (EISA) process,^{126,127} with surfaces of the pore being modified with a wide range of chemical moieties based mainly on silane coupling chemistries. In any case, a successful bio-compatible nanoparticle must exhibit low toxicity, size uniformity, large capacity for diverse cargos, high traceability, colloidal stability, selective cell-specific binding and internalization, and triggered cargo release.^{126,128}

Ma et al. described a hollow mesoporous silica nanoparticle (HMSNPs) based targeted drug/siRNA co-delivery system, aimed at overcoming MDR in ovarian cancer cells.¹²⁵ Perpendicular nanochannels connecting to the internal hollow cores were formed within the HMSNPs, facilitating drug loading and release. It was shown that the extra volume of the hollow core enhances the drug loading capacity by almost two fold as compared with conventional MSNP. The surface of the HMSNPs were coated with folic acid conjugated to polyethyleneimine (PEI-FA) under neutral conditions using electrostatic interactions between the phosphate groups on the HMSNP surfaces and the partially charged amino groups of PEI-FA, thereby blocking the mesopores and preventing leakage of the loaded drugs. Folic acid not only prevents drug leakage but also acts as a target ligand that allows HMSNP selective binding and internalization in the cancer cells. HMSNPs coated with PEI-FA showed enhanced siRNA binding capability on account of electrostatic interactions between the amino groups of PEI-FA and siRNA, as compared with that of conventional MSNPs. This electrostatic interaction helped to achieve the pH-controlled release of loaded drugs. *In vitro* pH-responsive drug/siRNA co-delivery experiments were conducted with two cancer cell lines-, HeLa cervical cancer cell lines having higher folic acid receptor expression and MCF-7 breast cancer cell lines with lower folic acid receptor expression. The pH-responsive intracellular drug/siRNA release greatly minimizes the prerelease and possible adverse side effects of the delivery system and its payloads. The co-delivery of DOX and siRNA against the Bcl-2 protein into HeLa cells was achieved via folic acid receptor mediated endocytosis. It was shown that the expression of the anti-apoptotic protein Bcl-2 was successfully suppressed, leading to enhanced therapeutic efficacy of DOX. Thus, the multifunctional nanoparticle shows promising potentials for controlled and targeted co-delivery of drug and gene in cancer treatment.¹²⁵

Meng et al. used a similar technique involving both chemo and gene therapy to effectively overcome MDR in human breast cancer xenografts. Meng et al. developed a MSNPs co-loaded with DOX and siRNA that targets the P-gp.¹²⁶ For the selection of the siRNA that targets P-gp, among a series of drug resistant targets, high throughput screening was performed in a MDR breast cancer cell line, MCF-7/MDR. Formulated MSNPs displayed a size of 50 nm with conjugation to polyethyleneimine-polyethylene glycol (PEI-PEG) copolymer. This conjugation protected the co-delivery of bound DTX and P-gp siRNA to the tumor site in MCF-7/MDR xenograft model. The effective biodistribution and reduced reticuloendothelial uptake, as a result of the MSNPs design, allowed Meng and coworkers to achieve an 8% enhanced permeability and retention effect at the tumor site. The co-delivery of both therapeutic agents resulted in synergistic inhibition of tumor growth *in vivo* as compared to free DTX or MSNPs loaded with either drug or siRNA alone. Multiple analysis of xenograft biopsies revealed significant P-gp knockdown at heterogeneous tumor sites. These regions correspond to the intracellular release of DTX and induced apoptosis. Meng and coworkers emphasized that the heterogeneity originates in the tumor microenvironment, which influences the vascular access, rather than heterogeneous P-gp expression in the MDR cells.¹²⁶ Similar to Ma et al., these data provide proof-of-principle testing for the use of a dual drug/siRNA loaded nanoparticles to overcome MDR in a xenograft model. This study also provided the first detailed analysis of the impact of heterogeneity in the tumor microenvironment on the efficacy of siRNA delivery *in vivo*.¹²⁶

MSNPs can have an array of multifunctional modular designs, suggesting that the next generation of nanoparticles will have multicomponent cargos that deliver their payload to target cells through the active recruitment of targeting ligands combined with biologically triggered responses that actuate molecular valves. The combination of molecular machines and increasingly complex and biomimetic supported lipid bilayers, -such as those derived from red blood cells, may allow unprecedented engineering of nanoparticle/cellular interactions and provide a universal platform for theranostics and personalized medicine.

Polymer-Drug Nano-Conjugates

Polymer-drug nano-conjugates-are the chemical conjugation of the therapeutic drug and polymer by a covalent bond. Polymer-drug nano-conjugates-have been widely explored for delivery of anticancer drugs for the treatment of various cancers.¹²⁹ One of the major advantages of polymer-drug nano-conjugates is the ability to escape filtration from the kidneys, resulting in increased blood circulation time. Increased blood circulation times allow for anticancer conjugates-to accumulate at the site of action, the tumor, by taking advantage of the EPR effect.¹²⁹ However, polymer-drug conjugates must also eventually be eliminated from the body to avoid any potential long term adverse side effects-the drug or polymer may elicit. Incorporating biodegradable systems allows for these conjugates, of a sufficient size, to-evade renal filtration-while allowing subsequent degradation and elimination from the body. These conjugates should have degradation rates slow enough to allow adequate biodistribution and accumulation at the site of action. The degradation of these conjugates should also result in the production of non-toxic degradation products that are eliminated from the body. A number of biologically degradable bonds have been described (Fig. 5(A)). The biodegradation of these conjugates usually occurs via hydrolysis, enzymatic cleavage, or reductive degradation. Some biodegradable polymers have been studied^{130, 131} and include-poly- α -amino acids such as poly(L-lysine),¹³² poly(L-glutamic acid),¹³³ and poly((N-hydroxyalkyl)glutamine)¹³⁴ as well as carbohydrate polymers such as dextrans,¹³⁵ hydroxyethylstarch (HES),¹³⁶ polysialic acid,¹³⁷ and the polyacetal Fleximer®.¹³⁸

OPAXIO™ (formerly branded XYOTAX) is a biodegradable polymer-drug nano-conjugate currently under phase III clinical development in the United States. OPAXIO™ is a conjugate of poly(L-glutamic acid) and the anticancer drug PTX.¹³⁹ The selection of poly(L-glutamic acid) was based on the biodegradation to L-glutamic acid which can then enter normal cellular metabolism. PTX was conjugated via an ester bond to the γ -carboxylic acid side chains of poly(L-glutamic acid). Due to the conjugation via the 2' hydroxyl of PTX, the conjugate is unable to bind tubulin and elicit a pharmacological response, rendering it inactive. In one particular example, the poly(L-glutamic acid) conjugate, having a molecular weight of 48 kDa and containing approximately 37% PTX by weight, - maintains water solubility. During preclinical investigation of this formulation, the conjugate demonstrated a higher maximum tolerated dose (MTD) and was more efficacious than PTX formulated in Cremophor EL/ethanol alone. Phase III clinical trials¹⁴⁰⁻¹⁴⁴ are still evaluating OPAXIO™ within prostate, breast, ovarian, colorectal, and lung cancer patients.

Biodegradable derivatives are being explored for more commonly used polymers such as PEG and HPMA copolymers. Biodegradable multi-arm PEGs containing ester bonds between PEG chains have entered clinical trials.¹⁴⁵ Research has also been done to see if biodegradable polymers consisting of small molecular weight PEG blocks can be linked together via enzymatically cleavable oligopeptide groups while linked to DOX.¹⁴⁶ Ulbrich et al. utilized a variety of approaches to synthesize biodegradable HPMA copolymer-drug conjugates. Such approaches include graft systems containing oligopeptide sequences and/or reductive disulfide bonds,¹⁴⁷ and the generation of biodegradable star HPMA copolymer-drug conjugates.¹⁴⁸ In a similar technique, poly-(amido amine) (PAMAM) dendrimers were modified with poly-HPMA grafts via enzymatically cleavable or reducible linkers. This allowed for degradation of the high molecular weight polymer. These star polymer conjugates displaying DOX showed prolonged blood circulation, increased tumor accumulation, and anti-tumor efficacy in lymphoma tumor bearing mice.¹⁴⁹

Biodegradable multiblock poly(HPMA) conjugates were also generated via a combination of RAFT polymerization and click chemistry.^{150, 151} The synthesis of multiblock poly(HPMA) was performed in three major steps (Fig. 5(B)). RAFT polymerization of HPMA was first performed using an enzyme-sensitive, Gly-Phe-Leu-Gly containing chain transfer agent with a terminal alkyne. Following polymerization, a post-polymer modification was performed to introduce a terminal azide, resulting in an α -alkyne, ω -azido-telechelic poly(HPMA). In the final step, a biodegradable multiblock poly(HPMA) was synthesized by click chemistry in the presence of a copper catalyst. It was shown that the end product, multiblock poly(HPMA), had a molecular weight of 291 kDa and a polydispersity index of 1.11. Upon incubation with model lysosomal enzymes, poly(HPMA) segments of similar molecular weights (42 kDa) were formulated.¹⁵¹ These results demonstrate how advances in chemistry (i.e., RAFT polymerization and click chemistry) can be utilized to synthesize newer biodegradable polymer-drug conjugates with well-defined physicochemical properties. The polymer-drug conjugate and its derivatives can then be implemented for the co-delivery of multiple drugs.

Wang et al. demonstrated the potential use of polymer-drug conjugates for combinatorial chemotherapy.¹⁵² Their research group combined the bioactivities of both oxaliplatin and demethylcantharidin (DMC) and co-delivered them via a polymer-drug conjugate system. It has been shown that oxaliplatin was released from the polymer-drug conjugate within cancer cell by reduction to attack nuclear DNA.¹⁵² At the same time, a dose of DMC was hydrolyzed which block DNA damage-induced defense mechanisms by serine/threonine phosphatase 2A inhibition. *In vitro* studies showed that the polymer-drug conjugate with dual modes of action displayed increased cytotoxicity against SKOV-3 ovarian cancer cells than that of free oxaliplatin and DMC. The enhanced cytotoxicity of this polymer-drug conjugate was attributed to the synergistic effect between oxaliplatin and DMC, as well as the effective intracellular internalization of the micelles observed by confocal laser scanning microscopy (CLSM) imaging.

Dendrimer Based Nanoparticles

Dendrimers are branched polymeric macromolecules forming a star-like structure. Dendrimers' unique structures allow conjugation of drugs to the surface, allowing for maximization of the potential of biological interactions. The synthesis of dendrimers can be done with a wide variety of chemistries, where the core, monomer units, and surface functionality determine the physiochemical characteristics.¹⁵³ The most important factor in formulating dendrimers for drug delivery applications is their biocompatibility. Other physiochemical properties to be considered are: solubility, surface group functionality, surface charge density, and stability of the dendrimers. Tomalia et al. first described the synthesis of PAMAM dendrimers in 1985.^{154, 155} Synthesis of dendrimers for each "generation" was performed in a step-wise fashion (Fig. 6(B)) resulting in dendrimers having precisely defined structures. As each synthetic step proceeds forward, increase in the generation resulted in a linear increase in radius and an exponential increase in surface groups.¹⁵⁶ For example, for the synthesis of PAMAM dendrimers an ethylenediamine core is first generated which is then followed by a subsequent half-generation addition by reaction with methyl acrylate. Ethylenediamine is used for the final and complete generation reaction step before PAMAM dendrimers are produced (Fig. 6(C)). This precision in synthetic production is one of the major advantages of dendrimers, as compared to most linear polymers. The end product of these reactions often yields mono-dispersed structures having polydispersity indices (Mw/Mn) of less than 1.05.¹⁵⁷ Another advantage dendrimers exhibit is the large number and density of functional groups displayed on their surface. These functional groups provides opportunities for conjugation of drugs,^{158, 159} targeting moieties,¹⁶⁰ imaging agents,¹⁶¹ etc. (Fig. 6(B)).

Much work with dendrimers focuses on their use for the encapsulation and formulation of drugs.¹⁶² Dendrimers often possess open cavities between adjacent branches of their hyper branched structure. These cavities allow for the encapsulation of drugs¹⁶³ and have been found to improve the solubility of poorly soluble drugs. In addition, drugs which have been formulated with dendrimers (physically mixing) have been investigated as both transdermal¹⁶⁴ and oral¹⁶⁵ delivery systems. It has also been investigated that dendrimers with positively charged surface functionalities, such as PAMAM and poly-(ethyleneimine) dendrimers, may act as gene carriers,¹⁶⁶ due to their ability to complex with negatively charged DNA.

The covalent attachment of drugs to dendrimers has been widely investigated.^{160–164} Many chemotherapeutic agents have been attached to the surface of dendrimers to help increase the drug's aqueous solubility and to provide specific delivery to tumor tissues. Multifunctional drug delivery platforms have been investigated that utilize dendrimers conjugated with imaging agents, drugs, and targeting moieties.¹⁶⁰ As described earlier, the synthesis of such conjugates begins with the ethylene diamine initiator core accompanied by repeated addition of methyl acrylate followed by subsequent methyl ester condensation with ethylene diamine to produce increasing generation PAMAM dendrimers (Fig. 6(C)). The resulting generation 5 (G5) dendrimer showed 128 primary amino groups on its surface. This will provide ample opportunity for further modification of the dendrimer's surface. In an effort to improve biocompatibility, partial acetylation of the primary amino groups has

been conducted in order to reduce the positive surface charge. The reaction was then followed by formation of a thiourea bond with fluorescein isothiocyanate (FITC) to enable *in vitro* imaging.¹⁶¹ PAMAM dendrimers were conjugated with folic acid, a targeting moiety, through the reaction of surface primary amines using an activated ester derivative of folic acid. The remaining primary amines were transformed into hydroxyl groups using a glycidolation reaction. Following this reaction, the chemotherapeutic agent, methotrexate, was attached by the formation of an ester bond. The characterization of the formulated dendrimers were carried out by size exclusion chromatography coupled with multiangle laser light scattering, nuclear magnetic resonance, and UV spectrometry. These methods helped to determine the content of the drug, fluorescent probes, and targeting agent.¹⁶⁷ *In vitro* analysis using confocal images revealed an increase in cellular uptake of tri-functional dendrimers when exposed to folic acid receptor expressing cells as compared to the untargeted controls.¹⁶⁷ *In vivo* evaluation was then performed in CB-17 severe combined immunodeficiency (SCID) mice bearing human KB cancer cell (over-expressing folic acid receptor) xenografts. A decrease in tumor growth and increase in survival were observed in mice treated with the tri-functional dendrimer conjugate for up to 84 days as compared to mice treated with equivalent doses of free methotrexate.¹⁶⁸ These results demonstrate that dendrimer-drug conjugates can be synthesized and utilized as a multifunctional drug delivery platform.

There have been increased interests for the use of dendrimers as a potential drug carrier to facilitate drug delivery across biological membranes. These biological membranes include skin (transdermal),^{164,169} intestinal epithelial,^{170,171} human placenta,¹⁷² and the blood-brain barrier.^{173–175} Biodegradable dendrimers,¹⁴⁹ glycodendrimers,^{176,177} amphiphilic dendrimers,^{178–180} and asymmetric dendrimers¹⁸¹ were also investigated as potential drug carriers. Dendrimers formulated as multifunctional drug delivery systems that are functionalized with chemotherapeutic agents, targeting moieties, and imaging agents have been the subject of several recent reviews.^{164,182,183}

There have been studies comparing dendritic carriers to more traditional polymeric carriers such as HPMA copolymers and PEG. In one study, branched and linear HPMA copolymer-DOX conjugates were evaluated for their anticancer activity against lymphoma and colorectal carcinoma cell lines. Results showed that branched HPMA copolymer-DOX conjugates demonstrated a 3 to 11 fold increase in anticancer activity as compared to linear HPMA copolymer-DOX.¹⁸⁴ Another study compared the anticancer activity of G4-PTX dendrimers and PEG-PTX. G4-PTX demonstrated enhanced *in vitro* anticancer activity against breast cancer cell lines as compared to free PTX. However, PEG-PTX showed significantly reduced anticancer activity as compared to free PTX.¹⁸⁵ These results demonstrate the unique potential of dendritic polymeric architectures as drug carriers.

Kaneshiro et al. have recently developed a new class of dendrimers, poly(l-lysine) dendrimers with a silsesquioxane cubic core (nanoglobules). These dendrimers have highly functionalized surfaces for attachment of various moieties along with compact globular and well-defined structures. These dendrimers can be used as versatile carriers for biomedical applications. In this study, a generation-3 (G3) nanoglobular dendrimer was used to conjugate a peptide c(RGDfK) with a PEG spacer for the co-delivery of DOX and siRNA.

DOX was coupled to the RGD targeted nanoglobule via a degradable disulfide spacer to give G3-[PEG-RGD]-[DOX]. Results demonstrated that G3-[PEG-RGD]-[DOX] dendrimers had higher cytotoxicity as compared to free DOX at high doses in glioblastoma U87 cancer cells. For co-delivery, G3-[PEG-RGD]-[DOX] was further complexed with siRNA. These co-loaded dendrimers were internalized by U87 cancer cells as shown by confocal microscopy. The co-delivery of siRNA and DOX dendrimer complexes having the targeted conjugate resulted in 50% gene silencing efficiency in U87-Luc cancer cells as compared to those of control conjugates G3-[PEG-RGD] and G3-[DOX] with approximately 25% gene silencing efficiency for each. These nanoglobules show potential as a carrier for the co-delivery of nucleic acids and chemotherapeutic agents.

It has been shown that microRNAs are deregulated in different types of cancer with miR-21 being a key player in the majority of cancers. Previous findings showed that the down-regulation of miR-21 in glioblastoma cancer cells leads to the repression of cell growth followed by increased cellular apoptosis and cell-cycle arrest. Taking advantage of these findings, Ren et al. used PAMAM dendrimers as a carrier to co-deliver antisense-miR-21 oligonucleotide (as-miR-21) and 5-fluorouracil (5-FU) to human glioblastoma cancer cells for enhancement of cytotoxicity in 5-FU antisense therapy. MTT assay was used to analyze the inhibitory effect toward brain tumors and to quantify the measurements of cell apoptosis and invasion using the U251 human brain glioma cell line. PAMAM dendrimers were formulated and co-loaded with both therapeutic agents while still maintaining a complex smaller than 100 nm in diameter. The co-delivery of as-miR-21 significantly improved the cytotoxicity of 5-FU with an 80% reduction in cell viability with increased apoptosis of U251 cells. The migration ability of the tumor cells was also decreased in the transwell assay. These results suggest that this co-delivery system will have important clinical applications for the treatment of miR-21-over expressing glioblastoma.

Clinical translation of dendrimers, used as drug delivery based systems, have been limited mainly due to the concerns over their biocompatibility and toxicity. Some studies have shown that dendrimers exhibit a high affinity for metal ions, bile salts, lipids, nucleic acids, and proteins, that may disrupt biological processes and leading to toxicity.¹⁸⁶ This molecular toxicity primarily depends on their surface functionalization. Dendrimers having a higher positive surface charge (~30+ mV) have been shown to elicit toxicities *in vitro*^{187,188} and *in vivo*.^{189,190} Most work involving dendrimers currently focuses on surface modification to design more biocompatible dendrimers to help increase biocompatibility. In addition, the difficulty and expense associated with dendrimer synthesis needs to be addressed before clinical translation can be achieved.

Miscellaneous Multifunctional Nanoparticles

Other multifunctional nanoparticles containing more than one therapeutic cargo for combinatorial chemotherapy include-oil nanoemulsions,^{191, 192} and iron oxide nanoparticle.^{42, 193} In oil emulsions, the hydrophobic drug mixture is homogenized along with oil. The drug will be loaded in the oil phase as a result of the nanoemulsion. The inorganic cores of iron oxide particles are functionalized with additional polymeric matrices to aid in carrying multiple drug payloads for combination chemotherapy. These

miscellaneous nanoparticles are in the development stage with cytotoxicity studies conducted to help validate them as potential drug carriers in the treatment of various cancers and diseases.

Taratula et al. developed, synthesized, and tested multifunctional nanostructured lipid nanocarrier-based system (NLCS) for the delivery of DOX or PTX and siRNA directly into the lungs by inhalation.¹⁹⁴ The formulated system contained-nanostructured lipid carriers (NLC); a DOX or PTX anticancer drug; siRNA targeted to MRP1 mRNA as a suppressor of pump drug resistance; siRNA targeted to BCL2 mRNA as a suppressor of nonpump cellular resistance and a modified synthetic analog of luteinizing hormone-releasing hormone (LHRH) as a targeting moiety specific to overexpressed receptors in the plasma membrane of lung cancer cells. Dynamic light scattering and atomic force microscopy studies revealed drug loaded NLC had a particle size of 110 ± 20 nm in diameter with a polydispersity index of 0.4. The NLCS formulations were tested *in vitro* using human lung cancer cells and *in vivo* utilizing mouse ortho-topic model of human lung cancer. Signs of cytotoxicity were seen against lung cancer cell lines for NLC displaying a positive charge (+60.3 mV). Cell viability decreased by approximately 20% when incubated with NLC. NLC-siRNA complexes showed a decrease in zeta potential, +45.5 mV, while caging with PEG almost completely eliminated the charge of formulated nanoparticles. In contrast, nanoparticles containing the drug were highly toxic *in vitro*. Data revealed that PTX incorporated into tumor-targeted nanoparticles increased toxicity to cancer cells overexpressing LHRH receptors by 7.5-fold. Simultaneous suppression of BCL2 and MRP1 proteins by siRNA led to the further enhancement of *in vitro* cytotoxicity. In fact, cytotoxicity of LHRH-NLC-PTX-siRNAs (MRP1 and BCL2) complexes was 120 and 16 times higher when compared with free drug and LHRH-NLC-PTX, respectively. It was found that in untreated animals, lung tumor progressively grew reaching 117.1 ± 18.7 mm³. Mice with lung cancer underwent inhalation treatment, 8 times within 4 weeks. -LHRH-NLC alone with no anticancer drug did not change the progression of the lung tumor, leading to an increase in volume up to 113.6 ± 1.5 mm³. Conjugated PTX to the NLC targeted to tumor cells by LHRH and local delivery by inhalation significantly enhanced antitumor activity of PTX itself. After treatment with LHRH-NLC-PTX, the tumor size decreased at the end of the experiment down to 20.8 ± 4.4 mm³. Finally, the suppression of both pump and nonpump cellular drug resistance in lung cancer cells led to almost complete regression of the tumor. In fact, the tumor size in animals treated with LHRH-NLC-TAX-siRNAs (MRP1 and BCL2) shrank down to 2.6 ± 3.0 mm³. These findings indicate almost complete disappearance of lung tumors in experimental animals. The data obtained demonstrated high efficiency of proposed NLCS for tumor-targeted local delivery by inhalation of anticancer drugs and mixture of siRNAs specifically to lung cancer cells and, as a result, efficient suppression of tumor growth and prevention of adverse side effects on healthy organs.

Yu et al. formulated cationic solid lipid nanoparticles (cSLN) co-delivering PTX and siRNA.¹⁹⁵ Emulsification solidification methods were used to prepare 1,2-dioleoyl-sn-glycero-3-ethylphosphocholine-based cSLN. PTX-loaded cSLN (PcSLN) did not significantly differ from those of empty cSLN without PTX (EcSLN), 140 nm and 151 nm, respectively. The use of cSLN increased cellular uptake of fluorescent dsRNA by 34.8-fold in human epithelial carcinoma KB cells, with PcSLN complexed to fluorescence-labeled

dsRNA promoting the greatest uptake as compared to cells treated with naked fluorescent dsRNA.¹⁹⁵ Specifically, $2.8 \pm 0.3\%$ of KB cells were fluorescence-positive after treatment with naked dsRNA, whereas $96.6 \pm 1.0\%$ and $91.3 \pm 1.2\%$ of cells were fluorescence-positive after the 4 h treatment with EcSLN and PcSLN, respectively. The co-delivery of therapeutic siRNA, human MCL1-specific siRNA (siMCL1) was complexed with PcSLN with luciferase-specific siRNA (siGL2) complexed to EcSLN or PcSLN being used as a control. MCL1 mRNA levels were significantly reduced by 50% in KB cells treated with siMCL1 complexed to PcSLN, but not in groups treated with siMCL1 alone or siGL2 complexed to PcSLN. *In vitro* results showed that siMCL1 complexed to PcSLN exerted the greatest anticancer effects in KB cells, followed by siMCL1 complexed to EcSLN, siGL2 complexed to PcSLN, PTX alone, and siMCL1 alone. *In vivo* studies using KB cell-xenografted mice, intratumoral injection of PcSLN complexed to siMCL1 significantly reduced the growth of tumors. Control mice treated with saline had an average tumor volume of $1373.1 \pm 241.0 \text{ mm}^3$ on day 16 after inoculation. Intratumoral administration of siMCL1 complexed to EcSLN plus free PTX decreased tumor volume to $714.2 \pm 230.0 \text{ mm}^3$. The highest inhibition of tumor growth was observed following intratumoral co-delivery of PTX and siMCL1 using PcSLN, decreasing tumor volume to $172.0 \pm 73.7 \text{ mm}^3$. Taken together, these results demonstrate the potential of cSLN for the development of co-delivery systems of various lipophilic anticancer drugs and therapeutic siRNAs.

TUMOR TARGETED NANOPARTICLES IN COMBINATORIAL CHEMOTHERAPEUTICS

The modification of nanoparticles with ligands has been widely accepted to enhance the therapeutic efficacy of its payloads while reducing adverse side effects relative to conventional therapeutics.¹⁹⁶ Ligand-conjugated nanoparticles not only have the ability to actively target specific cells but may also outperform first generation, non-targeted nanosystems. The necessity of targeted delivery depends on various-factors (e.g., disease, drugs and the delivery vehicle); a vast array of important benefits have been demonstrated.^{3, 197–199} It has been shown-in cancer therapy that the presence of targeting ligands enhances the cellular uptake of nanoparticles through receptor mediated endocytosis even though the physiochemical properties of the nanoparticle determines its accumulation at the site of action.^{196, 197} As a result, higher intracellular drug concentration with increased therapeutic activity is observed, –as (?) bioactive macromolecules, such as DNA and siRNA, require intracellular delivery for bioactivity.¹⁹⁶ Nanoparticle localization for endothelial targeting in cardiovascular diseases or immunological tissue targeting uses ligand-receptor interactions rather than the EPR.¹⁹⁸ Ligand-mediated targeting is also of importance for the transcytosis of nanodrugs across endothelial and epithelial barriers (i.e., blood-brain barrier).¹⁹⁹ MDR have also been combated using targeted nanoparticles.³ Also, targeted nanoparticles with a long systemic circulation may be able to locate and destroy cancers-cells that have metastasized elsewhere in the body. The clinical translation of targeted nanoparticles for treatment-has been slower with four-nanoparticle systems now in phase I/II clinical trials.³ The main barrier for clinical translation of these formulation systems is the complexity behind the manufacturing of targeted nanoparticles. The fabrication of targeted nanoparticles requires multiple steps such as-ligand coupling/insertion, purification and

low DTX versus cisplatin ratio HTCP NPs. The HTCP NPs showed a pH-sensitive release for both anticancer drugs. *In vitro* analysis was conducted using SK-BR-3 human breast adenocarcinoma and NIH3T3 mouse embryonic fibroblast cell lines to evaluate the therapeutic effects of HTCP NPs compared with Taxotere[®] and cisplatin alone. The HTCP NPs formulations of high, moderate and low DTX versus cisplatin ratios were analyzed with HTCP NPs of high DTX versus cisplatin ratio having the highest efficacy against selected cell lines. Using herceptin as a targeting ligand for HER2 overexpression, the value of targeted HTCP NPs demonstrated a lower IC₅₀ DTX (90.0201+ $\mu\text{g}/\text{mL}$) + cisplatin (0.00780 $\mu\text{g}/\text{mL}$) + herceptin (0.1629 $\mu\text{g}/\text{mL}$) against SK-BR-3 cells (having high HER2 overexpression), than that of IC₅₀ value of DTX (0.225+ $\mu\text{g}/\text{mL}$) + cisplatin (0.0875 $\mu\text{g}/\text{mL}$) + herceptin (1.827 $\mu\text{g}/\text{mL}$) against NIH3T3 cells (low HER2 overexpression), after 24 h incubation.²⁰⁶ The similar approach of TPGS prodrug nanoparticles can also be applied for targeted co-delivery of other hydrophilic and hydrophobic drugs.

Similarly, micellar nanoparticles self-assembled from biodegradable and amphiphilic copolymer poly-P-(MDS-co-CES) were recently developed by Lee et al.¹¹⁸ These cationic micellar nanoparticles have been shown to deliver small molecular drugs and bio-macromolecules such as genes and functional proteins individually or simultaneously into various types of cells.¹¹⁸ In this study, the cationic micellar nanoparticles co-delivered PTX and herceptin to achieve a targeted delivery of PTX to HER2/neu-overexpressing human breast cancer cells, thereby enhancing cytotoxicity through synergistic activities. Formulated PTX-loaded nanoparticles had an average size less than 120 nm with a zeta potential of about 60 mV. The surface of drug-loaded nanoparticles were then complexed with Herceptin to target HER2 overexpressed cancer breast cancer cells. Under physiological conditions drug-loaded herceptin complex remained stable displaying an average size of around 200 nm. BioPorter, a commercially available lipid-based protein carrier, was compared against formulated PTX-loaded Herceptin complexed nanoparticles. Results showed that the nanoparticles delivered Herceptin more efficiently than BioPorter and displayed an enhanced anticancer effectiveness. Treatments were repeated twice-daily with Herceptin formulations displaying significantly enhanced cytotoxicity in HER2-overexpressing breast cancer cells when compared against single drug-alone treatment. Further investigation was done-to evaluate the anticancer effects of co-delivered PTX-loaded Herceptin complex nanoparticles against human breast cancer cell lines with varying HER2 expressions levels, namely, MCF7, T47D, and BT474. It was observed that efficacy of co-delivered PTX and Herceptin was dependent on the HER2 expression levels. Confocal microscopy images revealed higher cellular uptake of formulated nanoparticles in HER2-overexpressing BT474 cancer cell lines as compared to HEK293 cells which express no HER2 receptors. Targeting ability of this co-delivery system was demonstrated through confocal imaging studies. This formulation may have important clinical implications against HER2-overexpressing breast cancers in the near future.

Hadjipanayis et al. co-delivered an anti-epidermal growth factor receptor (EGFR) deletion mutant antibody fabricated to amphiphilic triblock copolymer-coated iron oxide nanoparticles (IONPs) for targeted imaging and therapeutic treatment of glioblastoma.²⁰⁷ It has been shown that the EGFR variant III (EGFRvIII) deletion mutant is not expressed in normal brain tissue but is specifically expressed in malignant glioma cells. A polyclonal

rabbit antibody was developed for the synthesis of the 14-amino-acid fusion junction sequence (EGFRvIIIAb) for the selective binding of the mutant EGFR protein. The purified EGFRvIIIAb was then covalently conjugated to the amphiphilic triblock copolymer-coated iron oxide nanoparticles.²⁰⁸ The final formulation yielded a stable glioblastoma-targeting theranostic agent (EGFRvIIIAb-IONPs) (Fig. 7(A)). Convection enhanced delivery (CED), a continuous method of injection under a pressure gradient formed by the fluid containing the therapeutic agent, was used to effectively deliver EGFRvIIIAb-IONPs to the intratumoral and peritumoral regions in the brain.²⁰⁹ This CED method helps to prevent nanoparticles from becoming trapped in the spleen, liver, or within circulating macrophages after I.V. administration while also bypassing the blood-brain barrier. CED is a method that is therefore used increasingly in the distribution of therapeutic agents for the treatment of malignant gliomas.^{210–212} Human U87ΔEGFRvIII glioma model tumors were implanted in athymic nude mice were used to test the accuracy of MRI monitoring and the efficacy of antitumor effects of EGFRvIII-IONPs. There was a decrease in the T2-weighted MRI signal after CED of EGFRvIII-IONPs, with a total area signal drop being observed 7 days after CED treatment, indicating the nanoparticles had dispersed from the area. Animals that underwent CED treatment with either EFRvIIIAb or EGFRvIIIAb-IONPs had a significantly higher rate of survival, which may be a result of inhibition of EGFR-phosphorylation, whereas the CED untreated control or IONPs groups did not display an increase in survival rate (Figs. 7(B)–(F)). These results indicated that the MRI-guided CED of multifunctional EG-FRvIIIAb-IONPs results in the specific targeting of devastating brain tumors and may have potential for clinical applications.

Wei and Gao et al. used the similar targeted imaging and therapy method for delivery of multifunctional nanoparticles in the treatment of prostate cancer. A single chain anti-prostate stem cell antigen (PSCA) antibody (scAbP-SCA) is used as a specific ‘address tag’ for the targeted therapy and imaging of prostate.²¹³ The prostate stem cell antigen is a prostate-specific glycosyl phosphatidyl-inositol-anchored glycoprotein that is marginally expressed in normal prostate and overexpressed in prostate cancer tissues.²¹⁴ The multifunctional nanoparticles were prepared by cleaving intact AbPSCA with mercaptoethylamine (MEA), then linked to maleimide-PEG-carboxyl (MAL-PEG-COOH) with covalent conjugation to multifunctional polymeric vesicles formed by entrapping SPIO nanoparticles and DTX by amine-terminated PLGA. The final formulation yielded scAbP-SCA-DTX/SPIO-NPs having a size around 147 nm with SPIOs and DTX in the polymer matrix around 23 wt% and 6.02 wt%, respectively. A higher drug encapsulation efficiency was obtained by partitioning DTX into the oleic acid and oleylamine shell of the SPIOs, where it acted as a drug reservoir, giving a triphasic drug release pattern versus the common two-phase kinetic release pattern, which-includes burst effects of an initial release stage, as observed in vesicles without SPIOs. *In vitro* cytotoxicity studies revealed the anti-proliferative effects of the formulated multifunctional nanoparticles towards prostate cancer cell lines with an overall decrease in 80% cell viability as compared to non-treated cells. PC3 cells incubated with scAbPSCA-DTX/SPIO-NPs produced distinct darkened regions in the T2-weighted MRI as compared to polymeric vesicles without scAbPSCA or Endorem® (a commercial contrast, Guerbet, France).²¹³ These results demonstrated that the multifunctional scAbP-SCA-DTX/SPIO-

NPs can be used as MRI contrast agents for prostate-targeted imaging and real-time monitoring of therapeutic effects.

In a similar approach, Chen and Shuai et al. used scAb as a targeting ligand in the design of multifunctional nanoparticles.²¹⁵ Chen and Shuai et al. formulated a CD3 single chain antibody (scAbCD3) functionalized non-viral polymeric vector for gene delivery to *T*-cells.²¹⁵ As done by Wei et al., the polymeric vector was first complexed with SPIONs, which was then used to condense the therapeutic agent, a gene plasmid, as a dual-purpose probe (MRI contrast agent and T lymphocyte targeted gene delivery). -The engagement of *T*-cell antigen receptors, such as the CD3 receptors found on mature *T*-cells, may lead to the initiation of anergy. These receptors can also potentially mediate targeted gene delivery to *T*-cells. Therefore, scAbCD3-conjugated, poly(ethylene glycol)-grafted polyethyleneimine (PEG-g-PEI)-coated SPIONs (scAbCD3-PEG-g-PEI-SPION) were synthesized using bio-conjugation and ligand exchange methods.²¹⁶ The targeting multifunctional polyplexes (scAbCD3-PEG-g-PEI-SPION/DNA) then incorporated a diacylglycerol kinase (*DGK α*) gene that may potentially impair *T*-cell receptor (TCR) signaling, consequently resulting in the anergy of *T* cells.^{217, 218} T2-weighted MRI revealed that scAbCD3-immobilized polyplexes were efficiently taken up by target *T*-cells (HB8521) through CD3 receptor-mediated endocytosis. Flow cytometric analysis indicated high gene transfection efficiency of the targeted polyplexes (81.95%) as compared to polyplexes without scAbCD3 functionalization (7.39%). After *DGK α* genes were transferred into HB8521 cells, lower levels of cell proliferation and IL-2 expression were observed. This is mainly due to the response to immune stimulation in cells transfected with the targeted polyplexes-as compared to cells that hadn't been pre-transfected during stimulation. These data demonstrate that MRI-visible targeted nanoparticles can dampen TCR-induced diacylglycerol signaling.

Immunoliposomes (antibody-directed liposomes) are common pharmaceutical carriers for targeted drug delivery having the ability to encapsulate both hydrophilic and hydrophobic therapeutic agents using simple preparation techniques.²¹⁹ *In vivo* lung cancer targeted immunoliposomes were developed by Wu et al. using an anti-c-Met antibody.²¹⁹ It has been shown that c-Met, the receptor for hepatocyte growth factor (HGF), is abundantly expressed in 25% of non-small cell lung cancer patients. The activation of this protein has been reported to trigger cancer cell proliferation, migration, and invasion.^{220, 221} Wu et al. prepared individual targeted therapeutic vehicles and imaging probes. The anti-c-Met single chain variable fragment (scFv) antibody was first identified by phage display (Ms20, Kd value; 9.14 nM). Cysteine residues were then fused for a site-direct conjugation with maleimide-modified PEG-terminated liposomal DOX. The final formulation resulted in Ms20-conjugated liposomal DOX (Ms20-LD). Their study also utilized inorganic quantum dots (QD) as a targeted diagnostic tool (Ms20-QD). Due to the fact that c-Met expression appears in angiogenic endothelium as well as in tumor cells,²²² dual targeting properties, such as inhibition of tumor growth and prevention of angiogenesis, were observed in an Ms20-LD-injected H460-bearing SCID mouse xenograft model. It was also shown that Ms20-LD improved the chemotherapeutic drug delivery by inhibiting c-Met-transient or c-Met-constitutive activation of cancer cells. This study showed the *in vivo* tumor homing of

Ms20-QD, and it supported that Ms20-provides selective delivery to solid tumors. –Thus, Ms20 shows potential as a lung tumor targeted theranostic agent.

Peptide Based Targeted Nanoparticles

Peptides are attractive targeting molecules due to their small size, low immunogenicity, ease of manufacture and -lower cost.²²³ There are several methods for identifying peptide-based targeting ligands. One of the most common methods is obtained from the binding regions of a protein of interest. The phage display techniques may also be used in identifying peptide-targeting ligands. During a phage display screen, the bacteriophages–present a variety of targeting peptide sequences in a phage display library (~1011 different sequences), with the target peptides being selected by using a binding assay.²²⁴ The cyclic peptide, Cilengitide, has an integrin binding affinity and is currently in phase II clinical trials for the treatment of non-small cell lung cancer and pancreatic cancer.²²¹ Phase III clinical trials for the treatment of advanced solid tumors and non-Hodgkin's lymphoma-have also commenced for an Adnectin for human VEGF receptor 2 (Angiocept), a 40 amino acid thermostable and protease-stable oligopeptide. Peptides have limitations as well such as a low target affinity and susceptibility to proteolytic cleavage. These issues may be improved by displaying the peptides multivalently or using D-amino acids during the synthesis process.²²⁴ Recently, peptides have been used to fabricate multifunctional nanoparticles for targeted cancer imaging and therapy.

Medarova et al. specifically designed a breast tumor-targeted nanoparticle that would-deliver siRNA to human breast cancer while simultaneously allowing the siRNA delivery process through noninvasive techniques.²²⁵ The co-loaded-nanoparticles were made of SPIONs for MRI monitoring, and loaded with Cy5.5 fluorescence dye for near-infrared (IR) optical imaging, and siRNA to target the tumor-specific anti-apoptotic gene BIRC5. The magnetic iron oxide nanoparticles have been used extensively in combination with optical fluorescent dyes as multimodal imaging probes for the benefits of rapid screening and higher sensitivity. The tumor-associated under-glycosylated mucin-1 (uMUC-1) antigen has been shown to be overexpressed in >90% of breast cancers and also in >50% of all cancers in humans.²²⁶ Therefore, researchers have decorated nanoparticles with uMUC-1-targeting EPPT synthetic peptides for selective tumor targeting of breast cancer. Superparamagnetic iron oxide nanoparticles with functionalized amine groups are cross-linked with a dextran coating (MN) with Cy5.5 dye conjugated to its surface to produce MN-Cy5.5 nanoparticles (Fig. 8(A)). A heterofunctional cross-linker, *N*-succinimidyl 3-(2-pyridyldithio) propionate (SPDP), was then used to couple the thiol-modified, FITC-labeled EPPT peptides and siRNA to the MN-Cy5.5 nanoparticle. The final multifunctional co-loaded formulation, MN-EPPT-siBIRC5, exhibited super-paramagnetic and fluorescence properties. *In vivo* studies used mice with BT-20 tumors treated i.v. with the final formulation. The tumors were clearly imaged using the nanoparticles, as verified simultaneously by T2 MRI and near-IR optical imaging (Fig. 8(B)). It was shown that administration of the multifunctional nanoparticles once a week over a two-week period induced considerable levels of necrosis and apoptosis of the tumors themselves. This is a direct result of the siBIRC5-mediated inhibition of the anti-apoptotic survivin proto-oncogene which–resulted in a significant decrease in tumor growth rate (Fig. 8(C)). The tumor-targeted multifunctional imaging-capable nanoparticle

displays the potential of MRI-guided tumor treatment. This application, along with other MRI-guided tumor treatments described, can be used to quantify changes in the tumor volume over the treatment schedule as well as guide selection of an optimal treatment schedule.

Liu et al. evaluated porous silicon nanoparticles (PSi-NPs) as a potential carrier in multi-drug delivery for the co-loading of the hydrophobic drug indomethacin and the hydrophilic human peptide YY3-36 (PYY3-36).²²⁷ Their study showed that the sequential loading of these two drugs into PSi-NPs enhanced the drug release rate of each drug and also their amount permeated across Caco-2 and Caco-2/HT29 cell monolayers.²²⁷ Results showed that regardless of the loading approach used, dual or single loading into PSi-NPs, drug permeation profiles were in good correlation with the drug release behaviour. Permeation studies helped to indicate the critical role of the mucus intestinal layer and the paracellular resistance in the permeation of the therapeutic agents across the intestinal wall. It was also observed that the loading PYY3-36 greatly improved the cytocompatibility of the PSi-NPs. Conformational analysis revealed that the PYY3-36 still displayed biological activity after release from PSi-NPs and permeation across the intestinal cell monolayers. These results are the first to demonstrate the co-loading potential of PSi-NPs for simultaneous multi-drug delivery of both hydrophobic and hydrophilic therapeutic compounds.

Li et al. have reported that tetrandrine (Tet) effectively increases the stability of PTX-loaded nanoparticles when Tet is co-encapsulated with PTX into mPEG-PCL nanoparticles.²²⁸ Their study demonstrated that the synergistic antitumor effect of Tet and PTX against gastric cancer cells-provided the basis of co-administration of Tet and PTX using nanoparticles. It has been reported that the cellular chemo-resistance to PTX correlates with intracellular antioxidant capacity.²²⁸ Therefore, the depletion of cellular antioxidant capacity could enhance the cytotoxicity of PTX. Tet effectively induces intracellular ROS production.²²⁸ Their study provides a novel therapeutic strategy-based on “oxidation therapy” that it could amplify antitumor effects of PTX by employing Tet as a pro-oxidant. It was shown that more intracellular Tet accumulation by endocytosis of PTX/Tet-NPs than equivalent doses of free drug lead to more intracellular ROS induction, which efficiently enhanced the cytotoxicity of PTX through the sequential inhibition of ROS-dependent Akt pathways along with the activation of apoptotic pathways. The tumor inhibition is a result of synergistic action and mediated superior cytotoxicity of PTX/Tet-NPs over free drug. The preliminary results suggest that co-delivery of PTX and Tet via nanoparticles provided a novel therapeutic strategy based on “oxidation therapy” against gastric cancer and may be applied to other nanoparticle applications.

Taking advantage of the acidic extracellular tumor microenvironment (pH 5.8–7.1) may provide another strategy for increasing tumor selectivity. The acidic conditions around the tumor which-are caused by the hypoxic metabolic state, can provide a triggering signal for cancer-targeted drug delivery of nanoparticles.^{229–231} Zhang et al. designed a glioma targeting pH-sensitive siRNA nanovector using Caltex (CTX) based-on this strategy.²³² A multifunctional iron oxide magnetic nanoparticle was coated with various types of functional molecules; the primary amine group-blocked polyethyleneimine (PEI) acting as the pH-sensitive layer, siRNA as a therapeutic payload with CTX as a tumor targeting

ligand.²³² Citra-conic anhydride (2-methylmaleic anhydride) was reacted with the primary amine group of PEI, providing a terminal carboxylate, which could then be hydrolyzed under acidic conditions. Under acidic conditions, the reversible charge conversion from positive to negative in a pH-sensitive manner may help in reducing the cytotoxicity of PEI while minimizing nonspecific cellular up-take during physiological pH conditions.^{229, 233} The nanovectors were then synthesized using iron oxide nanoparticles with amine-functionalized previously coated with amine-terminated PEG. These primary amine groups were then reacted with Trauts reagent, providing thiol-modified NPs. Amine groups of PEI that remained unreacted after the citra-conylation reaction were activated with SPDP for conjugation onto the surface of the NPs. The formulation, pH-sensitive PEI-coated NPs, showed negligible cytotoxicity at pH 7.4 as a result of surface-exposed carboxylates on the NPs. However, cytotoxicity was triggered under acidic conditions where the NPs surface charge increased due to de-blocking of the primary amine groups and protonation of amine groups remaining in the PEI. Further conjugation with thiol-modified CTX and siRNA using succinimidyl ester-PEG-maleimide (NHS-PEG-MAL) linkages was done to test the targeted delivery and therapeutic properties of the NPs. *In vitro* analysis of C6 cells using MRI scans incubated with NPs-PEI-siRNA-CTX displayed higher intracellular up-take than that of NP-PEI-siRNA, indicating that the presence of CTX on the surfaces of the NPs assisted in the cellular internalization of the nanovectors themselves. CTX-conjugated NPs also mediated selectivity in gene silencing effects. -Cells incubated with NP-PEI-siRNA-CTX at pH 6.2 showed a significant reduction in GFP gene expression as compared to gene expression almost unchanged in cells treated with the same nanovector at pH 7.4. These results suggest that the nanovector pH-based system shows a good safety profile and may potentially be used as a brain tumor targeted theranostic agent in future studies.

Nanoporous silica shows potential as an attractive drug delivery system due to -its high surface area and binding capacity for therapeutic and diagnostic agents as compared to liposomes of similar size. Nanoporous silica cores easily load multicomponent cargos and therefore produce nanocarriers that can potentially be used for targeted multicomponent delivery of therapeutic agents. Ashley et al. synergistically combined the features of mesoporous silica particles and liposomes by developing porous silica nanoparticle-supported lipid bilayers (protocells) approximately 100–150 nm in diameter (Fig. 9). The combination of these two distinct carriers helped to address the multiple challenges of targeted delivery.²³⁴ An SP94-targeted peptide was then conjugated to the protocells. The SP94 peptide specifically binds to human hepatocellular carcinoma. Protocells were further conjugated with a histidine-rich fusogenic peptide which assists in endosomal escape once administered and also cytosolic dispersion of the encapsulated cargos. It was observed that the nanoporous support resulted in improved stability and enhanced lateral bilayer fluidity as compared to both liposomes and non-porous particles. As a result, it promoted multivalent interactions between the protocell and the target cancer cells while using only a minimal number of targeting peptides through peptide recruitment to the cell surface.²³⁴ A 1000-fold higher loading capacity of the drug DTX was observed in protocells due to their high surface area and porosity of their nanoporous cores when compared to liposomes of similar size. Protocells' unique properties help to solve the problem of achieving higher targeting specificity with enhanced cytotoxicity against the target cancer cells while sparing normal

healthy cells. Viability tests showed that protocells loaded with the therapeutic agent DTX maintained a 90% normal hepatocyte while killing over 97% MDR1+ hepatocellular carcinoma (Hep3B).²³⁴ Results also showed that protocells without fluidity on the surface or DTX loaded liposomes, were less effective at killing Hep3B cells while showing high cytotoxicity against non-cancerous cell lines. Protocells loaded with DTX demonstrated targeted delivery while sparing healthy cells as compared with free drug and DTX-loaded liposomes. The combination of two nanocarriers for a targeted multicomponent delivery of therapeutic agents shows great promise in overcoming loading capacity of drugs with increased therapeutic efficacy against target cancer cells.

As previously described, the combining of two different functional nanoparticles which communicate with one another may be constructed to target a specific disease. Bhatia et al. designed such a nanosystem in which they used ‘signaling’ modules (gold nanorods, NRs, or tumor-targeted tissue factor, tTF) as tumor-activating agents for selective delivery and ‘receiving’ nanoparticles (magneto-fluorescent iron oxide nanoworms, NWs, or DOX-loaded liposomes, LPs) for targeted imaging or therapeutic agents (Fig. 10(A)).³⁰ These NWs are elongated nanostructures formed by the assembly of iron oxide cores that exhibit strong magnetic properties and efficient tumor targeting.²³⁵ The multifunctional nanosystem contained two ‘signaling’ modules which activated the coagulation cascade in tumors, broadcasting the tumor’s location to receivers in circulation (Fig. 10(B)). External electromagnetic energy was converted into heat by NRs in circulation. The NRs passively target tumors and locally disrupt tumor vessels using the heat generated. Coagulation was induced upon the binding of the tTF to the angiogenic $\alpha v \beta 3$ receptors. Coagulation regions were then targeted by the receiving nanoparticles. Peptide substrates were then derivatized on NWs and LPs for the coagulation of trans-glutaminase FXIII or fibrin-binding. Results showed that after injection of signaling modules into MDA-MB-435 bearing mice at 45 °C, ‘receiving’ NWs or LPs displayed prominent extravascular accumulation around the tumor which helped to amplify the therapeutic outcome (Figs. 10(C) and (D)). These results demonstrated a heat-dependent increase in the passive accumulation and specific biochemical recognition of the coagulation process.²³⁵ It was shown that the communication coagulation cascade helped to improve the accumulation of the receiving modules by a factor of 40 as compared to receiving modules without communication. The combining of two different functional nanoparticles which communicated with one another improved extravascular tumor accumulation while amplifying the therapeutic outcome. These results show great promise in the field of combining functionalized nanoparticles as a co-delivery method for the treatment of cancer.

Small Molecules-Based Targeted Nanoparticles

Small molecules are relatively inexpensive to manufacture and are capable of an infinite array of diverse structures and properties.²⁰³ Folic acid (folate) is a heavily studied small molecule that plays a major role as a targeting moiety for the delivery of therapeutic agents. This small molecule is a water-soluble vitamin B6 that is essential in humans for growth and rapid cell division, especially during embryonic development.²²⁴ Folate receptors are over-expressed on various tumor cells, allowing folate, which has a high binding affinity for folate receptors ($Kd = 10^{-9}$ M), to be used as a targeting ligand for targeted delivery of

imaging and therapeutic agents to tumors. Several cancer imaging agents and therapeutics that use folate as a targeting moiety are currently being tested in clinical trials such as ¹¹¹In-DTPA-folate, ^{99m}Tc-folate conjugate (EC20), folate-linked fluorescent hepten (EC17), and diacetylvinyl-blastine hydrazide-folate conjugate (EC145).²⁰³ Folate is one of the promising small molecule targeting ligands used for co-delivery of therapeutic agents using organic or inorganic nanoparticles. Another class of small molecules which act as targeting ligands are carbohydrates. These small molecule targeting ligands can selectively recognize cell surface receptors such as lectin.²³⁶ Carbohydrates such as galactose, mannose, and arabinose may serve as effective targeting moieties in the treatment of liver diseases as they readily bind to the asialoglycoprotein receptor (ASGP-R) that is present only on hepatocytes at a high density, approximately 500, 000 receptors per cell.^{237–240}

Cellular metabolism requires an essential vitamin, riboflavin, and studies have shown that the riboflavin carrier protein (RCP) is highly up-regulated in metabolically active cells.^{241, 242} Therefore, flavin mononucleotide (FMN), which is an endogenous RCP ligand, may be used as a small molecule targeting ligand for metabolically active cancer or endothelial cells. Kiessling et al. synthesized a dual probe nanoparticle using FMN-coated ultrasmall superparamagnetic iron oxide nanoparticles (FLUSPIO) as MRI/optical probes for prostate cancer detection *in vivo*.²⁴³ Phosphate groups of FMN were used to coat USPIO with guanosine monophosphate to impart stability to the nanoparticle. FLUSPIO had a final hydrodynamic radius of 97 ± 3 nm with an intense fluorescence emission band observed at 530 nm due to FMN. PC3 prostate cancer cells and human umbilical vein endothelial (HUVEC) cells were used for *in vitro* cellular uptake of FLUSPIO. Characterization was analyzed by MRI (3T), TEM, and fluorescence microscopy. A significantly increased R2 relaxation rate of both PC3 cells and HUVEC cells after 1h incubation with FLUSPIO-was observed compared to that of non-targeted USPIO.²⁴³ Free FMN reduced uptake of the nanoparticles considerably by competitive blocking of RCP. Fluorescence microscopy revealed an enhanced green fluorescence in the cells after FLUSPIO incubation. Endosomal localization of the nanoparticles is suggested due to the perinuclear fluorescence signal. These data are consistent with TEM results and suggest that FMN may serve as a versatile building block for tumor-targeted imaging and therapeutic modalities in multifunctional nanoparticles.

A dual contrast agent (nuclear imaging/MRI) was developed by Jeong et al. using galactose-conjugated SPI-ONs to target hepatocytes in a mouse model.²⁴⁴ After i.v. injection, SPIONs are generally nonspecifically phagocytosed or endocytosed by the reticuloendothelial system in the liver, spleen, lymph, and bone marrow. Therefore, the evaluation of hepatocyte function under certain clinical conditions, such as partial liver transplant or hepatitis, is essential, and there is need for hepatocyte-selective imaging. Jeong et al. synthesized lactobionic acid (LBA) having a high affinity for ASGP-R. The LBA was immobilized onto SPIONs using amide linkages of the dopamine-modified SPIONs bearing a primary amine group and the LBA using 1-ethyl-3-(3-(dimethylamino)-propyl) carbodiimide/*N*-hydroxysuccinimide (EDC/NHS) chemistry.²⁴⁴ Nanoparticles were radiolabeled with ^{99m}Tc via diethylene tri-amine pentaacetic acid (DTPA), which were further conjugated to the remaining amine groups of dopamine-SPIONs. *In vivo* micro-single photon emission computed tomography (SPECT)/CT images and T2-weighted MR images analysis of

99mTC-LBA-SPION, after tail vein injection, revealed that nanoparticles accumulated in the liver within a few minutes. The blocking of ASGP-R using free galactose was conducted in a competitive study showing a large decrease in liver uptake. These data suggest that ASGP-R facilitated the uptake of 99mTC-LBA-SPIONs. It was then confirmed by TEM imaging that LBA-SPIONs were located within the mitochondrial matrix as well as the cytoplasm. This indicated that ASGP-R helped to facilitate internalization of the nanoparticles into the hepatocytes.

Small molecule-targeting ligands must demonstrate high specificity and affinity towards cellular receptors. The development of such a targeting ligand has been proven to be a challenging task.²⁰³ Multivalent binding effects may be a way to help improve the targeting of small molecule-conjugated nanoparticles. This would entail conjugating multiple ligands on the nanoparticle surface. High-throughput screening is another strategy for selecting small molecule-targeting ligands having high affinity and specificity for specific receptors. Weissleder et al. used high-throughput screening, with fluorescent magnetic nanoparticles, against several small molecular ligands from a library of 146 small molecules (500 Da), that specifically bind to endothelial cells, activated human macrophages, and pancreatic cancer cells.²⁴⁵ Overall, small molecules are relatively inexpensive to produce and are capable of an infinite array of diverse structures and properties with great potential as a class of targeting moieties.

Aptamer-Based Targeted Nanoparticles

Aptamers are small nucleic acid ligands (15–40 bases) that have high specificity to target binding sites due to the molecules' ability to fold into unique conformations with three-dimensional structures.²⁴⁶ The systematic evolution of ligands by exponential enrichment (SELEX) is the selection process used to identify aptamers.^{247–250} Through this process, it is possible to select aptamers displaying high affinity and specificity for a target from libraries consisting of more than 10¹⁵ random oligonucleotides. Aptamers as a targeting moiety have many advantages over antibodies: low immunogenicity, small size (~15 kDa), and easy scale-up preparation without batch-to-batch variations. Approximately more than 200 aptamers have been isolated to date.^{251, 252} AS1411, a nucleolin targeted aptamer, is in phase III of clinical development.²⁵³ Pegaptanib, a VEGF165 targeted aptamer, was approved by the FDA in 2004 for the treatment of neovascular macular degeneration.^{254–256} Aptamers also possess several deleterious properties such as rapid clearance from the blood due to nuclease degradation. To enhance aptamers' bioavailability and pharmacokinetic properties, chemical modification with PEG or pyrimidine modifications at the 2'-fluorine position were conducted on the aptamer molecule itself.²⁵⁷ One of the best characterized aptamers used for targeted delivery-is 2'-fluoropyridine-RNA. These aptamers are generated against the extracellular domain of prostate-specific membrane antigen (PSMA).²⁵⁸ The PSMA as targeting ligand was used for the delivery of DOX,²⁵⁹ incorporated into self-assembled polymeric nanoparticles,^{16, 260, 261} and quantum dots.²⁹ Recent studies utilize a PSMA aptamer-siRNA chimera system that was extended at the 3' end to contain a complementary nucleotide sequence directed toward the antisense strand of the siRNA.²⁶²

Alexis et al. co-delivered DOX and DTX using bio-compatible and biodegradable PLGA-b-PEG copolymer. The nanoprecipitation method was used to formulate DTX encapsulated NPs (~1 wt% Dtxl) having a diameter of $62 \pm 1\mu5$ nm. The surfaces of the nanoparticles were further functionalized with A10 PSMA aptamers which were pre-loaded with DOX.² The final formulation, NP-(DTX)-Apt- (Fig. 11) was further analyzed for cellular uptake and *in vitro* cytotoxicity. A hydrophobic dye, NBD-cholesterol, was used to visualize cellular uptake of both drugs using fluorescence microscopy having a fluorescence emission spectrum (excitation/emission = 460 nm/534 nm). Two cell lines chosen for analysis were LNCaP prostate adeno-carcinomas cells, which-express PSMA antigens on their plasma membrane, as the target cell line and PC3 prostate adenocarcinomas cells, which show no expression of the PSMA antigen acting as a negative control. It was shown that NBD-cholesterol and DOX were effectively delivered into LNCaP cells via NP-Apt bioconjugates. There was no uptake of NBD observed in PC3 cells, with only a relatively small amount of DOX signal appearing in the PC3 nucleus which may represent a portion of free DOX released from the NP-Apt bioconjugates during incubation with cells. *In vitro* cytotoxicity studies revealed that NP-(DTX)-Apt-formulations were significantly cytotoxic in both cell lines as compared to all controls. The relative cell viability of NP-(DTX)-Apt- was 54% in contrast to 58%, 86%, and 100% using NP-(DTX)-Apt, NP-Apt-, and NP-Apt, respectively. Alexis et al. examined a novel targeted drug delivery system which consisted of NP-Apt bioconjugates that simultaneously delivered both hydrophobic PTX and hydrophilic nucleic acid intercalating DOX drugs to prostate cancer cell lines.² This targeted co-delivery system may also allow for temporally distinct release of drugs, which may have implications for delivery to distinct anatomical locations.

Kim et al. developed multimodal imaging probes that were capable of concurrent radionuclide imaging, MRI, and fluorescence imaging *in vivo*.²⁶³ The multifunctional nanoparticles used a magnetic cobalt ferrite core-encased by a silica shell which contained the fluorescent rhodamine. The nanoparticles were further modified with various organo-silicon compounds, such as (MeO)₃Si-PEG or 3-aminopropyl triethoxysilane. An AS1411 aptamer was conjugated on the surface of nanoparticles and served as a nucleolin-targeting ligand²⁶⁴ and *p*-SCN-Bn-NOTA for 67Ga-citrate incorporation provided MFR-AS1411. Multimodal nanoparticles were injected into C6-bearing nude mice, and specific tumor targeting of MFR-AS1411 was observed using radionuclide images via 67Ga radioactivity, 24 h post-injection. In contrast, nanoparticles containing mutant AS1411 (MFR-AS1411mt) were rapidly cleared from the bloodstream following i.v. administration to mice. MFR-AS1411-injected mice were further analyzed using MRI imaging techniques where T2-weighted images displayed black spots at the tumor site. *Ex vivo* fluorescence imaging, and high fluorescence signals from the intestine, liver, and tumors further confirmed these results that MFR-AS1411 demonstrated tumor-specific accumulation. The development of this multimodal imaging system offers the benefits of complementary modalities and eliminates the shortcomings of individual imaging modalities. Multimodal nanoparticles provides a broad range of diagnostic and therapeutic imaging possibilities in human applications.²⁶⁵

Ellington et al. identified a newly anti-EGFR aptamer and its specific 'escort.' Conjugation with gold nanoparticles (GNPs) demonstrates the internalization properties of this new aptamer.²⁶⁶ A RNA pool spanning 62 random sequence positions-was used to identify

aptamers specific to EGFR. One aptamer predominated (aptamer J18) having a K_d value of 7 nM and was obtained after round 12 when analyzing selective binding species. GNPs (~20 nm) was conjugated to aptamer J18 by coating the GNPs with capture ONTs, followed by hybridization of an extended aptamer complementary to the capture ONTs.²⁶⁶ A431 cells incubated with aptamer J18-GNPs at 37 °C were analyzed by flow cytometry and fluorescence microscopy with results indicating specific binding to the cell line. These results demonstrated that the internalization of GNPs is due to the aptamer directed toward cell surface EGFR, which could lead to internalization via receptor-mediated endocytosis.²⁶⁶ This finding suggests that receptor-specific nucleic acids can overcome non-specific absorption and internalization of GNPs, which convey chronic disadvantages during conventional therapy.

Miscellaneous Targeted Approaches

The copolymer of N-acetyl D-glucosamine and D-glucuronic acid, Hyaluronic acid (HA), has been widely used as a targeting macromolecule for binding to cluster determinant 44 (CD44), -which is overexpressed in various tumors.²⁶⁷⁻²⁶⁹ Zhou et al. developed a thermo-responsive hybrid nanogel with HA as a targeting moiety for simultaneous temperature sensing, cancer cell targeting, fluorescence imaging, and combined chemo-photothermal treatment (Fig. 12).^{270, 271} Templated Ag nanoparticle was used to prepare the spherical hybrid nanogel through synthesis using a thermo-responsive non-linear PEG-based hydrogel coating as a shell. Strong hydrogen bonding between HA and PEG oligomers on the shell surface helped to immobilize HA, followed by the addition of AuCl_4^- to the hybrid nanogel to form an Ag–Au bimetallic core.²⁷⁰ High drug loading capacity (46.5 wt%) was achieved in the Ag–Au–PEG–HA hybrid nanogels mainly due to the stabilization by hydrogen bonds between the ether oxygen atoms of the nonlinear PEG gel shell and the amide groups of Temozolomide (TMZ), a model drug used in the formulation. Confocal imaging of Ag–Au–PEG–HA hybrid nanogel-incubated B16F10 murine metastatic melanoma cells (CD44+) revealed-significantly higher fluorescence intensity images as compared to nanogel without HA, demonstrating selective tumor targeting. Near-IR irradiation generalized localized heat during drug release profile studies and enhanced drug delivery by promoting a gradual transition from a hydrophilic to a hydrophobic PEG network.²⁷⁰ The gradual transition broke the PEG-TMZ bonds and also reduced the mesh size of the nanogels, further facilitating diffusion of the drug molecules from the nanocages. This combined chemo-photothermal treatment was investigated by measuring the cell viability of B16F10 cells incubated with empty or TMZ-loaded hybrid nanogels after near-IR irradiation. The combination of TMZ and photothermal treatment showed enhanced cytotoxicity as compared to other chemotherapy or photothermal treatments alone. It was shown that the combination therapy had significantly enhanced therapeutic efficacy—as compared with the additive therapeutic index achieved from chemo-and photothermal therapies, suggesting that the nanogels displayed synergistic effects.²⁷⁰

THERANOSTIC MULTIFUNCTIONAL NANOTECHNOLOGY IN CHEMOTHERAPY AND IMAGING

Theranostics, the combination of therapeutic and imaging methods on a single level, have reached new possibilities thanks to recent advances in nanotechnology.^{272–274} These nanotechnology advancements incorporate imaging probes for the enhancement of image resolution and specificity towards target tissues. Nanoparticles conjugated to active targeting ligands usually make up these imaging probes.^{203, 275} Nanoparticles having no active target ligand coupled to their surface will be passive targeting, mediated by the enhanced permeability and retention effect (EPR).^{276, 277} Theranostic nanomedicine has the potential for simultaneous and real time monitoring of drug delivery, trafficking of drug and therapeutic responses.

Small molecule drugs often display many disadvantages including the lack of sufficient specificity to the tumor, severe and toxic side effects in healthy tissues, limited delivery of hydrophobic drugs to the tumor cells, and the development of drug-resistance.^{42, 278} It has been described in this review that NPs can provide a potential solution to these problems in traditional chemotherapy.^{42, 279, 280} One such solution is the development of theranostic NPs which incorporates imaging agents and drugs such as DOX or PTX-used for simultaneous imaging and targeted chemotherapy of diseases and cancers.^{281, 282}

As described, theranostic NPs can simultaneously provide cancer detection, drug delivery, and real-time evaluation of therapeutic efficacy. Kim et al. developed chitosan-based NPs (CNPs) that were labeled with Cy5.5, a NIR fluorescence dye for imaging, and encapsulated with PTX for cancer therapy (PTX–Cy5.5–CNP) to produce a multifunctional theranostic NPs (Figs. 13(A) through (G)).^{283–286} SCC7 tumor-bearing mouse models-were treated dose-dependently with PTX–Cy5.5–CNP to the tumor sites which-were then visualized using optical imaging technology. Repeated injections at three-day intervals modulated and increased the therapeutic efficacy of PTX–Cy5.5–CNP. Strong NIR fluorescence signals were observed in the targeted tumors. This optimal protocol of repeated injections of PTX–CNPs at three-day intervals greatly increased the drug concentration in targeted tumors which resulted in enhanced therapeutic efficacy to tumor tissues while minimizing toxicity to normal tissues. This demonstrated that the optimal dosage of the drug in question may be identified using theranostic NPs, thereby increasing both effectiveness and safety of the drug. SCC7 tumor-bearing mouse models were also analyzed using NIR fluorescence imaging for direct monitoring of tumor growth in response to PTX–Cy5.5–CNP administration (Figs. 14(A) through (D)). The possibility-of determining the optimal dosage of drug for the individual patient at the right time using theranostic NPs may hold promise in paving the way for personalized medicine.

Similarly, Chen et al. recently demonstrated pH-responsive NPs encapsulated with DOX to better understand drug release behavior and intracellular localization (Fig. 15).²⁸⁷ Hydrophobic *N*-palmitoyl groups were conjugated to chitosan to prepare a PH-responsive polymer then followed by attachment with Cy5.5. PH-responsive polymers were able to self-assemble into NPs and encapsulate DOX within aqueous media, yielding DOX–Cy5–NPs. DOX (donor) and Cy5 (acceptor) in NPs were sufficiently close for energy transfer to occur

(FRET on) at pH = 7.0, whereas DOX and Cy5.5 were not in close proximity (FRET off) in the protonated form of DOX–Cy5–NPs at low pH.²⁸⁷ No fluorescence of DOX was observed, after internalization to cells, when DOX–Cy5–NPs was in the caveolae/caveosomes (FRET on with high efficiency) and having a weak fluorescence in the cytosol when DOX–Cy5–NPs was in slightly acidic early endosome (FRET on with low efficiency). However, strong fluorescence signals were observed in the cytosol when DOX–Cy5–NPs was in acidic late endosomes/lysosomes (FRET off) (Fig. 16). This study indicated that theragnostic NPs employing the FRET technique can allow intracellular monitoring of drug release.²⁸⁷

Intravital-microscopy has had a great deal of success when it comes to examining cellular behavior and molecular signals under conditions simulating a natural environment in living animals at subcellular resolution.^{288–290} Whole body imaging using fluorescence or bioluminescence usually provides only macroscopic resolution as compared to intravital microscopy. Intravital-microscopy includes an *in vivo* CLSM used to directly assess *in vivo* distribution of the drug carrier or drug across various cellular locations. Intravital microscopy may also be used to understand the delivery mechanism of nanoparticles and their payload to the targeted tissue.^{291, 292} Cabral et al. fabricated drug-loaded micelles composed of poly-(glutamic acid) and hydrophilic PEG block copolymer, and used them for intra-vital imaging.²⁹³ Highly permeable tumors (C26) and poorly permeable tumors (BxPC3) were used to observe *in vivo* bio-distribution and antitumor activity of drug-loaded micelles having a range of diameters. Alexa dye-labeled micelles were used for *in vivo* CLSM imaging. It was shown through real-time imaging via *in vivo* CLSM of a mouse, that various sized micelles (diameters of 30, 50, 70 and 100 nm) penetrated through highly permeable tumors; however, only 30 nm micelles accumulated in poorly permeable tumors to achieve an antitumor effect (Figs. 17(A) through (G)). These results indicated that *in vivo* CLSM can contribute to the analysis of cellular internalization, tissue penetration and the extravasation profile of NPs in living mice.²⁸⁷

During chemotherapy, theragnostic NPs are highly useful for providing real-time information on its location, release or efficacy of the contained drug and detecting residual tumor cells with various optical imaging techniques as shown in the above-mentioned studies. In addition, they enable the identification of the optimal dosage of the drug in question and may hold promise in the personalized medicines.

CONCLUSION AND FUTURE PROSPECTS

Considerable effort has been made toward the research and development of multifunctional co-loaded chemo/gene therapy nanoparticle systems for cancer targeted imaging and therapy. Magnetic nanoparticle-based theranostic systems showed particular promise. The intrinsic magnetic properties lend themselves to diagnostic MRI applications, with their surfaces easily modified using a variety of targeting moieties, such as antibodies, peptides, small molecules, aptamers, or therapeutic agents utilizing a number of conjugation strategies. Also, magnetic nanoparticles can be degraded to Fe ions in the body particularly in the acidic compartments of cells (e.g., lysosomes), relieving potential toxicity of long-term residence of the nanoparticles themselves as compared to other inorganic nanoparticles

such as gold-and carbon-based formulations. The newer and advanced characterization methodologies are also needed, including pharmacokinetics and long-term toxicity studies. It is critical to be aware of the design parameters discussed in this review for preparation of nanoparticles for potential clinical uses. The costs required to integrate multiple components for co-loading or multifunctional properties-are an additional consideration for commercial viability. One must also consider the regulatory hurdles encountered during clinical trials. The required regulatory processes become more-complex with the multifunctionalities of the nanoparticles as they consist of multiple additional components and also claim multiple indications with a single nanoparticle. Nonetheless, there is high probability that– multifunctional chemo/gene therapy nanoparticle systems for cancer-specific treatment–will be used in the clinic setting in the near future. The multifunctional chemo/gene therapy approaches will help to meet unmet medical needs for effective cancer treatments with minimal adverse effects.

Acknowledgments

The authors acknowledge the support of the National Institute of General Medical Science of the National Institutes of Health under award number SC3GM109873. The authors acknowledge Hawai'i Community Foundation, Honolulu, HI 96813, USA, for research support on asthma and mesothelioma research (Leahi Fund) in 2011 and 2013, respectively. The authors would like to acknowledge the 2013 George F. Straub Trust and Robert C. Perry Fund of the Hawai'i Community Foundation, Honolulu, HI 96813, USA, for research support on lung cancer. The authors also acknowledge a seed grant from the Research Corporation of the University of Hawai'i at Hilo, Hilo, HI 96720, USA, and The Daniel K. Inouye College of Pharmacy, University of Hawaii at Hilo, Hilo, HI 96720, USA, for providing start-up financial support to their research group. The authors gratefully thank Ann Gleason, Instructor at the University of Hawaii at Hilo English Language Institute, for assisting with the editing of this review article. The authors would also like to thank the scholarship foundations for their continued support of minorities in the pharmaceutical science research field: Kamehameha Schools, Honolulu, HI 96813, USA; Liko A'e Foundation, Kahului, HI 96732, USA; Hawai'i Community Foundation, Honolulu, HI 96813, USA; Ke Ola Mau program, Hilo, HI 96720, USA; and the University of Hawai'i Foundation, Honolulu, HI 96822, USA.

Biographies



Micah D. K. Glasgow is currently the only Native Hawaiian Ph.D. in Pharmaceutical Sciences Candidate at the Daniel K. Inouye College of Pharmacy, University of Hawaii at Hilo. Mr. Glasgow is in his fourth year of professional graduate study with an anticipated graduation date of May 2015. He is an active member of American Association of Pharmaceutical Scientists, American Association for the Advancement of Science and the Controlled Release Society. Mr. Glasgow is the recipient of over 20 scholarships throughout his Ph.D. tenure. His main thesis project focuses on the co-delivery of synergistic acting drugs for the treatment of Neuroblastoma using hybrid nanotechnology. Mr. Glasgow's side project, funded in-part by the National Science Foundation, focuses on monitoring the on-set of nucleation (crystal formation) to better control downstream processes during the manufacturing and processing of active pharmaceutical ingredients (APIs). *Research*

Interests: combinatorial chemotherapy, hybrid nanotechnology, nucleation, crystallization, cancer therapy.



Mahavir B. Chougule, is an Assistant Professor of the Department of Pharmaceutical Sciences, Daniel K. Inouye College of Pharmacy, University of Hawaii at Hilo. He has more than three years of Post-Doc research-experience and two years of industrial research experience. Chougule's research has also focused on development of drug and/siRNA based nanoparticle systems for the treatment of cancer and pulmonary disorders. Chougule has 25 publications, 8 patents, 3 review articles, 5 book chapters, and 50 scientific presentations to his credit. He is also a member of the editorial boards of five pharmaceutical journals. He is an active member of American Association of Cancer Research and American Association of Pharmaceutical Scientists based on his scientific contributions. Dr. Chougule is a recipient of several national and international awards including recent American Association of Cancer Research (AACR) Minority-Serving Institution Faculty Scholar in Cancer Research Award, USA. *Research Interests:* gene therapy, chemotherapy, nanotechnology based novel delivery systems, lung and breast cancer, molecular biology, tumor models.

References

1. Bangham A, Horne R. Negative staining of phospholipids and their structural modification by surface-active agents as observed in the electron microscope. *J Mol Biol.* 1964; 8:660. [PubMed: 14187392]
2. Zhang L, Radovic-Moreno AF, Alexis F, Gu FX, Basto PA, Bagalkot V, Jon S, Langer RS, Farokhzad OC. Co-delivery of hydrophobic and hydrophilic drugs from nanoparticle-aptamer bioconjugates. *Chem Med Chem.* 2007; 2:1268. [PubMed: 17600796]
3. Davis M, Chen Z, Shin D. Nanoparticle therapeutics: An emerging treatment modality for cancer. *Nat Rev Drug Discov.* 2008; 7:771. [PubMed: 18758474]
4. Wagner V, Dullaart A, Bock AK, Zweck A. The emerging nanomedicine landscape. *Nat Biotechnol.* 2006; 24:1211. [PubMed: 17033654]
5. Northfelt DW, Dezube BJ, Thommes JA, Miller BJ, Fischl MA, Friedman-Kien A, Kaplan LD, Du Mond C, Mamelok RD, Henry DH. Pegylated-liposomal doxorubicin versus doxorubicin, bleomycin, and vincristine in the treatment of AIDS-related Kaposi's sarcoma: Results of a randomized phase III clinical trial. *J Clin Oncol.* 1998; 16:2445. [PubMed: 9667262]
6. Harries M, Ellis P, Harper P. Nanoparticle albumin-bound paclitaxel for metastatic breast cancer. *J Clin Oncol.* 2005; 23:7768. [PubMed: 16204007]
7. Zhang L, Gu FX, Chan JM, Wang AZ, Langer RS, Farokhzad OC. Nanoparticles in medicine: Therapeutic applications and developments. *Clin Pharmacol Ther.* 2008; 83:761. [PubMed: 17957183]
8. Peer D, Karp JM, Hong S, Farokhzad OC, Margalit R, Langer R. Nanocarriers as an emerging platform for cancer therapy. *Nat Nanotechnol.* 2007; 2:751. [PubMed: 18654426]
9. Matsumura Y, Maeda H. A new concept for macromolecular therapeutics in cancer chemotherapy: Mechanism of tumorotropic accumulation of proteins and the antitumor agent smancs. *Cancer Res.* 1986; 46:6387. [PubMed: 2946403]

10. Greco F, Vicent MJ. Combination therapy: Opportunities and challenges for polymer-drug conjugates as anticancer nanomedicines. *Adv Drug Deliver Rev.* 2009; 61:1203.
11. Dong JT. Prevalent mutations in prostate cancer. *J Cell Biochem.* 2006; 97:433. [PubMed: 16267836]
12. Hanahan D, Weinberg RA. The Hallmarks of cancer. *Cell.* 2000; 100:57. [PubMed: 10647931]
13. Suggitt M, Bibby MC. 50 years of preclinical anticancer drug screening: Empirical to target-driven approaches. *Clin Cancer Res.* 2005; 11:971. [PubMed: 15709162]
14. Ismael GF, Rosa DD, Mano MS, Awada A. Novel cytotoxic drugs: Old challenges, new solutions. *Cancer Treat Rev.* 2008; 34:81. [PubMed: 17905518]
15. Aryal S, Hu CM, Zhang L. Combinatorial drug conjugation enables nanoparticle dual-drug delivery. *Small.* 2010; 6:1442. [PubMed: 20564488]
16. Kolishetti N, Dhar S, Valencia P, Lin L, Karnik R, Lippard S, Langer R, Farokhzad O. Engineering of self-assembled nanoparticle platform for precisely controlled combination drug therapy. *P Natl Acad Sci USA.* 2010; 107:17939.
17. James JS, Dubs G. FDA approves new kind of lymphoma treatment. *Food and Drug Administration. AIDS Treat News.* 1997:2–3.
18. Albanell J, Baselga J. Trastuzumab, a humanized anti-HER2 monoclonal antibody, for the treatment of breast cancer. *Drug Today.* 1999; 35:931.
19. Liu LH, Xu KJ, Wang HY, Tan PKJ, Fan WM, Venkatraman SS, Li LJ, Yang YY. Self-assembled cationic peptide nanoparticles as an efficient antimicrobial agent. *Nat Nanotechnol.* 2009; 4:457. [PubMed: 19581900]
20. Liu LH, Guo K, Lu J, Venkatraman SS, Luo D, Ng KC, Ling EA, Moochhala S, Yang YY. Biologically active core/shell nanoparticles self-assembled from cholesterol-terminated PEG-TAT for drug delivery across the blood-brain barrier. *Biomaterials.* 2008; 10:1509. [PubMed: 18155137]
21. Krakovicova H, Etrych T, Ulbrich K. HPMA-based polymer conjugates with drug combination. *Eur J Pharm Sci.* 2009; 37:405. [PubMed: 19491032]
22. Tekade RK, Dutta T, Gajbhiye V, Jain NK. Exploring dendrimer towards dual drug delivery: pH responsive simultaneous drug-release kinetics. *J Microencapsul.* 2009; 26:287. [PubMed: 18791906]
23. Ganta S, Amiji M. Coadministration of paclitaxel and curcumin in nanoemulsion formulations to overcome multidrug resistance in tumor cells. *Mol Pharm.* 2009; 6:928. [PubMed: 19278222]
24. Chen A, Zhang M, Wei D, Stueber D, Taratula O, Minko T, He H. Co-delivery of doxorubicin and Bcl-2 siRNA by mesoporous silica nanoparticles enhances the efficacy of chemotherapy in multidrug-resistant cancer cells. *Small.* 2009; 5:2673. [PubMed: 19780069]
25. Mayer LD, Janoff AS. Optimizing combination chemotherapy by controlling drug ratios. *Mol Interv.* 2007; 7:216. [PubMed: 17827442]
26. Wang Y, Gao S, Ye WH, Yoon HS, Yang YY. Co-delivery of drugs and DNA from cationic core-shell nanoparticles self-assembled from a biodegradable copolymer. *Nat Mater.* 2006; 5:791. [PubMed: 16998471]
27. Saad M, Garbuzenko OB, Minko T. Co-delivery of siRNA and an anticancer drug for treatment of multidrug-resistant cancer. *Nanomedicine-UK.* 2008; 3:761.
28. Debbage P, Jaschke W. Molecular imaging with nanoparticles: Giant roles for dwarf actors. *Histochem Cell Biol.* 2008; 130:845. [PubMed: 18825403]
29. Bagalkot V, Zhang L, Levy-Nissenbaum E, Jon S, Kantoff PW, Langer R, Farokhzad OC. Quantum dot-aptamer conjugates for synchronous cancer imaging, therapy, and sensing of drug delivery based on bi-fluorescence resonance energy transfer. *Nano Lett.* 2007; 7:3065. [PubMed: 17854227]
30. Park JH, Maltzahn G, Zhang L, Schwartz M, Ruoslahti E, Bhatia S, Sailor M. Magnetic iron oxide nanoworms for tumor targeting and imaging. *Adv Mater.* 2008; 20:1630. [PubMed: 21687830]
31. Nasongkla N, Bey E, Ren J, Ai H, Khemtong C, Guthi JS, Chin SF, Sherry AD, Boothman DA, Gao J. Multifunctional polymeric micelles as cancer-targeted, MRI-ultrasensitive drug delivery systems. *Nano Lett.* 2006; 6:2427. [PubMed: 17090068]

32. McCarthy JR, Weissleder R. Multifunctional magnetic nanoparticles for targeted imaging and therapy. *Adv Drug Deliver Rev.* 2008; 60:1241.
33. Sanhai WR, Sakamoto JH, Canady R, Ferrari M. Seven challenges for nanomedicine. *Nat Nanotechnol.* 2008; 3:242. [PubMed: 18654511]
34. Riehemann K, Schneider SW, Luger TA, Godin B, Ferrari M, Fuchs H. Nanomedicine—challenge and perspectives. *Angew Chem Int Ed Engl.* 2009; 48:872. [PubMed: 19142939]
35. Sheng Y, Liao LD, Thakor NV, Tan MC. Nanoparticles for molecular imaging. *J Biomed Nanotechnol.* 2014; 10:2641. [PubMed: 25992413]
36. Dubertret B, Skourides P, Norris DJ, Noireaux V, Brivanlou AH, Libchaber A. *In vivo* imaging of quantum dots encapsulated in phospholipid micelles. *Science.* 2002; 298:1759. [PubMed: 12459582]
37. Shi HT, Wei JF, Qiang L, Chen X, Meng XW. Fluorescent carbon dots for bioimaging and biosensing applications. *J Biomed Nanotechnol.* 2014; 10:2677. [PubMed: 25992414]
38. Chanda N, Kattumuri V, Shukla R, Zambre A, Katti K, Upendran A, Kulkarni RR, Kan P, Fent GM, Casteel SW, Smith CJ, Boote E, Robertson JD, Cutler C, Lever JR, Katti KV, Kannan R. Bombesin functionalized gold nanoparticles show *in vitro* and *in vivo* cancer receptor specificity. *P Natl Acad Sci USA.* 2010; 107:8760.
39. Nie LB, Liu FH, Ma P, Xiao XY. Applications of gold nanoparticles in optical biosensors. *J Biomed Nanotechnol.* 2014; 10:2700. [PubMed: 25992415]
40. De La Zerda A, Zavaleta C, Keren S, Vaithilingam S, Bodapati S, Liu Z, Levi J, Smith BR, Ma TJ, Oralkan O, Cheng Z, Chen X, Dai H, Khuri-Yakub BT, Gambhir SS. Carbon nanotubes as photoacoustic molecular imaging agents in living mice. *Nat Nanotechnol.* 2008; 3:557. [PubMed: 18772918]
41. Ramon-Azcon J, Ahadian S, Obregon R, Shiku H, Ramalingam M, Matsue T. Applications of carbon nanotubes in stem cell research. *J Biomed Nanotechnol.* 2014; 10:2539. [PubMed: 25992408]
42. Shapira A, Livney YD, Broxterman HJ, Assaraf YG. Nanomedicine for targeted cancer therapy: Towards the overcoming of drug resistance. *Drug Resist Update.* 2011; 14:150.
43. Chiu GN, Wong MY, Ling LU, Shaikh IM, Tan KB, Chaudhury A, Tan BJ. Lipid-based nanoparticulate systems for the delivery of anti-cancer drug cocktails: Implications on pharmacokinetics and drug toxicities. *Curr Drug Metab.* 2009; 10:861. [PubMed: 20214582]
44. Gottesman MM. Mechanisms of cancer drug resistance. *Annu Rev Med.* 2002; 53:615. [PubMed: 11818492]
45. Koval M, Preiter K, Adles C, Stahl PD, Steinberg TH. Size of IgG-opsonized particles determines macrophage response during internalization. *Exp Cell Res.* 1998; 242:265. [PubMed: 9665824]
46. Huwyler J, Cerletti A, Fricker G, Eberle AN, Drewe J. Bypassing of P-glycoprotein using immunoliposomes. *J Drug Target.* 2002; 10:73. [PubMed: 11996089]
47. Rejman J, Oberle V, Zuhorn IS, Hoekstra D. Size-dependent internalization of particles via the pathways of clathrin- and caveolae-mediated endocytosis. *Biochem J.* 2004; 377:159. [PubMed: 14505488]
48. Bebawy M, Chetty M. Gender differences in p-glycoprotein expression and function: Effects on drug disposition and outcome. *Curr Drug Metab.* 2009; 10:322. [PubMed: 19519340]
49. Bradshaw DM, Arceci RJ. Clinical relevance of transmembrane drug efflux as a mechanism of multidrug resistance. *J Clin Oncol.* 1998; 16:3674. [PubMed: 9817290]
50. Hennessy M, Spiers JP. A primer on the mechanics of P-gly coprotein the multidrug transporter. *Pharmacol Rev.* 2007; 55:1.
51. Andres, RP.; Datta, S.; Janes, DB.; Kubiak, CP.; Reifengerger, R. The design, fabrication and electronic properties of self-assembled molecular nanostructures. In: Nalwa, HS., editor. *Handbook of Nanostructured Materials and Nanotechnology.* Vol. 3. American Press; San Diego, CA: 2000. p. 179-231.
52. Sumpter, BG.; Noid, DW.; Barnes, MD.; Otaigbe, JU. Encyclopedia of Nanoscience and Nanotechnology. Nalwa, HS., editor. Vol. 8. American Scientific Publisher; Los Angeles: 2004/2011. p. 873-903.

53. Zhou, W. Encyclopedia of Nanoscience and Nanotechnology. Nalwa, HS., editor. Vol. 10. American Scientific Publisher; Los Angeles: 2004/2011. p. 149-160.
54. Imae, T.; Funayama, K.; Nakanishi, Y.; Yoshii, K. Encyclopedia of Nanoscience and Nanotechnology. Nalwa, HS., editor. Vol. 3. American Scientific Publisher; Los Angeles: 2004/2011. p. 685-702.
55. Walde, P. Encyclopedia of Nanoscience and Nanotechnology. Nalwa, HS., editor. Vol. 9. American Scientific Publisher; Los Angeles: 2004/2011. p. 43-80.
56. Nalwa HS. A special issue on reviews in nanomedicine, drug delivery and vaccine development. J Biomed Nanotechnol. 2014; 10:1635. [PubMed: 25992435]
57. Nalwa HS. A special issue on reviews in biomedical applications of nanomaterials, tissue engineering, stem cells, bioimaging, and toxicity. J Biomed Nanotechnol. 2014; 10:2421. [PubMed: 25992404]
58. Bangham AD, Standish MM, Watkins JC. Diffusion of univalent ions across the lamellae of swollen phospholipids. J Mol Biol. 1965; 13:238. [PubMed: 5859039]
59. Bayne WF, Mayer LD, Swenson CE. Pharmacokinetics of CPX-351 (cytarabine/daunorubicin HCl) liposome injection in the mouse. J Pharm Sci. 2009; 98:2540. [PubMed: 19009594]
60. Aas T, Borresen AL, Geisler S, Smith-Sorensen B, Johnsen H, Varhaug JE, Akslen LA, Lonning PE. Specific P53 mutations are associated with de novo resistance to doxorubicin in breast cancer patients. Nat Med. 1996; 2:811. [PubMed: 8673929]
61. Persidis A. Cancer multidrug resistance. Nat Biotechnol. 1999; 17:94. [PubMed: 9920278]
62. Anand A, Huberman M. Peripheral neurotoxicity of taxol in patients previously treated with cisplatin. Cancer. 1995; 76:916. [PubMed: 8625200]
63. Parhi P, Mohanty C, Sahoo SK. Nanotechnology-based combinational drug delivery: An emerging approach for cancer therapy. Drug Discov Today. 2012; 17:1044. [PubMed: 22652342]
64. Wu S, Singh RK. Resistance to chemotherapy and molecularly targeted therapies: Rationale for combination therapy in malignant melanoma. Curr Mol Med. 2011; 11:553. [PubMed: 21707515]
65. Chen Y, Zhu X, Zhang X, Liu B, Huang L. Nanoparticles modified with tumor-targeting scFv deliver siRNA and miRNA for cancer therapy. Mol Ther. 2010; 18:1650. [PubMed: 20606648]
66. Li N, Fu H, Tie Y, Hu Z, Kong W, Wu Y, Zheng X. miR-34a inhibits migration and invasion by down-regulation of c-Met expression in human hepatocellular carcinoma cells. Cancer Lett. 2009; 275:44. [PubMed: 19006648]
67. de Nigris F, Balestrieri ML, Napoli C. Targeting c-Myc, Ras and IGF cascade to treat cancer and vascular disorders. Cell Cycle. 2006; 5:1621. [PubMed: 16921263]
68. Halaby MJ, Yang DQ. p53 translational control: A new facet of p53 regulation and its implication for tumorigenesis and cancer therapeutics. Genetics. 2007; 395:1.
69. Grothey A. Future directions in vascular endothelial growth factor-targeted therapy for metastatic colorectal cancer. Semin Oncol. 2006; 33:S41. [PubMed: 17145524]
70. Kang SH, Cho HJ, Shim G, Lee S, Kim SH, Choi HG, Kim CW, Oh YK. Cationic liposomal co-delivery of small interfering RNA and a MEK inhibitor for enhanced anticancer efficacy. Pharm Res. 2011; 28:3069. [PubMed: 21879387]
71. Shim G, Han SE, Yu YH, Lee S, Lee HY, Kim K, Kwon IC, Park TG, Kim YB, Choi YS, Kim CW, Oh YK. Trilysinoyl oleylamide-based cationic liposomes for systemic co-delivery of siRNA and an anticancer drug. J Control Release. 2011; 155:60. [PubMed: 20971142]
72. Grossman D, Kim PJ, Schechner JS, Altieri DC. Inhibition of melanoma tumor growth *in vivo* by survivin targeting. P Natl Acad Sci USA. 2001; 98:635.
73. Zhang M, Garbuzenko OB, Reuhl KR, Rodriguez-Rodriguez L, Minko T. Two-in-one: Combined targeted chemo and gene therapy for tumor suppression and prevention of metastases. Nanomedicine-UK. 2012; 7:185.
74. Sawant RR, Vaze OS, Rockwell K, Torchilin VP. Palmitoyl ascorbate-modified liposomes as nanoparticle platform for ascorbate-mediated cytotoxicity and paclitaxel co-delivery. Eur J Pharm Biopharm. 2010; 75:321. [PubMed: 20433922]

75. Sawant RR, Vaze OS, Rockwell K, Torchilin VP. Palmitoyl ascorbate-modified liposomes as nanoparticle platform for ascorbate-mediated cytotoxicity and paclitaxel co-delivery. *Eur J Pharm Biopharm.* 2010; 75:321. [PubMed: 20433922]
76. Unsal-Kacmaz K, Ragunathan S, Rosfjord E, Dann S, Upeslacis E, Grillo M, Hernandez R, Mack F, Klippel A. The interaction of PKN3 with RhoC promotes malignant growth. *Mol Oncol.* 2012; 6:284. [PubMed: 22217540]
77. Aleku M, Schulz P, Keil O, Santel A, Schaeper U, Dieckhoff B, Janke O, Endruschat J, Durieux B, Roder N, Loffler K, Lange C, Fechtner M, Mopert K, Fisch G, Dames S, Arnold W, Jochims K, Giese K, Wiedenmann B, Scholz A, Kaufmann J. Atu027, a liposomal small interfering RNA formulation targeting protein kinase N3, inhibits cancer progression. *Cancer Res.* 2008; 68:9788. [PubMed: 19047158]
78. Strumberg D, Schultheis B, Traugott U, Vank C, Santel A, Keil O, Giese K, Kaufmann J, Drevs J. First-in-human phase I study of Atu027, a liposomal small interfering RNA formulation, targeting protein kinase N3 (PKN3) in patients with advanced solid tumors. *J Clin Oncol.* 2011; 29:1. [PubMed: 21115866]
79. Dai W, Jin W, Zhang J, Wang X, Wang J, Zhang X, Wan Y, Zhang Q. Spatiotemporally controlled co-delivery of anti-vasculature agent and cytotoxic drug by octreotide-modified stealth liposomes. *Pharm Res.* 2012; 29:2902. [PubMed: 22723122]
80. Hu J, Chen LJ, Liu L, Chen X, Chen PL, Yang G, Hou WL, Tang MH, Zhang F, Wang XH, Zhao X, Wei YQ. Liposomal honokiol, a potent antiangiogenesis agent, in combination with radiotherapy produces a synergistic antitumor efficacy without increasing toxicity. *Exp Mol Med.* 2008; 40:617. [PubMed: 19116447]
81. Huber PE, Bischof M, Jenne J, Heiland S, Peschke P, Saffrich R, Grone HJ, Debus J, Lipson KE, Abdollahi A. Trimodal cancer treatment: Beneficial effects of combined antiangiogenesis, radiation, and chemotherapy. *Cancer Res.* 2005; 65:3643. [PubMed: 15867359]
82. Maitani Y, Saito H, Seishi Y, Iwase Y, Yamauchi T, Higashiyama K, Sugino T. A combination of liposomal sunitinib plus liposomal irinotecan and liposome co-loaded with two drugs enhanced antitumor activity in PC12-bearing mouse. *J Drug Target.* 2012; 20:873. [PubMed: 23050928]
83. Sochanik A, Mitrus I, Smolarczyk R, Cichon T, Snietura M, Czaja M, Szala S. Experimental anticancer therapy with vascular-disruptive peptide and liposome-entrapped chemotherapeutic agent. *Arch Immunol Ther Ex.* 2010; 58:235.
84. Zhang YF, Wang JC, Bian DY, Zhang X, Zhang Q. Targeted delivery of RGD-modified liposomes encapsulating both combretastatin A-4 and doxorubicin for tumor therapy: *In vitro* and *in vivo* studies. *Eur J Pharm Biopharm.* 2010; 74:467. [PubMed: 20064608]
85. Zucker D, Andriyanov AV, Steiner A, Raviv U, Barenholz Y. Characterization of PEGylated nanoliposomes co-remotely loaded with topotecan and vincristine: Relating structure and pharmacokinetics to therapeutic efficacy. *J Control Release.* 2012; 160:281. [PubMed: 22019556]
86. Wong MY, Chiu GN. Liposome formulation of co-encapsulated vincristine and quercetin enhanced antitumor activity in a trastuzumab-insensitive breast tumor xenograft model. *Nanomedicine-UK.* 2011; 7:834.
87. Feldman EJ, Kolitz JE, Trang JM, Liboiron BD, Swenson CE, Chiarella MT, Mayer LD, Louie AC, Lancet JE. Pharmacokinetics of CPX-351; a nanoscale liposomal fixed molar ratio formulation of cytarabine: Daunorubicin, in patients with advanced leukemia. *Leukemia Res.* 2012; 36:1283. [PubMed: 22840315]
88. Lim WS, Tardi PG, Dos Santos N, Xie X, Fan M, Liboiron BD, Huang X, Harasym TO, Bermudes D, Mayer LD. Leukemia-selective uptake and cytotoxicity of CPX-351, a synergistic fixed-ratio cytarabine: Daunorubicin formulation, in bone marrow xenografts. *Leukemia Res.* 2010; 34:1214. [PubMed: 20138667]
89. Riviere K, Kieler-Ferguson HM, Jerger K, Szoka FC Jr. Anti-tumor activity of liposome encapsulated fluoroorotic acid as a single agent and in combination with liposome irinotecan. *J Control Release.* 2011; 153:288. [PubMed: 21600250]
90. Tardi P, Johnstone S, Harasym N, Xie S, Harasym T, Zisman N, Harvie P, Bermudes D, Mayer L. *In vivo* maintenance of synergistic cytarabine: Daunorubicin ratios greatly enhances therapeutic efficacy. *Leukemia Res.* 2009; 33:129. [PubMed: 18676016]

91. Ko YT, Falcao C, Torchilin VP. Cationic liposomes loaded with proapoptotic peptide D-(KLAKLAK)(2) and Bcl-2 antisense oligodeoxynucleotide G3139 for enhanced anticancer therapy. *Mol Pharm.* 2009; 6:971. [PubMed: 19317442]
92. Bajelan E, Haeri A, Vali AM, Ostad SN, Dadashzadeh S. Co-delivery of doxorubicin and PSC 833 (Valspodar) by stealth nanoliposomes for efficient overcoming of multidrug resistance. *J Pharm Pharm Sci.* 2012; 15:568. [PubMed: 23106959]
93. Avci P, Erdem SS, Hamblin MR. Photodynamic therapy: One step ahead with self-assembled nanoparticles. *J Biomed Nanotechnol.* 2014; 10:1937. [PubMed: 25580097]
94. Bolfarini GC, Siqueira-Moura MP, Demets GJ, Morais PC, Tedesco AC. *In vitro* evaluation of combined hyperthermia and photodynamic effects using magnetoliposomes loaded with cucurbituril zinc phthalocyanine complex on melanoma. *J Photoch Photobio B.* 2012; 115:1.
95. Strickley RG. Solubilizing excipients in oral and injectable formulations. *Pharm Res.* 2004; 21:201. [PubMed: 15032302]
96. Yokoyama M, Kwon GS, Okano T, Sakurai Y, Seto T, Kataoka K. Preparation of micelle-forming polymer-drug conjugates. *Bioconjugate Chem.* 1992; 3:295.
97. Kabanov A, Vinogradov S, Suzdaltseva Y, Vyu A. Water-soluble block polycations as carriers for oligonucleotide delivery. *Bioconjugate Chem.* 1995; 6:639.
98. Hu CM, Zhang L. Nanoparticle-based combination therapy toward overcoming drug resistance in cancer. *Biochem Pharmacol.* 2012; 83:1104. [PubMed: 22285912]
99. Torchilin VP. Micellar nanocarriers: Pharmaceutical perspectives. *Pharm Res.* 2007; 24:1. [PubMed: 17109211]
100. Hu Y, Jiang Z, Chen R, Wu W, Jiang X. Degradation and degradation-induced re-assembly of PVP-PCL micelles. *Biomacromolecules.* 2010; 11:481. [PubMed: 20073456]
101. Orienti I, Zuccari G, Fini A, Rabasco AM, Carosio R, Raffaghello L, Montaldo PG. Modified doxorubicin for improved encapsulation in PVA polymeric micelles. *Drug Deliv.* 2005; 12:15. [PubMed: 15801716]
102. Mishra D, Kang HC, Bae YH. Reconstitutable charged polymeric (PLGA)(2)-b-PEI micelles for gene therapeutics delivery. *Biomaterials.* 2011; 32:3845. [PubMed: 21354616]
103. Blanco E, Kessinger CW, Sumer BD, Gao J. Multifunctional micellar nanomedicine for cancer therapy. *Exp Biol Med (Maywood).* 2009; 234:123. [PubMed: 19064945]
104. Chandran T, Katragadda U, Teng Q, Tan C. Design and evaluation of micellar nanocarriers for 17-allylamino-17-demethoxygeldanamycin (17-AAG). *Int J Pharm.* 2010; 392:170. [PubMed: 20363305]
105. Torchilin VP. Structure and design of polymeric surfactant-based drug delivery systems. *J Control Release.* 2001; 73:137. [PubMed: 11516494]
106. Kabanov AV, Batrakova EV, Alakhov VY. Pluronic block copolymers as novel polymer therapeutics for drug and gene delivery. *J Control Release.* 2002; 82:189. [PubMed: 12175737]
107. Mikhail AS, Allen C. Poly(ethylene glycol)-b-poly(epsilon-caprolactone) micelles containing chemically conjugated and physically entrapped docetaxel: Synthesis, characterization, and the influence of the drug on micelle morphology. *Biomacromolecules.* 2010; 11:1273. [PubMed: 20369884]
108. Kakizawa Y, Furukawa S, Kataoka K. Block copolymer-coated calcium phosphate nanoparticles sensing intracellular environment for oligodeoxynucleotide and siRNA delivery. *J Control Release.* 2004; 97:345. [PubMed: 15196761]
109. Lavasanifar A, Samuel J, Kwon GS. Poly(ethylene oxide)-block-poly(l-amino acid) micelles for drug delivery. *Adv Drug Deliver Rev.* 2002; 54:169.
110. Chytil P, Etrych T, Konak C, Sirova M, Mrkván T, Bouček J, Rihova B, Ulbrich K. New HPMA copolymer-based drug carriers with covalently bound hydrophobic substituents for solid tumour targeting. *J Control Release.* 2008; 127:121. [PubMed: 18304673]
111. Jia Z, Wong L, Davis TP, Bulmus V. One-pot conversion of RAFT-generated multifunctional block copolymers of HPMA to doxorubicin conjugated acid- and reductant-sensitive crosslinked micelles. *Biomacromolecules.* 2008; 9:3106. [PubMed: 18844406]

112. Chandran SS, Nan A, Rosen DM, Ghandehari H, Denmeade SR. A prostate-specific antigen activated N-(2-hydroxypropyl) methacrylamide copolymer prodrug as dual-targeted therapy for prostate cancer. *Mol Cancer Ther.* 2007; 6:2928. [PubMed: 18025277]
113. Lele BS, Leroux JC. Synthesis and micellar characterization of novel amphiphilic A–B–A triblock copolymers of N-(2-Hydroxypropyl)methacrylamide or N-Vinyl-2-pyrrolidone with Poly(α -caprolactone). *Macromolecules.* 2002; 35:6714.
114. Neradovic D, van Steenberg MJ, Vansteelant L, Meijer YJ, van Nostrum CF, Hennink WE. Degradation mechanism and kinetics of thermosensitive polyacrylamides containing lactic acid side chains. *Macromolecules.* 2003; 36:7491.
115. Soga O, van Nostrum CF, Fens M, Rijcken CJ, Schiffelers RM, Storm G, Hennink WE. Thermosensitive and biodegradable polymeric micelles for paclitaxel delivery. *J Control Release.* 2005; 103:341. [PubMed: 15763618]
116. Talelli M, Rijcken CJ, van Nostrum CF, Storm G, Hennink WE. Micelles based on HPMA copolymers. *Adv Drug Deliver Rev.* 2010; 62:231.
117. Krimmer SG, Pan H, Liu J, Yang J, Kopecek J. Synthesis and characterization of poly(epsilon-caprolactone)-block-poly[N-(2-hydroxypropyl)methacrylamide] micelles for drug delivery. *Macromol Biosci.* 2011; 11:1041. [PubMed: 21567954]
118. Lee AL, Wang Y, Cheng HY, Pervaiz S, Yang YY. The co-delivery of paclitaxel and herceptin using cationic micellar nanoparticles. *Biomaterials.* 2009; 30:919. [PubMed: 19042015]
119. Oerlemans C, Bult W, Bos M, Storm G, Nijssen JF, Hennink WE. Polymeric micelles in anticancer therapy: Targeting, imaging and triggered release. *Pharm Res.* 2010; 27:2569. [PubMed: 20725771]
120. Danhier F, Ansorena E, Silva JM, Coco R, Le Breton A, Preat V. PLGA-based nanoparticles: An overview of biomedical applications. *J Control Release.* 2012; 161:505. [PubMed: 22353619]
121. Zhu H, Chen H, Zeng X, Wang Z, Zhang X, Wu Y, Gao Y, Zhang J, Liu K, Liu R, Cai L, Mei L, Feng SS. Co-delivery of chemotherapeutic drugs with vitamin E TPGS by porous PLGA nanoparticles for enhanced chemotherapy against multi-drug resistance. *Biomaterials.* 2014; 35:2391. [PubMed: 24360574]
122. Wang H, Zhao Y, Wu Y, Hu Y-l, Nan K, Nie G, Chen H. Enhanced anti-tumor efficacy by co-delivery of doxorubicin and paclitaxel with amphiphilic methoxy PEG-PLGA copolymer nanoparticles. *Biomaterials.* 2011; 32:8281. [PubMed: 21807411]
123. Lu Y, Yang Y, Sellinger A, Lu M, Huang J, Fan H, Haddad R, Lopez G, Burns A, Sasaki D, Shelnett J, Brinker C. Self-assembly of mesoscopically ordered chromatic polydiacetylene/silica nanocomposites. *Nature.* 2001; 410:913. [PubMed: 11309612]
124. Roy A, Singh MS, Upadhyay P, Bhaskar S. Nanoparticle mediated co-delivery of paclitaxel and a TLR-4 agonist results in tumor regression and enhanced immune response in the tumor microenvironment of a mouse model. *Int J Pharm.* 2013; 445:171. [PubMed: 23376226]
125. Ma X, Zhao Y, Ng KW, Zhao Y. Integrated hollow mesoporous silica nanoparticles for target drug/siRNA co-delivery. *Chem-Eur J.* 2013; 19:15593. [PubMed: 24123533]
126. Meng H, Mai W, Zhang H, Xue M, Xia T, Lin S, Wang X, Zhao Y, Ji Z, Zink J, Nel A. Codelivery of an optimal drug/siRNA combination using mesoporous silica nanoparticles to overcome drug resistance in breast cancer *in vitro* and *in vivo*. *ACS nano.* 2013; 7:994. [PubMed: 23289892]
127. Hao NJ, Li LF, Tang FQ. Shape-mediated biological effects of mesoporous silica nanoparticles. *J Biomed Nanotechnol.* 2014; 10:2508. [PubMed: 25992407]
128. Li LL, Liu TL, Fu CH, Liu HY, Tan LF, Meng XW. Multifunctional silica-based nanocomposites for cancer nanotheranostics. *J Biomed Nanotechnol.* 2014; 10:1784. [PubMed: 25992441]
129. Fang J, Nakamura H, Maeda H. The EPR effect: Unique features of tumor blood vessels for drug delivery, factors involved, and limitations and augmentation of the effect. *Adv Drug Deliver Rev.* 2011; 63:136.
130. Sun H, Meng F, Dias AA, Hendriks M, Feijen J, Zhong Z. Alpha-amino acid containing degradable polymers as functional biomaterials: Rational design, synthetic pathway, and biomedical applications. *Biomacromolecules.* 2011; 12:1937. [PubMed: 21469742]
131. De Souza R, Zahedi P, Allen CJ, Piquette-Miller M. Polymeric drug delivery systems for localized cancer chemotherapy. *Drug Deliver.* 2010; 17:365.

132. Couffin-Hoarau AC, Aubertin AM, Boustta M, Schmidt S, Fehrentz JA, Martinez J, Vert M. Peptide-poly(L-lysine citramide) conjugates and their *in vitro* anti-HIV behavior. *Biomacromolecules*. 2009; 10:865. [PubMed: 19296658]
133. Yang D, Van S, Liu J, Wang J, Jiang X, Wang Y, Yu L. Physicochemical properties and biocompatibility of a polymer-paclitaxel conjugate for cancer treatment. *Intl J Nanomed*. 2011; 6:2557.
134. Metselaar JM, Bruin P, de Boer LW, de Vringer T, Snel C, Oussoren C, Wauben MH, Crommelin DJ, Storm G, Hennink WE. A novel family of L-amino acid-based biodegradable polymer-lipid conjugates for the development of long-circulating liposomes with effective drug-targeting capacity. *Bioconjugate Chem*. 2003; 14:1156.
135. Baldwin AD, Kiick KL. Polysaccharide-modified synthetic polymeric biomaterials. *Biopolymers*. 2010; 94:128. [PubMed: 20091875]
136. Kemp JD, Cardillo T, Stewart BC, Kehrberg E, Weiner G, Hedlund B, Naumann PW. Inhibition of lymphoma growth *in vivo* by combined treatment with hydroxyethyl starch deferoxamine conjugate and IgG monoclonal antibodies against the transferrin receptor. *Cancer Res*. 1995; 55:3817. [PubMed: 7641199]
137. Pisal DS, Kosloski MP, Balu-Iyer SV. Delivery of therapeutic proteins. *J Pharm Sci*. 2010; 99:2557. [PubMed: 20049941]
138. Yurkovetskiy AV, Fram RJ. XMT-1001, a novel polymeric camptothecin pro-drug in clinical development for patients with advanced cancer. *Adv Drug Deliver Rev*. 2009; 61:1193.
139. Chipman SD, Oldham FB, Pezzoni G, Singer JW. Biological and clinical characterization of paclitaxel poliglumex (PPX, CT-2103), a macromolecular polymer-drug conjugate. *Intl J Nanomed*. 2006; 1:375.
140. Beer TM, Ryan C, Alumkal J, Ryan CW, Sun J, Eilers KM. A phase II study of paclitaxel poliglumex in combination with transdermal estradiol for the treatment of metastatic castration-resistant prostate cancer after docetaxel chemotherapy. *Colloq Inse*. 2010; 21:433.
141. Mita M, Mita A, Sarantopoulos J, Takimoto CH, Rowinsky EK, Romero O, Angiuli P, Allievi C, Eisenfeld A, Verschraegen CF. Phase I study of paclitaxel poliglumex administered weekly for patients with advanced solid malignancies. *Cancer Chemoth Pharm*. 2009; 64:287.
142. Sabbatini P, Sill MW, O'Malley D, Adler L, Secord AA. S Gynecologic Oncology Group. A phase II trial of paclitaxel poliglumex in recurrent or persistent ovarian or primary peritoneal cancer (EOC): A gynecologic oncology group study. *Gynecol Oncol*. 2008; 111:455. [PubMed: 18829087]
143. O'Brien ME, Socinski MA, Popovich AY, Bondarenko IN, Tomova A, Bilynsky BT, Hotko YS, Ganul VL, Kostinsky IY, Eisenfeld AJ, Sandalic L, Oldham FB, Bandstra B, Sandler AB, Singer JW. Randomized phase III trial comparing single-agent paclitaxel Poliglumex (CT-2103, PPX) with single-agent gemcitabine or vinorelbine for the treatment of PS 2 patients with chemotherapy-naïve advanced non-small cell lung cancer. *J Thorac Oncol*. 2008; 3:728. [PubMed: 18594318]
144. Man M, Rugo H. Paclitaxel poliglumex. *Cell Therapeutics/Chugai Pharmaceutical IDrugs*. 2005; 8:739. [PubMed: 16118697]
145. Sapra P, Zhao H, Mehlig M, Malaby J, Kraft P, Longley C, Greenberger LM, Horak ID. Novel delivery of SN38 markedly inhibits tumor growth in xenografts, including a camptothecin-11-refractory model. *Clin Cancer Res*. 2008; 14:1888. [PubMed: 18347192]
146. Pechar M, Ulbrich K, Subr V, Seymour LW, Schacht EH. Poly(ethylene glycol) multiblock copolymer as a carrier of anti-cancer drug doxorubicin. *Bioconjugate Chem*. 2000; 11:131.
147. Etrych T, Chytil P, Mrkvan T, Sirova M, Rihova B, Ulbrich K. Conjugates of doxorubicin with graft HPMA copolymers for passive tumor targeting. *J Control Release*. 2008; 132:184. [PubMed: 18534705]
148. Etrych T, Strohalm J, Chytil P, Cernoch P, Starovoytova L, Pechar M, Ulbrich K. Biodegradable star HPMA polymer conjugates of doxorubicin for passive tumor targeting. *Eur J Pharm Sci*. 2011; 42:527. [PubMed: 21392579]

149. Etrych T, Kovar L, Strohalm J, Chytil P, Rihova B, Ulbrich K. Biodegradable star HEMA polymer-drug conjugates: Biodegradability, distribution and anti-tumor efficacy. *J Control Release*. 2011; 154:241. [PubMed: 21699933]
150. Yang J, Luo K, Pan H, Kopeckova P, Kopecek J. Synthesis of biodegradable multiblock copolymers by click coupling of RAFT-generated heterotelechelic polyhpa conjugates. *React Funct Polym*. 2011; 71:294. [PubMed: 21499527]
151. Luo K, Yang J, Kopeckova P, Kopecek J. Biodegradable multiblock poly[N-(2-hydroxypropyl)methacrylamide] via reversible addition-fragmentation chain transfer polymerization and click chemistry. *Macromolecules*. 2011; 44:2481. [PubMed: 21552355]
152. Wang E, Xiong H, Zhou D, Xie Z, Huang Y, Jing X, Sun X. Co-delivery of oxaliplatin and demethylcantharidin via a polymer-drug conjugate. *Macromol Biosci*. 2014; 14:588. [PubMed: 24254404]
153. Kaneshiro TL, Lu ZR. Targeted intracellular codelivery of chemotherapeutics and nucleic acid with a well-defined dendrimer-based nanoglobular carrier. *Biomaterials*. 2009; 30:5660. [PubMed: 19595449]
154. Tomalia DA, Baker H, Dewald J, Hall M, Kallos G, Martin S, Roeck J, Ryder J, Smith P. A new class of polymers: Starburst-dendritic macromolecules. *Polym J*. 1985; 17:117.
155. Tomalia DA, Baker H, Dewald J, Hall M, Kallos G, Martin S, Roeck J, Ryder J, Smith P. Dendritic macromolecules: Synthesis of starburst dendrimers. *Macromolecules*. 1986; 19:2466.
156. Esfand R, Tomalia DA. Poly(amidoamine) (PAMAM) dendrimers: From biomimicry to drug delivery and biomedical applications. *Drug Discover Today*. 2001; 6:427.
157. Svenson S, Tomalia DA. Dendrimers in biomedical applications—reflections on the field. *Adv Drug Deliver Rev*. 2005; 57:2106.
158. Thiagarajan G, Ray A, Malugin A, Ghandehari H. PAMAM-camptothecin conjugate inhibits proliferation and induces nuclear fragmentation in colorectal carcinoma cells. *Pharm Res*. 2010; 27:2307. [PubMed: 20552256]
159. Vijayalakshmi N, Ray A, Malugin A, Ghandehari H. Carboxyl-terminated PAMAM-SN38 conjugates: Synthesis, characterization, and *in vitro* evaluation. *Bioconjugate Chem*. 2010; 21:1804.
160. Majoros IJ, Williams CR, Becker A, Baker JR Jr. Methotrexate delivery via folate targeted dendrimer-based nanotherapeutic platform. *Wiley Interdiscip Rev Nanomed Nanobiotechnol*. 2009; 1:502. [PubMed: 20049813]
161. Menjoge AR, Kannan RM, Tomalia DA. Dendrimer-based drug and imaging conjugates: Design considerations for nanomedical applications. *Drug Discover Today*. 2010; 15:171.
162. Gajbhiye V, Palanirajan VK, Tekade RK, Jain NK. Dendrimers as therapeutic agents: A systematic review. *J Pharm Pharmacol*. 2009; 61:989. [PubMed: 19703342]
163. Bhadra D, Bhadra S, Jain S, Jain NK. A PEGylated dendritic nanoparticulate carrier of fluorouracil. *Int J Pharm*. 2003; 257:111. [PubMed: 12711167]
164. Cheng Y, Xu Z, Ma M, Xu T. Dendrimers as drug carriers: Applications in different routes of drug administration. *J Pharm Sci*. 2008; 97:123. [PubMed: 17721949]
165. Goldberg DS, Ghandehari H, Swaan PW. Cellular entry of G3.5 poly (amido amine) dendrimers by clathrin- and dynamin-dependent endocytosis promotes tight junctional opening in intestinal epithelia. *Pharm Res*. 2010; 27:1547. [PubMed: 20411406]
166. Xu Q, Wang CH, Pack DW. Polymeric carriers for gene delivery: Chitosan and poly(amidoamine) dendrimers. *Curr Pharm Des*. 2010; 16:2350. [PubMed: 20618156]
167. Majoros IJ, Thomas TP, Mehta CB, Baker JR Jr. Poly(amidoamine) dendrimer-based multifunctional engineered nanodevice for cancer therapy. *J Med Chem*. 2005; 48:5892. [PubMed: 16161993]
168. Kukowska-Latallo JF, Candido KA, Cao Z, Nigavekar SS, Majoros IJ, Thomas TP, Balogh LP, Khan MK, Baker JR Jr. Nanoparticle targeting of anticancer drug improves therapeutic response in animal model of human epithelial cancer. *Cancer Res*. 2005; 65:5317. [PubMed: 15958579]
169. Filipowicz A, Wolowicz S. Solubility and *in vitro* transdermal diffusion of riboflavin assisted by PAMAM dendrimers. *Int J Pharm*. 2011; 408:152. [PubMed: 21272625]

170. Wiwattanapatapee R, Carreno-Gomez B, Malik N, Duncan R. Anionic PAMAM dendrimers rapidly cross adult rat intestine *in vitro*: A potential oral delivery system? *Pharm Res*. 2000; 17:991. [PubMed: 11028947]
171. Sadekar S, Ghandehari H. Transepithelial transport and toxicity of PAMAM dendrimers: Implications for oral drug delivery. *Adv Drug Deliver Rev*. 2012; 64:571.
172. Menjoge AR, Rinderknecht AL, Navath RS, Faridnia M, Kim CJ, Romero R, Miller RK, Kannan RM. Transfer of PAMAM dendrimers across human placenta: Prospects of its use as drug carrier during pregnancy. *J Control Release*. 2011; 150:326. [PubMed: 21129423]
173. Beg S, Samad A, Alam M, Nazish I. Dendrimers as novel systems for delivery of neuropharmaceuticals to the brain. *CNS Neurol Disord-Dr*. 2011; 10:576.
174. He H, Li Y, Jia XR, Du J, Ying X, Lu WL, Lou JN, Wei Y. PEGylated poly(amidoamine) dendrimer-based dual-targeting carrier for treating brain tumors. *Biomaterials*. 2011; 32:478. [PubMed: 20934215]
175. Ke W, Shao K, Huang R, Han L, Liu Y, Li J, Kuang Y, Ye L, Lou J, Jiang C. Gene delivery targeted to the brain using an angiopep-conjugated polyethyleneglycol-modified polyamidoamine dendrimer. *Biomaterials*. 2009; 30:6976. [PubMed: 19765819]
176. Sebestik J, Niederhafner P, Jezek J. Peptide and glycopeptide dendrimers and analogous dendrimeric structures and their biomedical applications. *Amino Acids*. 2011; 40:301. [PubMed: 21058024]
177. Li Y, Cheng Y, Xu T. Design, synthesis and potent pharmaceutical applications of glycodendrimers: A mini review. *Curr Drug Discov Technol*. 2007; 4:246. [PubMed: 18045087]
178. Frechet JM. Dendrimers and supramolecular chemistry. *P Natl Acad Sci USA*. 2002; 99:4782.
179. Jin Y, Ren X, Wang W, Ke L, Ning E, Du L, Bradshaw J. A 5-fluorouracil-loaded pH-responsive dendrimer nanocarrier for tumor targeting. *Int J Pharm*. 2011; 420:378. [PubMed: 21925254]
180. Raghupathi KR, Azagarsamy MA, Thayumanavan S. Guest-release control in enzyme-sensitive, amphiphilic-dendrimer-based nanoparticles through photochemical crosslinking. *Chem-Eur J*. 2011; 17:11752. [PubMed: 21887830]
181. Lee CC, Gillies ER, Fox ME, Guillaudeu SJ, Frechet JM, Dy EE, Szoka FC. A single dose of doxorubicin-functionalized bow-tie dendrimer cures mice bearing C-26 colon carcinomas. *P Natl Acad Sci USA*. 2006; 103:16649.
182. Medina SH, El-Sayed ME. Dendrimers as carriers for delivery of chemotherapeutic agents. *Chem Rev*. 2009; 109:3141. [PubMed: 19534493]
183. Longmire M, Choyke PL, Kobayashi H. Dendrimer-based contrast agents for molecular imaging. *Curr Top Med Chem*. 2008; 8:1180. [PubMed: 18855704]
184. Jelinkova M, Strohalm J, Etrych T, Ulbrich K, Rihova B. Starlike versus classic macromolecular prodrugs: Two different antibody-targeted HPMA copolymers of doxorubicin studied *in vitro* and *in vivo* as potential anticancer drugs. *Pharm Res*. 2003; 20:1558. [PubMed: 14620507]
185. Khandare JJ, Jayant S, Singh A, Chandna P, Wang Y, Vorsa N, Minko T. Dendrimer versus linear conjugate: Influence of polymeric architecture on the delivery and anticancer effect of paclitaxel. *Bioconjugate Chem*. 2006; 17:1464.
186. Cheng Y, Zhao L, Li Y, Xu T. Design of biocompatible dendrimers for cancer diagnosis and therapy: Current status and future perspectives. *Chem Soc Rev*. 2011; 40:2673. [PubMed: 21286593]
187. Goldberg DS, Vijayalakshmi N, Swaan PW, Ghandehari H. G3.5 PAMAM dendrimers enhance transepithelial transport of SN38 while minimizing gastrointestinal toxicity. *J Control Release*. 2011; 150:318. [PubMed: 21115079]
188. Mukherjee SP, Lyng FM, Garcia A, Davoren M, Byrne HJ. Mechanistic studies of *in vitro* cytotoxicity of poly(amidoamine) dendrimers in mammalian cells. *Toxicol Appl Pharm*. 2010; 248:259.
189. Greish K, Thiagarajan G, Herd H, Price R, Bauer H, Hubbard D, Burckle A, Sadekar S, Yu T, Anwar A, Ray A, Ghandehari H. Size and surface charge significantly influence the toxicity of silica and dendritic nanoparticles. *Nanotoxicology*. 2012; 6:713. [PubMed: 21793770]

190. Ziembra B, Janaszewska A, Ciepluch K, Krotewicz M, Fogel WA, Appelhans D, Voit B, Bryszewska M, Klajnert B. *In vivo* toxicity of poly(propyleneimine) dendrimers. *J Biomed Mater Res A*. 2011; 99:261. [PubMed: 21976451]
191. Chen AM, Zhang M, Wei D, Stueber D, Taratula O, Minko T, He H. Co-delivery of doxorubicin and Bcl-2 siRNA by mesoporous silica nanoparticles enhances the efficacy of chemotherapy in multidrug-resistant cancer cells. *Small*. 2009; 5:2673. [PubMed: 19780069]
192. Dilnawaz F, Singh A, Mohanty C, Sahoo SK. Dual drug loaded superparamagnetic iron oxide nanoparticles for targeted cancer therapy. *Biomaterials*. 2010; 31:3694. [PubMed: 20144478]
193. Singh A, Dilnawaz F, Mewar S, Sharma U, Jagannathan N, Sahoo S. Composite polymeric magnetic nanoparticles for co-delivery of hydrophobic and hydrophilic anticancer drugs and MRI imaging for cancer therapy. *ACS Appl Mater Interfaces*. 2011; 3:842. [PubMed: 21370886]
194. Taratula O, Kuzmov A, Shah M, Garbuzenko OB, Minko T. Nanostructured lipid carriers as multifunctional nanomedicine platform for pulmonary co-delivery of anticancer drugs and siRNA. *J Control Release*. 2013; 171:349. [PubMed: 23648833]
195. Yu YH, Kim E, Park DE, Shim G, Lee S, Kim YB, Kim CW, Oh YK. Cationic solid lipid nanoparticles for co-delivery of paclitaxel and siRNA. *Eur J Pharm Biopharm*. 2012; 80:268. [PubMed: 22108492]
196. Bartlett DW, Su H, Hildebrandt IJ, Weber WA, Davis ME. Impact of tumor-specific targeting on the biodistribution and efficacy of siRNA nanoparticles measured by multimodality *in vivo* imaging. *P Natl Acad Sci USA*. 2007; 104:15549.
197. Pirolo KF, Chang EH. Does a targeting ligand influence nanoparticle tumor localization or uptake? *Trends Biotechnol*. 2008; 26:552. [PubMed: 18722682]
198. Farokhzad OC, Langer R. Impact of nanotechnology on drug delivery. *ACS Nano*. 2009; 3:16. [PubMed: 19206243]
199. Gabathuler R. Approaches to transport therapeutic drugs across the blood-brain barrier to treat brain diseases. *Neurobiol Dis*. 2010; 37:48. [PubMed: 19664710]
200. Gu F, Zhang L, Teply BA, Mann N, Wang A, Radovic-Moreno AF, Langer R, Farokhzad OC. Precise engineering of targeted nanoparticles by using self-assembled biointegrated block copolymers. *P Natl Acad Sci USA*. 2008; 105:2586.
201. Allen TM, Cullis PR. Drug delivery systems: Entering the mainstream. *Science*. 2004; 303:1818. [PubMed: 15031496]
202. Jung H, Yang T, Lasagna MD, Shi J, Reinhart GD, Cremer PS. Impact of hapten presentation on antibody binding at lipid membrane interfaces. *Biophys J*. 2008; 94:3094. [PubMed: 18199665]
203. Yu MK, Park J, Jon S. Targeting strategies for multifunctional nanoparticles in cancer imaging and therapy. *Theranostics*. 2012; 2:3. [PubMed: 22272217]
204. Ferrara N. VEGF as a therapeutic target in cancer. *Oncology*. 2005; 69(Suppl 3):11. [PubMed: 16301831]
205. Van Cutsem E, Kohne CH, Hitre E, Zaluski J, Chang Chien CR, Makhson A, D'Haens G, Pinter T, Lim R, Bodoky G, Roh JK, Folprecht G, Ruff P, Stroh C, Tejpar S, Schlichting M, Nippgen J, Rougier P. Cetuximab and chemotherapy as initial treatment for metastatic colorectal cancer. *N Engl J Med*. 2009; 360:1408. [PubMed: 19339720]
206. Mi Y, Zhao J, Feng SS. Targeted co-delivery of docetaxel, cisplatin and herceptin by vitamin E TPGS-cisplatin pro-drug nanoparticles for multimodality treatment of cancer. *J Control Release*. 2013; 169:185. [PubMed: 23403395]
207. Hadjipanayis CG, Machaidze R, Kaluzova M, Wang L, Schuette AJ, Chen H, Wu X, Mao H. EGFRvIII antibody-conjugated iron oxide nanoparticles for magnetic resonance imaging-guided convection-enhanced delivery and targeted therapy of glioblastoma. *Cancer Res*. 2010; 70:6303. [PubMed: 20647323]
208. Gao X, Cui Y, Levenson RM, Chung LW, Nie S. *In vivo* cancer targeting and imaging with semiconductor quantum dots. *Nat Biotechnol*. 2004; 22:969. [PubMed: 15258594]
209. Raghavan R, Brady ML, Rodriguez-Ponce MI, Hartlep A, Pedain C, Sampson JH. Convection-enhanced delivery of therapeutics for brain disease, and its optimization. *Neurosurg Focus*. 2006; 20:E12. [PubMed: 16709017]

210. Bobo RH, Laske DW, Akbasak A, Morrison PF, Dedrick RL, Oldfield EH. Convection-enhanced delivery of macromolecules in the brain. *P Natl Acad Sci USA*. 1994; 91:2076.
211. Hadjipanayis CG, Fellows-Mayle W, Deluca NA. Therapeutic efficacy of a herpes simplex virus with radiation or temozolomide for intracranial glioblastoma after convection-enhanced delivery. *Mol Ther*. 2008; 16:1783. [PubMed: 18728637]
212. Morrison PF, Laske DW, Bobo H, Oldfield EH, Dedrick RL. High-flow microinfusion: Tissue penetration and pharmacodynamics. *Am J Physiol*. 1994; 266:R292. [PubMed: 8304553]
213. Ling Y, Wei K, Luo Y, Gao X, Zhong S. Dual docetaxel/superparamagnetic iron oxide loaded nanoparticles for both targeting magnetic resonance imaging and cancer therapy. *Biomaterials*. 2011; 32:7139. [PubMed: 21726899]
214. Wente M, Jain A, Kono E, Berberat P, Giese T, Reber H, Friess H, Büchler M, Reiter R, Hines O. Prostate stem cell antigen is a putative target for immunotherapy in pancreatic cancer. *Pancreas*. 2005; 31:119. [PubMed: 16024997]
215. Chen G, Chen W, Wu Z, Yuan R, Li H, Gao J, Shuai X. MRI-visible polymeric vector bearing CD3 single chain antibody for gene delivery to *T* cells for immunosuppression. *Biomaterials*. 2009; 30:1962. [PubMed: 19162315]
216. Tromsdorf UI, Bigall NC, Kaul MG, Bruns OT, Nikolic MS, Mollwitz B, Sperling RA, Reimer R, Hohenberg H, Parak WJ, Forster S, Beisiegel U, Adam G, Weller H. Size and surface effects on the MRI relaxivity of manganese ferrite nanoparticle contrast agents. *Nano Lett*. 2007; 7:2422. [PubMed: 17658761]
217. Olenchock BA, Guo R, Carpenter JH, Jordan M, Topham MK, Koretzky GA, Zhong XP. Disruption of diacyl-glycerol metabolism impairs the induction of *T* cell anergy. *Nat Immunol*. 2006; 7:1174. [PubMed: 17028587]
218. Zhong XP, Hainey EA, Olenchock BA, Zhao H, Topham MK, Koretzky GA. Regulation of *T* cell receptor-induced activation of the Ras-ERK pathway by diacylglycerol kinase zeta. *J Biol Chem*. 2002; 277:31089. [PubMed: 12070163]
219. Lu RM, Chang YL, Chen MS, Wu HC. Single chain anti-c-Met antibody conjugated nanoparticles for *in vivo* tumor-targeted imaging and drug delivery. *Biomaterials*. 2011; 32:3265. [PubMed: 21306768]
220. Birchmeier C, Birchmeier W, Gherardi E, Vande Woude GF. Met, metastasis, motility and more. *Nat Rev Mol Cell Biol*. 2003; 4:915. [PubMed: 14685170]
221. Cappuzzo F, Marchetti A, Skokan M, Rossi E, Gajapathy S, Felicioni L, Del Grammastro M, Sciarrotta MG, Buttitta F, Incarbone M, Toschi L, Finocchiaro G, Destro A, Terracciano L, Roncalli M, Alloisio M, Santoro A, Varella-Garcia M. Increased MET gene copy number negatively affects survival of surgically resected non-small-cell lung cancer patients. *J Clin Oncol*. 2009; 27:1667. [PubMed: 19255323]
222. Ding S, Merkulova-Rainon T, Han ZC, Tobelem G. HGF receptor up-regulation contributes to the angiogenic phenotype of human endothelial cells and promotes angiogenesis *in vitro*. *Blood*. 2003; 101:4816. [PubMed: 12595309]
223. Wang AZ, Gu F, Zhang L, Chan JM, Radovic-Moreno A, Shaikh MR, Farokhzad OC. Biofunctionalized targeted nanoparticles for therapeutic applications. *Expert Opin Biol Th*. 2008; 8:1063.
224. McCarthy JR, Bhaumik J, Karver MR, Erdem SS, Weissleder R. Targeted nanoagents for the detection of cancers. *Mol Oncol*. 2010; 4:511. [PubMed: 20851695]
225. Kumar M, Yigit M, Dai G, Moore A, Medarova Z. Image-guided breast tumor therapy using a small interfering RNA nanodrug. *Cancer Res*. 2010; 70:7553. [PubMed: 20702603]
226. Perey L, Hayes DF, Maimonis P, Abe M, O'Hara C, Kufe DW. Tumor selective reactivity of a monoclonal antibody prepared against a recombinant peptide derived from the DF3 human breast carcinoma-associated antigen. *Cancer Res*. 1992; 52:2563. [PubMed: 1373671]
227. Liu D, Bimbo LM, Makila E, Villanova F, Kaasalainen M, Herranz-Blanco B, Caramella CM, Lehto VP, Salonen J, Herzig KH, Hirvonen J, Santos HA. Co-delivery of a hydrophobic small molecule and a hydrophilic peptide by porous silicon nanoparticles. *J Control Release*. 2013; 170:268. [PubMed: 23756152]

228. Li X, Lu X, Xu H, Zhu Z, Yin H, Qian X, Li R, Jiang X, Liu B. Paclitaxel/tetrandrine coloaded nanoparticles effectively promote the apoptosis of gastric cancer cells based on oxidation therapy. *Mol Pharm*. 2012; 9:222. [PubMed: 22171565]
229. Mok H, Park JW, Park TG. Enhanced intracellular delivery of quantum dot and adenovirus nanoparticles triggered by acidic pH via surface charge reversal. *Bioconjugate Chem*. 2008; 19:797.
230. Min KH, Kim JH, Bae SM, Shin H, Kim MS, Park S, Lee H, Park RW, Kim IS, Kim K, Kwon IC, Jeong SY, Lee DS. Tumoral acidic pH-responsive MPEG-poly(beta-amino ester) polymeric micelles for cancer targeting therapy. *J Control Release*. 2010; 144:259. [PubMed: 20188131]
231. Sethuraman VA, Na K, Bae YH. pH-responsive sulfonamide/PEI system for tumor specific gene delivery: An *in vitro* study. *Biomacromolecules*. 2006; 7:64. [PubMed: 16398499]
232. Mok H, Veiseh O, Fang C, Kievit FM, Wang FY, Park JO, Zhang M. pH-Sensitive siRNA nanovector for targeted gene silencing and cytotoxic effect in cancer cells. *Mol Pharm*. 2010; 7:1930. [PubMed: 20722417]
233. Lee Y, Fukushima S, Bae Y, Hiki S, Ishii T, Kataoka K. A protein nanocarrier from charge-conversion polymer in response to endosomal pH. *J Am Chem Soc*. 2007; 129:5362. [PubMed: 17408272]
234. Simberg D, Duza T, Park JH, Essler M, Pilch J, Zhang L, Derfus AM, Yang M, Hoffman RM, Bhatia S, Sailor MJ, Ruoslahti E. Biomimetic amplification of nanoparticle homing to tumors. *P Natl Acad Sci USA*. 2007; 104:932.
235. Perez EA. Impact, mechanisms, and novel chemotherapy strategies for overcoming resistance to anthracyclines and taxanes in metastatic breast cancer. *Breast Cancer Res Tr*. 2009; 114:195.
236. Zhang H, Ma Y, Sun XL. Recent developments in carbohydrate-decorated targeted drug/gene delivery. *Med Res Rev*. 2010; 30:270. [PubMed: 19626595]
237. Shen Z, Wei W, Tanaka H, Kohama K, Ma G, Dobashi T, Maki Y, Wang H, Bi J, Dai S. A galactosamine-mediated drug delivery carrier for targeted liver cancer therapy. *Pharmacol Res*. 2011; 64:410. [PubMed: 21723392]
238. Kim EM, Jeong HJ, Park IK, Cho CS, Moon HB, Yu DY, Bom HS, Sohn MH, Oh IJ. Asialoglycoprotein receptor targeted gene delivery using galactosylated polyethylenimine-graft-poly(ethylene glycol): *In vitro* and *in vivo* studies. *J Control Release*. 2005; 108:557. [PubMed: 16253376]
239. Yang Y, Zhang Z, Chen L, Gu W, Li Y. Galactosylated poly(2-(2-aminoethoxy)ethoxy)phosphazene/DNA complex nanoparticles: *In vitro* and *in vivo* evaluation for gene delivery. *Biomacromolecules*. 2010; 11:927. [PubMed: 20302354]
240. Jiang HL, Kwon JT, Kim EM, Kim YK, Arote R, Jere D, Jeong HJ, Jang MK, Nah JW, Xu CX, Park IK, Cho MH, Cho CS. Galactosylated poly(ethylene glycol)-chitosan-graft-polyethylenimine as a gene carrier for hepatocyte-targeting. *J Control Release*. 2008; 131:150. [PubMed: 18706946]
241. Lu W, Xiong C, Zhang G, Huang Q, Zhang R, Zhang JZ, Li C. Targeted photothermal ablation of murine melanomas with melanocyte-stimulating hormone analog-conjugated hollow gold nanospheres. *Clin Cancer Res*. 2009; 15:876. [PubMed: 19188158]
242. Foraker AB, Khantwal CM, Swaan PW. Current perspectives on the cellular uptake and trafficking of riboflavin. *Adv Drug Deliver Rev*. 2003; 55:1467.
243. Karande AA, Sridhar L, Gopinath KS, Adiga PR. Riboflavin carrier protein: A serum and tissue marker for breast carcinoma. *Int J Cancer*. 2001; 95:277. [PubMed: 11494224]
244. Jayapaul J, Hoenius M, Arns S, Lederle W, Lammers T, Comba P, Kiessling F, Gaetjens J. FMN-coated fluorescent iron oxide nanoparticles for RCP-mediated targeting and labeling of metabolically active cancer and endothelial cells. *Biomaterials*. 2011; 32:5863. [PubMed: 21605902]
245. Lee CM, Jeong HJ, Kim EM, Kim DW, Lim ST, Kim HT, Park IK, Jeong YY, Kim JW, Sohn MH. Super-paramagnetic iron oxide nanoparticles as a dual imaging probe for targeting hepatocytes *in vivo*. *Magn Reson Med*. 2009; 62:1440. [PubMed: 19859969]
246. Wilson DS, Szostak JW. *In vitro* selection of functional nucleic acids. *Annu Rev Biochem*. 1999; 68:611. [PubMed: 10872462]

247. Tuerk C, Gold L. Systematic evolution of ligands by exponential enrichment: RNA ligands to bacteriophage T4 DNA polymerase. *Science*. 1990; 249:505. [PubMed: 2200121]
248. Liu B, Zhang JN, Liao J, Liu J, Chen K, Tong GX, Yuan P, Liu ZX, Pu Y, Liu HX. Aptamer-functionalized nanoparticles for drug delivery. *J Biomed Nanotechnol*. 2014; 10:3189. [PubMed: 26000380]
249. Xi ZJ, Huang RR, Deng Y, He NY. Progress in selection and biomedical applications of aptamers. *J Biomed Nanotechnol*. 2014; 10:3043. [PubMed: 25992428]
250. Aravind A, Varghese S, Veerananarayanan S, Mathew A, Nagaoka Y, Iwai S, Fukuda T, Hasumura T, Yoshida Y, Maekawa T, Kumar DS. Aptamer-labeled PLGA nanoparticles for targeting cancer cells. *Cancer Nanotechnol*. 2012; 3:1. [PubMed: 26069492]
251. Lee JF, Hesselberth JR, Meyers LA, Ellington AD. Aptamer database. *Nucleic Acids Res*. 2004; 32:D95. [PubMed: 14681367]
252. Lee JF, Stovall GM, Ellington AD. Aptamer therapeutics advance. *Curr Opin Chem Biol*. 2006; 10:282. [PubMed: 16621675]
253. Rosenberg JE, Bambury RM, Van Allen EM, Drabkin HA, Lara PN Jr, Harzstark AL, Wagle N, Figlin RA, Smith GW, Garraway LA, Choueiri T, Erlandsson F, Laber DA. A phase II trial of AS1411 (a novel nucleolin-targeted DNA aptamer) in metastatic renal cell carcinoma. *Invest New Drug*. 2014; 32:178.
254. Bates PJ, Kahlon JB, Thomas SD, Trent JO, Miller DM. Antiproliferative activity of G-rich oligonucleotides correlates with protein binding. *J Biol Chem*. 1999; 274:26369. [PubMed: 10473594]
255. Bates PJ, Laber DA, Miller DM, Thomas SD, Trent JO. Discovery and development of the G-rich oligonucleotide AS1411 as a novel treatment for cancer. *Exp Mol Pathol*. 2009; 86:151. [PubMed: 19454272]
256. Mongelard F, Bouvet P. AS-1411, a guanosine-rich oligonucleotide aptamer targeting nucleolin for the potential treatment of cancer, including acute myeloid leukemia. *Curr Opin Mol Ther*. 2010; 12:107. [PubMed: 20140822]
257. Bouchard PR, Hutabarat RM, Thompson KM. Discovery and development of therapeutic aptamers. *Annu Rev Pharmacol*. 2010; 50:237.
258. Lupold SE, Hicke BJ, Lin Y, Coffey DS. Identification and characterization of nuclease-stabilized RNA molecules that bind human prostate cancer cells via the prostate-specific membrane antigen. *Cancer Res*. 2002; 62:4029. [PubMed: 12124337]
259. Bagalkot V, Farokhzad OC, Langer R, Jon S. An aptamer-doxorubicin physical conjugate as a novel targeted drug-delivery platform. *Angew Chem Int Ed Engl*. 2006; 45:8149. [PubMed: 17099918]
260. Farokhzad OC, Cheng J, Teply BA, Sherifi I, Jon S, Kantoff PW, Richie JP, Langer R. Targeted nanoparticle-aptamer bioconjugates for cancer chemotherapy *in vivo*. *P Natl Acad Sci USA*. 2006; 103:6315.
261. Farokhzad OC, Jon S, Khademhosseini A, Tran TN, Lavan DA, Langer R. Nanoparticle-aptamer bioconjugates: A new approach for targeting prostate cancer cells. *Cancer Res*. 2004; 64:7668. [PubMed: 15520166]
262. Dassie JP, Liu XY, Thomas GS, Whitaker RM, Thiel KW, Stockdale KR, Meyerholz DK, McCaffrey AP, McNamara JO 2nd, Giangrande PH. Systemic administration of optimized aptamer-siRNA chimeras promotes regression of PSMA-expressing tumors. *Nat Biotechnol*. 2009; 27:839. [PubMed: 19701187]
263. Hwang do W, Ko HY, Lee JH, Kang H, Ryu SH, Song IC, Lee DS, Kim S. A nucleolin-targeted multimodal nanoparticle imaging probe for tracking cancer cells using an aptamer. *J Nucl Med*. 2010; 51:98. [PubMed: 20008986]
264. Derenzini M, Sirri V, Trere D, Ochs RL. The quantity of nucleolar proteins nucleolin and protein B23 is related to cell doubling time in human cancer cells. *Lab Invest*. 1995; 73:497. [PubMed: 7474921]
265. Antunes P, Ginj M, Zhang H, Waser B, Baum RP, Reubi JC, Maecke H. Are radiogallium-labelled DOTA-conjugated somatostatin analogues superior to those labelled with other radiometals? *Eur J Nucl Med Mol I*. 2007; 34:982.

266. Li N, Larson T, Nguyen HH, Sokolov KV, Ellington AD. Directed evolution of gold nanoparticle delivery to cells. *Chem Commun.* 2010; 46:392.
267. Gunthert U, Hofmann M, Rudy W, Reber S, Zoller M, Haussmann I, Matzku S, Wenzel A, Ponta H, Herrlich P. A new variant of glycoprotein CD44 confers metastatic potential to rat carcinoma cells. *Cell.* 1991; 65:13. [PubMed: 1707342]
268. Platt VM, Szoka FC Jr. Anticancer therapeutics: Targeting macromolecules and nanocarriers to hyaluronan or CD44, a hyaluronan receptor. *Mol Pharm.* 2008; 5:474. [PubMed: 18547053]
269. Bhang SH, Won N, Lee TJ, Jin H, Nam J, Park J, Chung H, Park HS, Sung YE, Hahn SK, Kim BS, Kim S. Hyaluronic acid-quantum dot conjugates for *in vivo* lymphatic vessel imaging. *ACS Nano.* 2009; 3:1389. [PubMed: 19476339]
270. Wu W, Shen J, Banerjee P, Zhou S. Core-shell hybrid nanogels for integration of optical temperature-sensing, targeted tumor cell imaging, and combined chemo-photothermal treatment. *Biomaterials.* 2010; 31:7555. [PubMed: 20643481]
271. Pekkanen AM, DeWitt MR, Rylander MN. Nanoparticle enhanced optical imaging and phototherapy of cancer. *J Biomed Nanotechnol.* 2014; 10:1677. [PubMed: 25992437]
272. Yoo D, Lee JH, Shin TH, Cheon J. Theranostic magnetic nanoparticles. *Accounts Chem Res.* 2011; 44:863.
273. Rosen JE, Chan L, Shieh DB, Gu FX. Iron oxide nanoparticles for targeted cancer imaging and diagnostics. *Nanomedicine-UK.* 2012; 8:275.
274. Singh R, Nalwa HS. Medical applications of nanoparticles in biological imaging, cell labeling, antimicrobial agents, and anti-cancer nanodrugs. *J Biomed Nanotechnol.* 2011; 7:489. [PubMed: 21870454]
275. Gu FX, Karnik R, Wang AZ, Alexis F, Levy-Nissenbaum E, Hong S, Langer RS, Farokhzad OC. Targeted nanoparticles for cancer therapy. *Nano Today.* 2007; 2:14.
276. Nurunnabi M, Khatun Z, Moon WC, Lee G, Lee YK. Heparin based nanoparticles for cancer targeting and noninvasive imaging. *Quant Imaging Med Surg.* 2012; 2:219. [PubMed: 23256083]
277. Cai WB, Chen XY. Nanoplatforams for targeted molecular imaging in living subjects. *Small.* 2007; 3:1840. [PubMed: 17943716]
278. Khemtong C, Kessinger CW, Gao J. Polymeric nanomedicine for cancer MR imaging and drug delivery. *Chem Commun.* 2009:3497–510.
279. Gelperina S, Kisich K, Iseman MD, Heifets L. The potential advantages of nanoparticle drug delivery systems in chemotherapy of tuberculosis. *Am J Resp Crit Care.* 2005; 172:1487.
280. Park JH, Saravanakumar G, Kim K, Kwon IC. Targeted delivery of low molecular drugs using chitosan and its derivatives. *Adv Drug Deliver Rev.* 2010; 62:28.
281. Ahmed N, Fessi H, Elaissari A. Theranostic applications of nanoparticles in cancer. *Drug Discov Today.* 2012; 17:928. [PubMed: 22484464]
282. Kelkar SS, Reineke TM. Theranostics: Combining imaging and therapy. *Bioconjugate Chem.* 2011; 22:1879.
283. Kim K, Kim JH, Park H, Kim YS, Park K, Nam H, Lee S, Park JH, Park RW, Kim IS, Choi K, Kim SY, Park K, Kwon IC. Tumor-homing multifunctional nanoparticles for cancer theragnosis: Simultaneous diagnosis, drug delivery, and therapeutic monitoring. *J Control Release.* 2010; 146:219. [PubMed: 20403397]
284. Min KH, Park K, Kim YS, Bae SM, Lee S, Jo HG, Park RW, Kim IS, Jeong SY, Kim K, Kwon IC. Hydrophobically modified glycol chitosan nanoparticles-encapsulated camptothecin enhance the drug stability and tumor targeting in cancer therapy. *J Control Release.* 2008; 127:208. [PubMed: 18336946]
285. Na JH, Koo H, Lee S, Min KH, Park K, Yoo H, Lee SH, Park JH, Kwon IC, Jeong SY, Kim K. Real-time and non-invasive optical imaging of tumor-targeting glycol chitosan nanoparticles in various tumor models. *Biomaterials.* 2011; 32:5252. [PubMed: 21513975]
286. Ryu JH, Kim SA, Koo H, Yhee JY, Lee A, Na JH, Youn I, Choi K, Kwon IC, Kim BS, Kim K. Cathepsin B-sensitive nanoprobe for *in vivo* tumor diagnosis. *J Mater Chem.* 2011; 21:17631.
287. Chen KJ, Chiu YL, Chen YM, Ho YC, Sung HW. Intracellularly monitoring/imaging the release of doxorubicin from pH-responsive nanoparticles using Forster resonance energy transfer. *Biomaterials.* 2011; 32:2586. [PubMed: 21251711]

288. Kobayashi H, Choyke PL. Target-cancer-cell-specific activatable fluorescence imaging probes: Rational design and *in vivo* applications. *Accounts Chem Res.* 2011; 44:83.
289. Pittet MJ, Weissleder R. Intravital imaging. *Cell.* 2011; 147:983. [PubMed: 22118457]
290. Bullen A. Microscopic imaging techniques for drug discovery. *Nat Rev Drug Discov.* 2008; 7:54. [PubMed: 18079755]
291. Amornphimoltham P, Masedunskas A, Weigert R. Intravital microscopy as a tool to study drug delivery in preclinical studies. *Adv Drug Deliver Rev.* 2011; 63:119.
292. Eichhorn ME, Strieth S, Luedemann S, Kleespies A, Noth U, Passon A, Brix G, Jauch KW, Bruns CJ, Dellian M. Contrast enhanced MRI and intravital fluorescence microscopy indicate improved tumor microcirculation in highly vascularized melanomas upon short-term anti-VEGFR treatment. *Cancer Biol Ther.* 2008; 7:1006. [PubMed: 18398295]
293. Cabral H, Matsumoto Y, Mizuno K, Chen Q, Murakami M, Kimura M, Terada Y, Kano MR, Miyazono K, Uesaka M, Nishiyama N, Kataoka K. Accumulation of sub-100 nm polymeric micelles in poorly permeable tumours depends on size. *Nat Nanotechnol.* 2011; 6:815. [PubMed: 22020122]

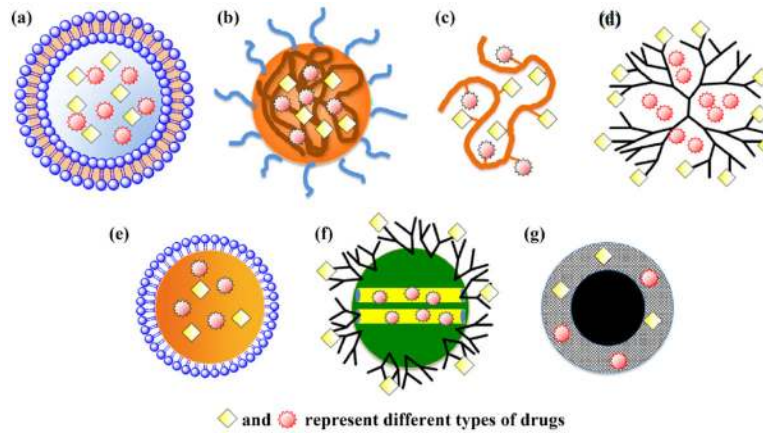


Figure 1. Schematic illustration of nanoscale drug carriers used for combinatorial drug delivery: (a) liposome, (b) polymeric micelle, (c) polymer-drug conjugate, (d) dendrimer, (e) oil nanoemulsion, (f) mesoporous silica nanoparticle, and (g) iron oxide nanoparticle. Reprinted with permission from [98], C. M. Hu and L. Zhang, Nanoparticle-based combination therapy toward overcoming drug resistance in cancer. *Biochemical pharmacology* 83, 1104 (2012). © 2012, Elsevier.

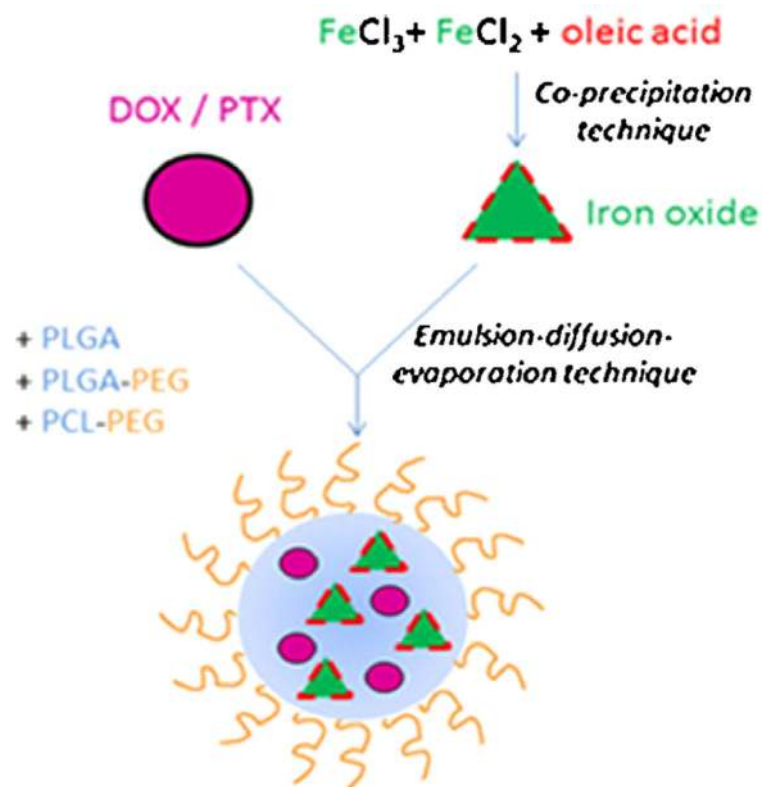


Figure 2. Schematic representation of SPIO/PTX-loaded PLGA-based nanoparticles. Reprinted with permission from [277], N. Schleich, et al., Dual anticancer drug/superparamagnetic iron oxide-loaded PLGA-based nanoparticles for cancer therapy and magnetic resonance imaging. *Int. J. Pharm.* 447, 94 (2013). © 2013, Elsevier.

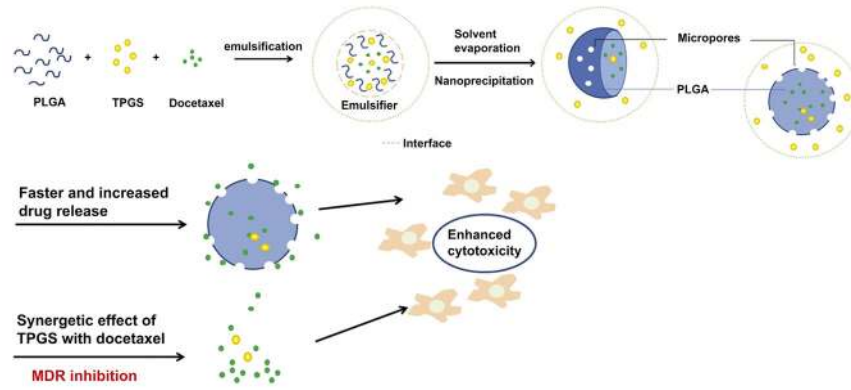


Figure 3. Schematic graph of TPGS functions as a pore former and promotes anti-tumor activity of DTX-loaded Nps. Reprinted with permission from [110], H. Zhu, et al., Co-delivery of chemotherapeutic drugs with vitamin E TPGS by porous PLGA nanoparticles for enhanced chemotherapy against multi-drug resistance. *Biomaterials* 35, 2391 (2014). © 2014, Elsevier.

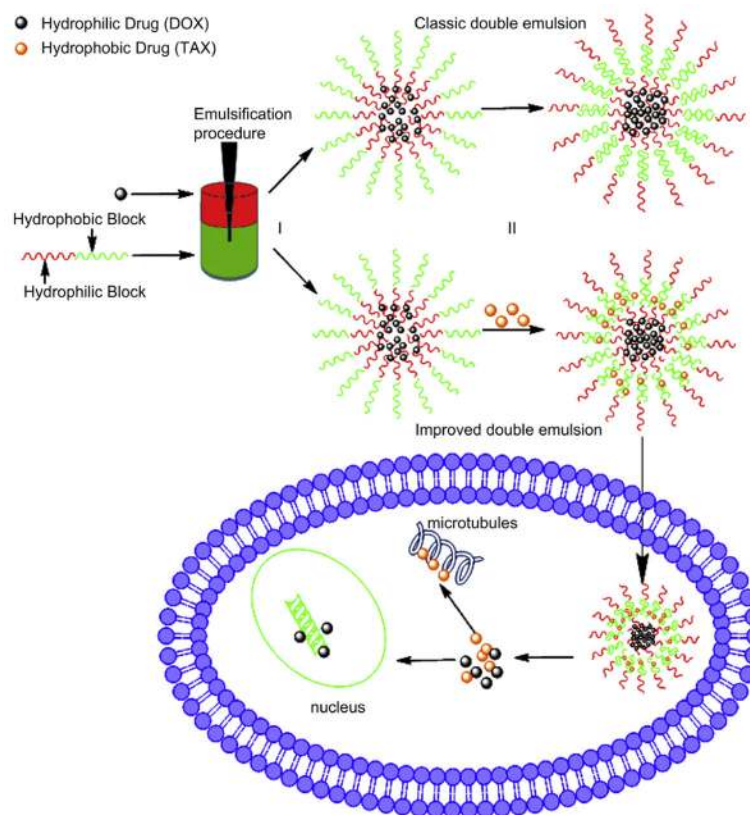
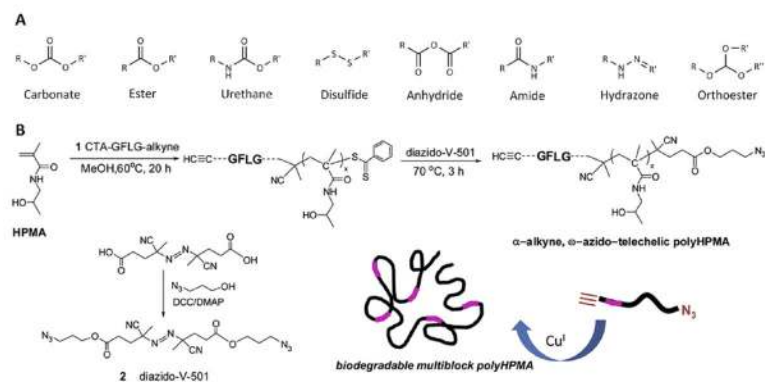


Figure 4.

Illustration of biodegradable amphiphilic copolymer NPs loaded with both DOX and TAX using improved double emulsion method. Emulsification procedure used to generate double emulsions. Step (I), generating water-in-oil for encapsulations of DOX; Step (II), generating water-in-oil-in-water for encapsulations of TAX. Green represents the oil phase containing amphiphilic copolymer and red the aqueous phase containing DOX. Reprinted with permission from [111], H. Wang, et al., Enhanced anti-tumor efficacy by co-delivery of doxorubicin and paclitaxel with amphiphilic methoxy PEG-PLGA copolymer nanoparticles. *Biomaterials* 32, 8281 (2011). © 2011, Elsevier.

**Figure 5.**

(A) Examples of bonds utilized in the synthesis of biodegradable polymer-drug conjugates. Biodegradation typically occurs via hydrolysis (via reduction for disulfides). (B) Overall strategy for the synthesis of multiblock polyHPMA copolymers. HPMA copolymer blocks are linked together via lysosomally degradable Gly-Phe-Leu-Gly (GFLG) linkages introduced via a combination of RAFT polymerization and click chemistry. Reprinted with permission from [137], J. Yang, et al., Synthesis of biodegradable multiblock copolymers by click coupling of RAFT-generated heterotelechelic polyhpma conjugates. *Reactive and Functional Polymers* 71, 294 (2011). © 2011, Elsevier.

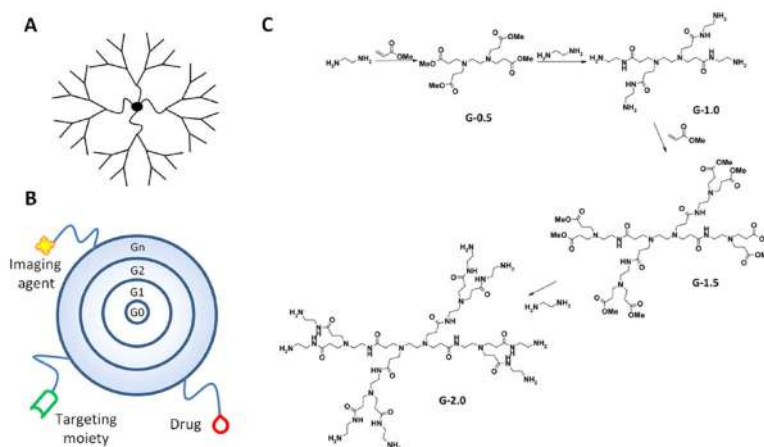


Figure 6. (A) Dendrimers are hyperbranched, star-link polymers. Drugs can be either conjugated to the dendrimer surface or encapsulated within “void” spaces between adjacent branches. (B) Dendrimers grow linearly in size and exponentially in surface area with each successive “generation.” They can be utilized as multifunctional nanocarriers, bearing drugs, imaging agents, and/or targeting moieties. (C) Synthesis of poly(amido amine) (PAMAM) dendrimers occurs from a ethylenediamine core with alternating reactions with methyl acrylate and ethylenediamine to produce each generation. Reprinted with permission from [278], N. Larson and H. Ghandehari, Polymeric conjugates for drug delivery. *Chem. Mater.* 24, 840 (2012). © 2012, American Chemical Society.

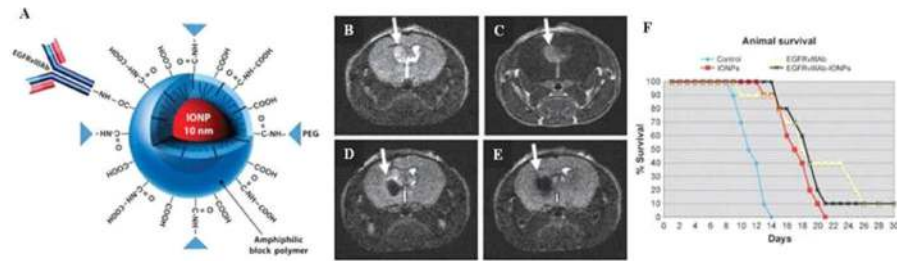


Figure 7.

(A) Schematic diagram showing EGFRvIII-IONPs. (B)–(F) Survival studies of nude mice implanted with the U87 Δ EGFRvIII glioma model. (B) T2-weighted MRI showing a tumor region with a bright signal 7 days after tumor implantation (arrow). (C) A tumor is shown (arrow) after injection of a gadolinium contrast agent (Gd-DTPA). (D) The MRI signal decreased (arrow) after CED of EGFRvIIIAb-IONPs. (E) EGFRvIIIAb-IONP dispersion and T2 signal decrease (arrow) 4 days after CED. (F) Survival curve of the nude mice bearing U87 Δ EGFRvIII cells after a treatment regimen of MRI-guided CED: the untreated control, IONPs, EGFRvIIIAb, or EGFRvIIIAb-IONPs. Reprinted with permission from [194], C. G. Hadjipanayis, et al., EGFRvIII antibody-conjugated iron oxide nanoparticles for magnetic resonance imaging-guided convection-enhanced delivery and targeted therapy of glioblastoma. *Cancer Res.* 70, 6303 (2010). © 2010, Cancer Research.

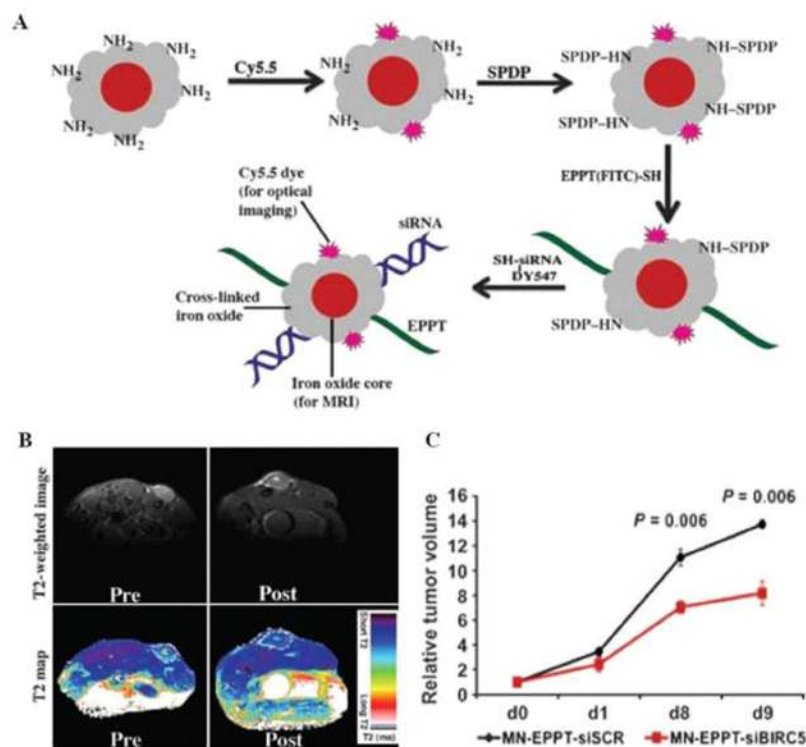


Figure 8.

(A) Schematic diagram showing the synthesis of MN-EPPT-siBIRC5. (B) Representative pre-contrast images and 24 h post-contrast T2-weighted images (top), and color-coded T2 maps (bottom) of the tumor-bearing mice i.v. injected with MN-EPPT-siBIRC5 (10 mg/kg Fe). (C) Relative tumor volume measurements of MN-EPPT-siBIRC5- and MN-EPPT-siSCR-injected animals over the course of treatment. Reprinted with permission from [212], M. Kumar, et al., Image-guided breast tumor therapy using a small interfering RNA nanodrug. *Cancer Res.* 70, 7553 (2010). © 2010, Cancer Research.

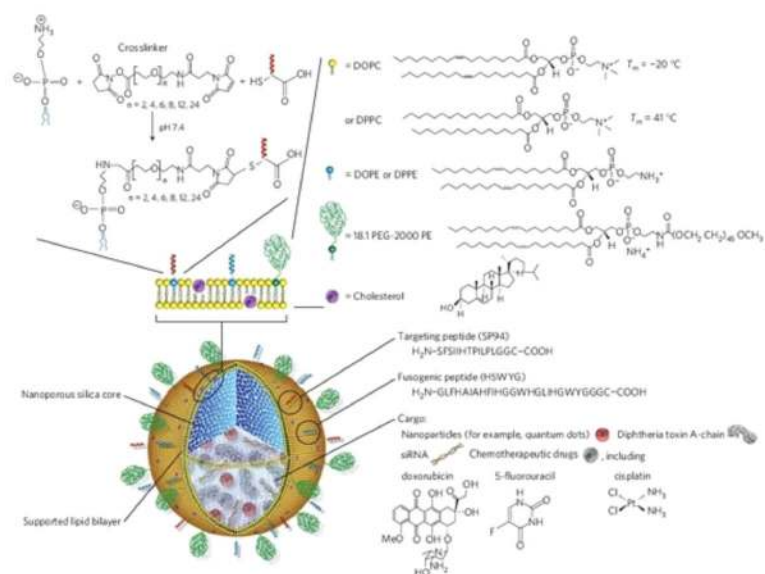


Figure 9. Schematic illustration of the silica nanoporous particle-supported lipid bilayer, depicting the disparate types of therapeutic and diagnostic agents that can be loaded within the nanoporous silica core, as well as the ligands that can be displayed on the surface of the nanoparticle. Reprinted with permission from [279], C. E. Ashley, et al., The targeted delivery of multicomponent cargos to cancer cells by nanoporous particle-supported lipid bilayers. *Nature materials* 10, 389 (2011). © 2011, Nature Publishing Group.

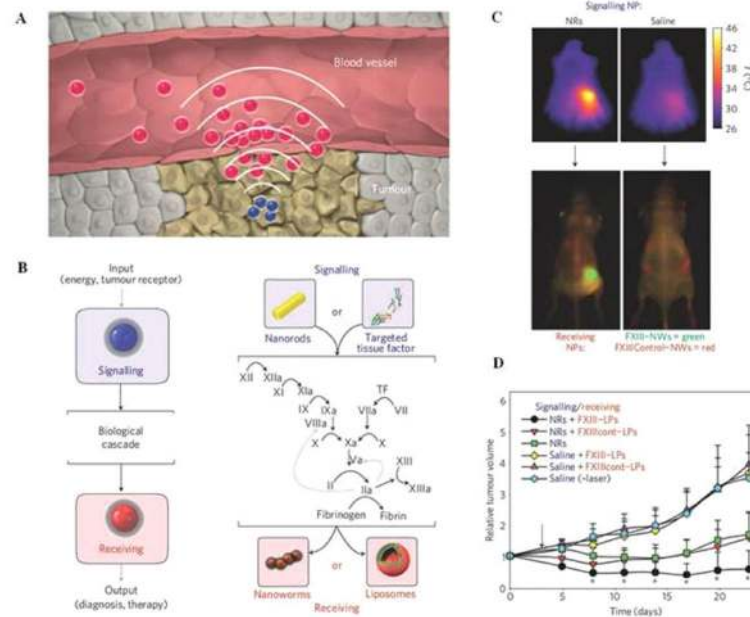


Figure 10.

(A) Schematic representation of nanoparticle communication to achieve amplified tumor targeting. Tumor-targeted signaling nanoparticles (blue) broadcast the tumor location to the receiving nanoparticles (red) present in circulation. (B) Shown are the harnessing of the biological cascade to transmit and amplify nanoparticle communication and the molecular signaling pathway between the signaling and receiving components. (C) Thermographic images of the photothermal NRs with heating. Seventy-two hours after NR or saline injection, mice were co-injected with FXIII-NWs and untargeted control-NWs, and their right flanks were broadly irradiated (top). Twenty-four hours post-irradiation, whole-animal fluorescence imaging revealed the distribution of the receiving nanoparticles (bottom). (D) Amplified tumor therapy with communicating nanoparticles. Tumor volumes following a single treatment with the communicating nanoparticle systems and controls. Reprinted with permission from [280], G. von Maltzahn, et al., Nanoparticles that communicate *in vivo* to amplify tumour targeting. *Nature Materials* 10, 545 (2011). © 2011, Nature Publishing Group.

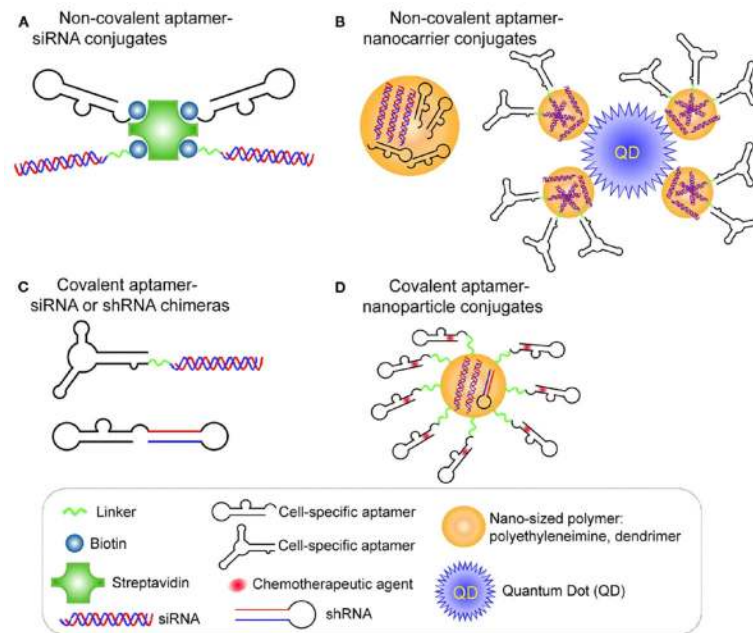


Figure 11.

Schematic illustration of (A) the intercalation of a hydrophilic anthracycline drug, such as DOX within the A10 PSMA aptamer; (B) the encapsulation of a hydrophobic drug, such as Dtxl, within the PLGA-b-PEG nanoparticles using the nano-precipitation method; and (C) nanoparticle–aptamer (NP–Apt) bioconjugates comprised of PLGA-b-PEG nanoparticles surface functionalized with the A10 PSMA aptamer for co-delivery of Dtxl and DOX. Both drugs can be released from the bioconjugates over time. Reprinted with permission from [281], J. Zhou, et al., Current progress of RNA aptamer-based therapeutics. *Frontiers in Genetics* 3, 234 (2012). © 2012, Cancer Research.

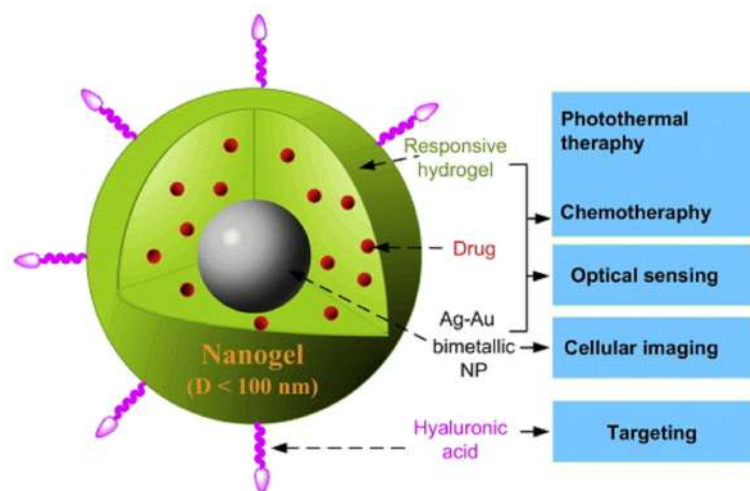


Figure 12.

Schematic illustration of multifunctional core-shell hybrid nanogels. The Ag–Au bimetallic NP (10 ± 3 nm) core is NIR resonant and highly fluorescent. The thermo-responsive nonlinear PEG-based gel shell cannot only manipulate the fluorescence intensity of Ag–Au NP core, but also trigger the release of drug molecules encapsulated in the gel shell under the local temperature increase of targeted pathological zones or the heat generated upon NIR irradiation. HA, a known targeting ligand, can be readily semi-interpenetrated into the surface networks of gel shell at a light penetration depth. Reprinted with permission from [254], W. Wu, et al., Core-shell hybrid nanogels for integration of optical temperature-sensing, targeted tumor cell imaging, and combined chemo-photothermal treatment. *Biomaterials* 31, 7555 (2010). © 2010, Elsevier.

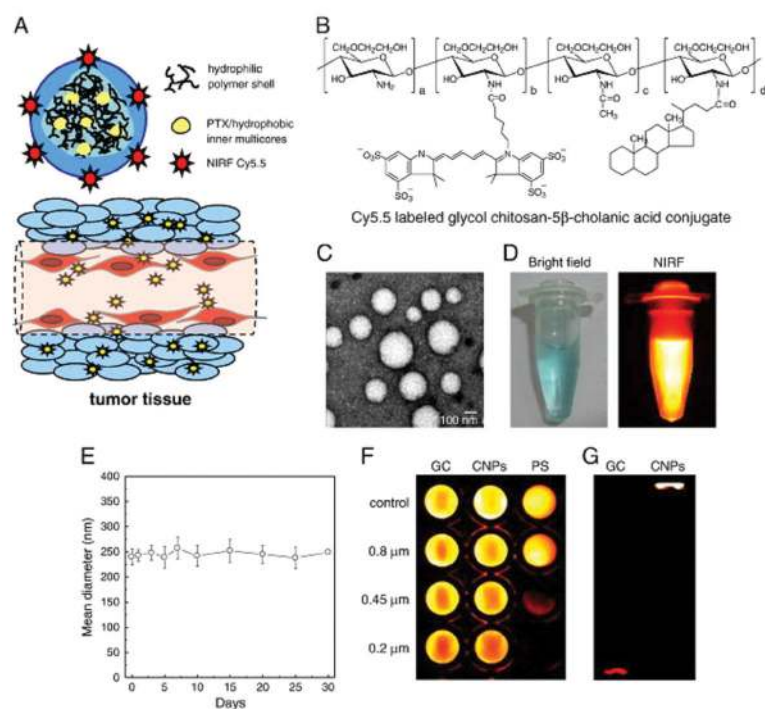
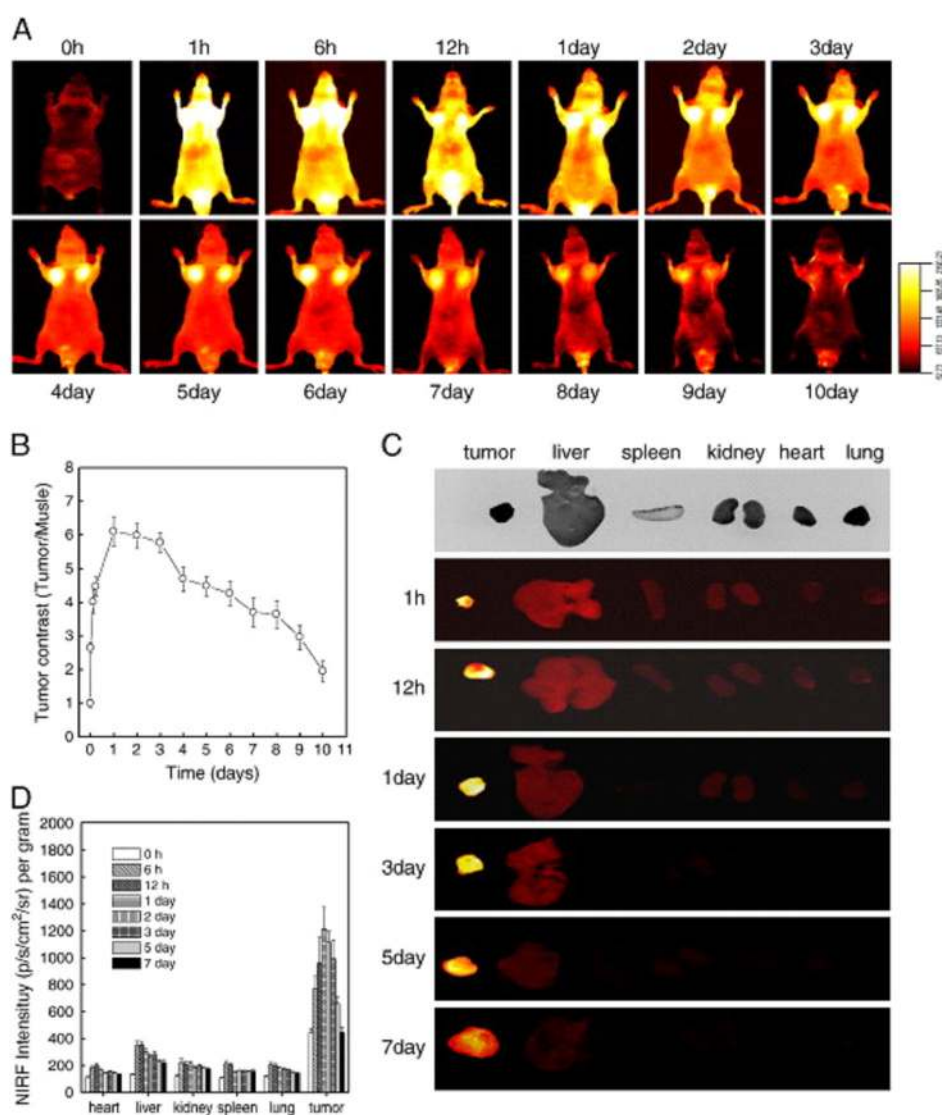


Figure 13.

(A) Conceptual description of a theragnostic nanoscale particle designed for cancer imaging and treatment. The theragnostic chitosan-based nanoparticles (CNPs) can preferentially accumulate at the tumor tissue by the enhanced permeation and retention (EPR) effect due to their unique properties, such as stability in blood, deformability, and fast cellular uptake. (B) Chemical structure of the glycol chitosan conjugates labeled with Cy5.5, a near-infrared fluorescent (NIRF) dye, and modified with hydrophobic 5β -cholanic acid. (C) A TEM image of Cy5.5-labeled CNPs (1 mg/ml) in distilled water. (D) Bright field and NIRF images of the Cy5.5-labeled CNPs in PBS. The NIRF image was obtained using a Cy5.5 filter set (ex = 674 nm, em = 695 nm). (E) Time-dependant size distribution of Cy5.5-labeled CNPs in PBS at 37 °C was confirmed using dynamic light scattering. (F) Filtration of water-soluble glycol chitosan (GC), CNPs, and polystyrene (PS) beads through filters of different pore sizes (0.8 μm , 0.45 μm , and 0.2 μm). The amount of each particle passed through the filters was quantified through NIRF intensity of the filtrate. (G) *In vitro* stability of the Cy5.5-labeled CNPs was determined using an SDS-PAGE test. Cy5.5-labeled GC polymers and CNPs were incubated in 10% serum for 6 h at 37 °C and their migratory positions were monitored using a Cy5.5 filter set. Reprinted with permission from [265], K. Kim, et al., Tumor-homing multifunctional nanoparticles for cancer theragnosis: Simultaneous diagnosis, drug delivery, and therapeutic monitoring. *J. Cntrl. Release* 146, 219 (2010). © 2010, Elsevier.

**Figure 14.**

(A) *In vivo* biodistribution of Cy5.5-labeled CNPs in SCC7 tumor-bearing mice. After tumor diameters reached 7–8 mm, 3.3 μmol of Cy5.5-labeled CNPs (5 mg/kg) were i.v. injected into the tumor-bearing C3H/HeN nude mice. (NIRF signal scale: 45–2680). (B) Time-dependent tumor contrast after administration of Cy5.5-labeled CNPs into tumor-bearing mice ($n = 3$). (C) NIRF images of the dissected major organs harvested from Cy5.5-labeled CNP-treated mice. The first row represents the bright field images of individual organs. A strong NIRF signal was observed in tumor tissues at all experimental times. (D) *Ex vivo* imaging of SCC7 xenograft tumor showed higher NIRF signal than other organs at all time points. A quantification of *in vivo* targeting characteristics of Cy5.5-labeled CNPs was recorded as total photons per centimeter squared per steradian (p/s/cm²/sr) per milligram of each organ at all time points ($n = 3$ mice per group). All data represent mean \pm s.e. Reprinted with permission from [265], K. Kim, et al., Tumor-homing multifunctional nanoparticles for

cancer theragnosis: Simultaneous diagnosis, drug delivery, and therapeutic monitoring. *J. Cntrl. Release* 146, 219 (2010). © 2010, Elsevier.

Author Manuscript

Author Manuscript

Author Manuscript

Author Manuscript

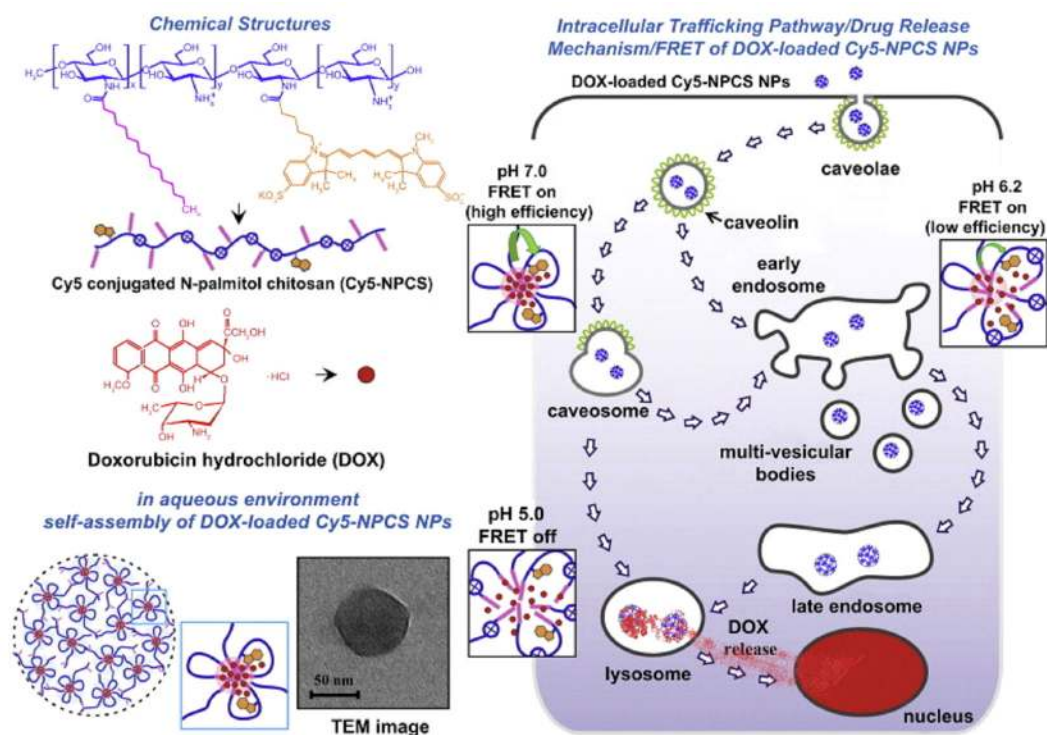


Figure 15. Schematic illustrations of the concept of the study. pH-responsive DOX (DOX)-loaded nanoparticles (NPs), made of *N*-palmitoyl chitosan bearing a Cy5 moiety (Cy5-NPCS), were prepared as an anticancer delivery device. Using the technique of Förster resonance energy transfer (FRET), the drug release behavior of DOX-loaded Cy5-NPCS NPs can be monitored/imaged intracellularly. Reprinted with permission from [269], K. J. Chen, et al., Intracellularly monitoring/imaging the release of doxorubicin from pH-responsive nanoparticles using Förster resonance energy transfer. *Biomaterials* 32, 2586 (2011). © 2011, Elsevier.

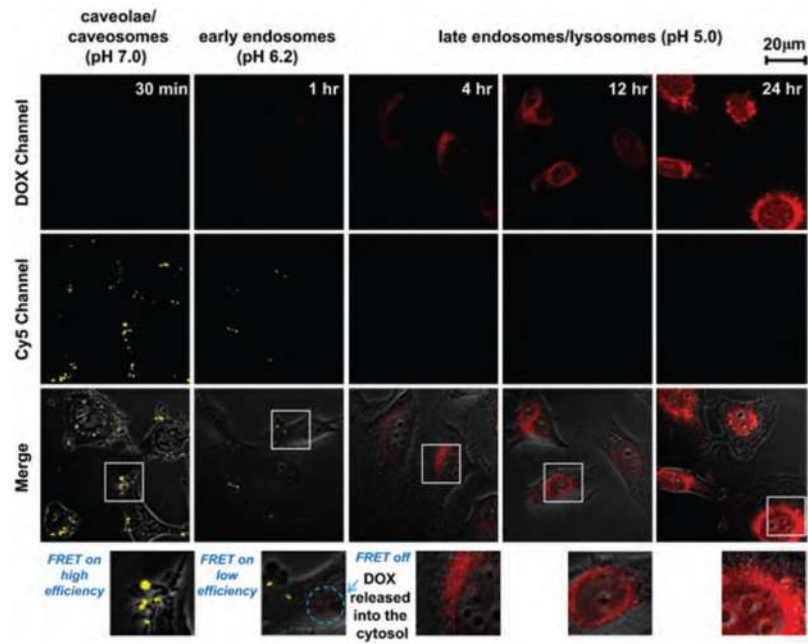


Figure 16. Dual-emission fluorescence images of HT1080 cells; cells were incubated with DOX-loaded Cy5–NPCS nanoparticles (NPs) for distinct durations and fluorescence images were then taken by CLSM in optical windows between 560–600 nm (DOX imaging channel) and 660–700 nm (Cy5 imaging channel) when irradiating NP suspensions at 488 nm. Reprinted with permission from [269], K. J. Chen, et al., Intracellularly monitoring/imaging the release of doxorubicin from pH-responsive nanoparticles using Forster resonance energy transfer. *Biomaterials* 32, 2586 (2011). © 2011, Elsevier.

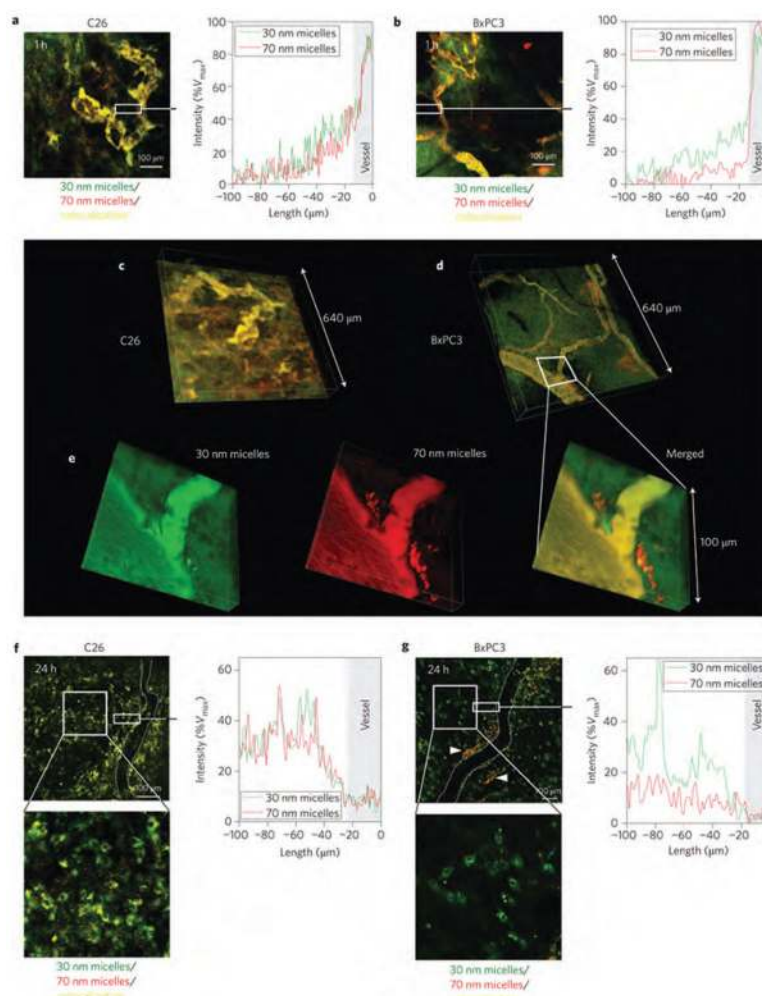


Figure 17.

In vivo real-time microdistribution of DACHPt/m with different diameters in tumours. (a), (b) Microdistribution of fluorescently labelled 30 nm (green) and 70 nm (red) micelles 1 h after injection into C26 (a) and BxPC3 (b) tumours. Their colocalization is shown in yellow. Right panels in (a) and (b) show fluorescence intensity profile from the blood vessel (0–10 mm; grey area) to the tumour tissue (10–100 mm) in the selected region (indicated by a white rectangle) expressed as a percentage of the maximum fluorescence intensity attained in the vascular region (%V_{max}). (c), (d) Z-stack volume reconstruction of C26 (c) and BxPC3 (d) tumours 1 h after co-injection of the fluorescent micelles. (e) Magnification of the perivascular region (indicated by a white trapezium) of the z-stack volume image of BxPC3 tumours. (f), (g) Distribution of 30 and 70 nm micelles 24 h after injection into C26 tumours (f) and BxPC3 tumours (g). White arrows in (g) indicate 70 nm micelles localizing at perivascular regions. Right panels show fluorescence intensity profile from the blood vessel (0–10 mm; grey area) to the tumour tissue (10–100 mm) in the selected region (indicated by white rectangle). Reprinted with permission from [275], H. Cabral, et al., Accumulation of sub-100 nm polymeric micelles in poorly permeable tumours depends on size. *Nature nanotechnology* 6, 815 (2011). © 2011, Nature Publishing Group.